2008

Development and testing of a combined catalyst/sorbent core-in-shell material for the production of high concentration hydrogen

Karl O. Albrecht
Iowa State University

Development and testing of a combined catalyst/sorbent core-in-shell material for the production of high concentration hydrogen

by

Karl Oscar Albrecht

A dissertation submitted to the graduate faculty

in partial fulfillment of the requirements for the degree of

DOCTOR OF PHILOSOPHY

Major: Chemical Engineering

Program of Study Committee:
Brent H. Shanks, Major Professor
Thomas D. Wheelock
Robert C. Brown
Kristen P. Constant
Thomas D. McGee

Iowa State University

Ames, Iowa

2008

Table of Contents

Abstract

A combined catalyst and sorbent for the production of hydrogen from CH_4 or CO was developed and tested. The combined catalyst and sorbent was a spherical multi-layered material having a CaO-based sorbent core and an outer shell composed mainly of alumina. The CaO sorbent core was employed to absorb CO_2, one of the reaction products. The alumina shell protected the friable CaO core and also supported a Ni catalyst. The development of the material focused separately on the development of the core and shell. First, since the CO_2 absorption capacity of CaO-based sorbents diminishes as they are repeatedly used and regenerated, the development of a more stable CaO-based sorbent was investigated. Both the addition of MgO, which acted as a sintering inhibitor, and severe initial calcination conditions for the CaO precursor limestone produced a more stable CaO sorbent. Second, an alumina-based material with good physical strength and high surface area was developed to serve as the shell of the core-in-shell material. The addition of either fine particle limestone or lanthanum oxide to the alumina shell formulation produced a material with enhanced physical strength, which was most likely due to the formation of a binding aluminate phase.

Reaction testing of the core-in-shell pellets with a 3:1 molar ratio of H_2O:CH_4 in the feed produced a high concentration of H_2 via simultaneous application of the steam-methane reforming reaction, the water-gas shift reaction and the reaction of CO_2 with CaO. This testing was conducted with a tubular fixed bed reactor over a temperature range of 550-650°C and a pressure range of 1.0-10.0 atm. The rapid absorption of CO_2 by CaO produced CH_4 and CO conversions greater than would have been possible without a sorbent. Lifecycle testing determined that a high concentration of H_2 could be produced over 10 cycles of H_2

production and sorbent regeneration. However, the length of time that H_2 was produced diminished with each cycle due to a loss of CO_2 absorption capacity by the CaO sorbent. Physical characterization of the pellets after lifecycle testing also revealed that some pellets fractured during lifecycle testing and that the Ni catalyst sintered.

Core-in-shell pellets with alternate shell formulations were also tested in the fixed bed reactor for the production of high concentrations of H_2 from a mixture of CO and steam via the water-gas shift reaction. Three alumina shell formulations were tested: a formulation with mostly alumina in the shell, a formulation with 10 wt% Fe_2O_3 added to the alumina shell formulation and a formulation with Ni impregnated onto the shell. The rapid absorption of CO_2 by the sorbent allowed for a high concentration of H_2 to be produced and a high CO conversion to be achieved between 550-600°C at 1.0 atm with any of these formulations. However, once the CaO sorbent became loaded, only the formulation with Ni present converted CO to reaction equilibrium levels. On the other hand, by absorbing CO_2 the formulation with mainly alumina in the shell appeared to be an attractive material for the production of H_2 from syngas. Furthermore, this formulation would be resistant to sulfurous gases that might be present.

Chapter 1. General Introduction

Introduction

Hydrogen is an important chemical used in numerous applications. As of 2000, two-thirds of the hydrogen demand was for the production of bulk chemicals such as ammonia and methanol and for the production and refinement of gasoline.[1] Additionally, hydrogen demand in the future will dramatically increase if fuel cell technology is successfully implemented for automobiles. A recent National Research Council report found that the demand for hydrogen could experience a 100-fold increase by 2050 with the implementation of automobile fuel cells in 2015.[2] Thus, research focused on the efficient and economical production of hydrogen has several potential benefits.

The current method for the commercial production of hydrogen is a complicated multi-step process. The steam reforming of methane or heavier hydrocarbons is the most widely used industrial practice for hydrogen production.[3] The steam-methane reforming (SMR) reaction is given by:

$$CH_4 + H_2O \leftrightarrow CO + 3H_2 \qquad \Delta H_{25°C} = 206 \text{ kJ/mol} \qquad (1)$$

Reaction 1 is highly endothermic and CH_4 conversion is limited by thermodynamic equilibrium at low temperatures. Thus, commercial application of the SMR reaction is typically carried out at 800-1100°C with a Ni catalyst. The CO produced through application of reaction 1 can be further reacted with steam through the water-gas shift (WGS) reaction, which is given by:

$$CO + H_2O \leftrightarrow H_2 + CO_2 \qquad \Delta H_{25°C} = -41 \text{ kJ/mol} \qquad (2)$$

The WGS reaction is mildly exothermic and high temperatures limit CO conversion. In order to maximize CO conversion, the WGS reaction is commonly employed by using a two-step reaction process. First, the reaction mixture is fed to a reactor operating between 350 and 450°C that contains an iron oxide/chromium oxide catalyst. This reactor operates at a higher temperature to increase the kinetics of the WGS reaction. Next, the process stream is fed to a second reactor operating between 200 and 215°C that is loaded with a copper-zinc oxide catalyst. This reactor is operated at the lower temperature in order to maximize the conversion of CO. The product stream exiting the second WGS reactor is primarily a mixture of CO_2 and H_2 that must be separated, typically by employing an amine scrubber for CO_2 removal.

Several recent investigations have focused on simplifying the production of H_2. These studies have focused on the selective removal of either H_2 or CO_2 from the reacting gas phase in order to enhance feedstock conversions while simultaneously separating the reaction products. For the selective removal of hydrogen, membranes made of palladium or other novel materials have been used.[4, 5] However, a technological breakthrough is needed for membrane technology to become practical and economic on a large scale. On the other hand, selective removal of CO_2 can be achieved by employing a solid sorbent in the reaction system. While different sorbents can be used, one of the most promising is CaO, which removes CO_2 by the following reaction:

$$CaO + CO_2 \leftrightarrow CaCO_3 \qquad \Delta H_{25°C} = -175 \text{ kJ/mol} \qquad (3)$$

Simultaneous application of reactions 1,2 and 3 has been shown to remove CO_2 while enhancing CH_4 and CO conversions to levels greater than allowed by thermodynamic equilibrium, thereby making it possible to produce high concentration H_2 in a single step.[6-8]

While several studies have demonstrated the feasibility of simultaneously performing the SMR and WGS reactions combined with CO_2 absorption by CaO, most of the studies have utilized packed beds of powders. Scale up of a reactor packed with powder could encounter gas channeling and significant pressure drop across the bed that could interfere with commercial applications. Pelletization of the catalyst and sorbent can address this challenge. However, pelletized CaO is friable. In order to produce a robust sorbent, a protective outer shell can be applied to pelletized CaO.[9-12] Furthermore, if the shell is porous, it can be impregnated with a Ni catalyst to create a combined catalyst and sorbent material capable of producing concentrated H_2 in a single reactor.[13, 14]

Such a combined catalyst and sorbent material for producing H_2 from CH_4 or other hydrocarbons and steam has been under development for several years.[13-15] The dual layered core-in-shell pellets are composed of a core made of a CaO-based sorbent and a shell made of an alumina-based formulation. The alumina-based shell serves to protect the fragile core and to support a Ni catalyst. Initial testing of the combined catalyst and sorbent produced highly encouraging results. However, several opportunities for improving both the core and shell materials were suggested along with the need for further reaction testing over a wider range of temperature and pressure.

The present dissertation focuses on the further development and performance testing of the combined catalyst and sorbent core-in-shell material. A stable CaO-based sorbent capable of CO_2 absorption and subsequent regeneration over many cycles was developed. A physically strong alumina-based material with high surface area for increasing the dispersion of the Ni catalyst was also developed for the shell of the core-in-shell material. Core-in-shell pellets made with two of the more promising shell formulations were subjected to

performance testing in a fixed bed reactor to determine the effectiveness of the formulations for producing H_2 from a mixture of CH_4 and steam. Additionally, the pellets were subjected to limited lifecycle testing to determine how well the pellets stood up to H_2 production and sorbent regeneration. Finally, the versatility of the core-in-shell pellets was demonstrated through application of shell formulations with three alternative catalysts for the water-gas shift reaction.

Dissertation Organization

This dissertation is organized into six chapters. Figure and Table numbers are specific for each chapter; i.e., there is a Figure 1 in Chapter 1 as well as in Chapters 2, 3 and so on. Chapter 1 contains a general introduction as well as a review of the relevant literature pertaining to sorption enhanced hydrogen production. Chapter 2 deals with the development of a stable CaO-based sorbent, which has implications not only for sorption enhanced hydrogen production but also for the separation of CO_2 from other gas mixtures that could be important because CO_2 is a greenhouse gas. Chapter 3 documents efforts to develop an alumina-based material with good physical strength and high surface area for application as the shell of the core-in-shell material. Chapter 4 deals with the results of pressurized reaction testing of two of the promising shell formulations developed in Chapter 3. Chapter 4 also contains results obtained from conducting lifecycle testing of the core-in-shell pellets. Chapter 5 deals with the results of water-gas shift reaction performance testing of three different shell formulations, each based on a different catalyst, one of the catalysts being the Al_2O_3 shell material itself, a second the Al_2O_3 with added Fe_2O_3, and a third the Al_2O_3 with

added Ni. Finally, Chapter 6 presents the overall general conclusions of the research together with recommendations for future research.

Literature Review

The production of hydrogen from different hydrocarbons in a single step with *in-situ* CO_2 removal has been the focus of several investigations. Harrison[6] recently published a review article covering numerous investigations pertaining to the enhanced production of H_2 using different solid CO_2 sorbents. The present literature review begins with an overall review of the thermodynamics of sorption enhanced hydrogen production when a CaO sorbent is utilized. The review continues by covering the results of several investigations and the materials and feedstocks used in them for the production of hydrogen with simultaneous CO_2 absorption. Last, the evolution, composition, and application of the core-in-shell pelletized material is reviewed.

Thermodynamic Analysis

The ability of CaO to reversibly absorb and desorb CO_2 is a function of the equilibrium vapor pressure of CO_2 over CaO. Baker[16] determined the following relationship for the equilibrium vapor pressure of CO_2 over CaO, which is also plotted in Figure 1.

$$\log_{10} P_{eq} = 7.079 - \frac{8308}{T} \tag{4}$$

In equation 4, P_{eq} is the equilibrium vapor pressure of CO_2 over CaO and T is the temperature of the system in K.

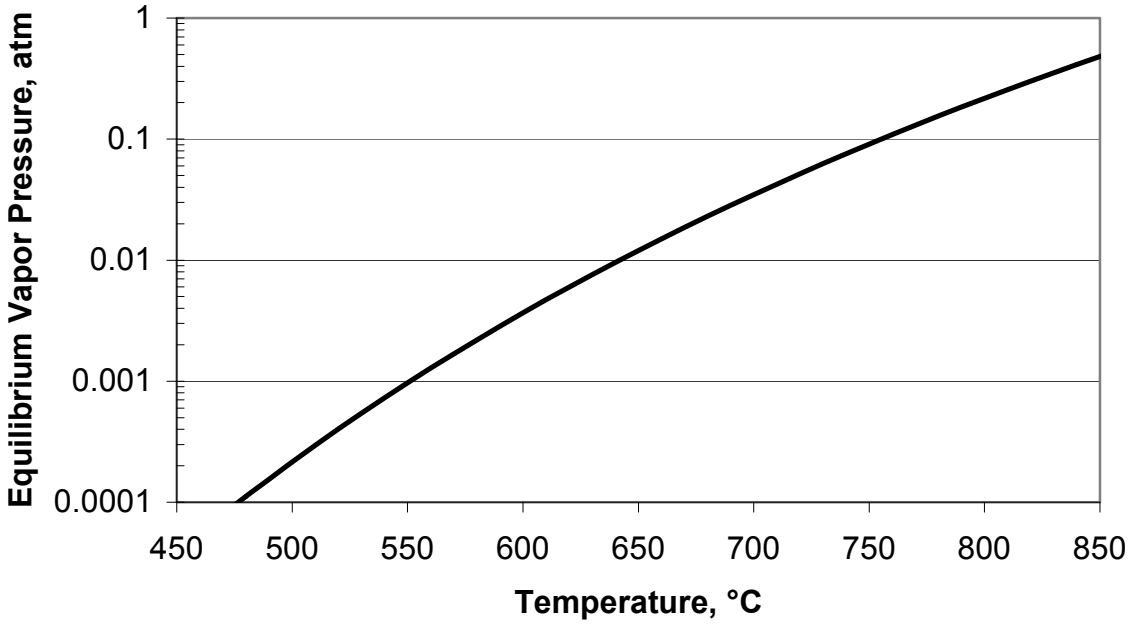

Figure 1. The equilibrium vapor pressure of CO_2 over CaO.

Above the equilibrium line in Figure 1, CO_2 is absorbed by CaO while below the line $CaCO_3$ decomposes into CaO and CO_2. Thus, a CaO sorbent can be regenerated through pressure swing, temperature swing or a combination of both.

The ability of CaO to react with steam to produce $Ca(OH)_2$ in a reaction environment must also be considered when utilizing CaO as a sorbent for enhanced hydrogen production. At 470°C, the equilibrium partial pressure of water vapor is 1.0 atm in the presence of $Ca(OH)_2$.[17] At atmospheric pressure, $Ca(OH)_2$ formation is not thermodynamically favored above 470°C. However, increasing the pressure of a system allows for the formation of $Ca(OH)_2$ at higher temperatures. A thermodynamic analysis by Balasubramanian et al.[8] determined that at 15 atm with a CH_4:H_2O molar feed ratio of 1:4 the concentration of H_2 in the product gas was decreased due to the formation of $Ca(OH)_2$ up to approximately 625°C.

Satrio et al.[13] performed a thermodynamic analysis of simultaneous application of the SMR and WGS reactions with and without CO_2 absorption by CaO. This analysis was based on a 3:1 mole ratio of H_2O:CH_4 at 1.0 atm. Figure 2 illustrates the results of this analysis for different temperatures. Gas composition is on a dry basis. Figure 2 indicates that between 550°C and 740°C that the highest concentration of H_2 is obtained when CO_2 is absorbed by CaO.

Figure 2 also reveals that CH_4 concentrations decrease as the temperature increases. This is because the SMR reaction is endothermic and CH_4 conversion is favored by higher temperature. The concentration of CO increases with increasing temperature due to the exothermic nature of the water-gas shift reaction. Introduction of CO_2 absorption via the carbonation of CaO results in greater conversions of CH_4 and CO than would otherwise be possible in a single step, resulting in diminished concentrations of CH_4 and CO. Of particular interest is the low concentration of CO in the presence of CO_2 absorption at 550-600°C, especially when considering that commercial application of the water-gas shift reaction typically takes place at a maximum temperature of 450°C.[18]

Another thermodynamic point of interest in Figure 2 is the near lack of temperature dependence on the concentration of CH_4 in a system at equilibrium with CO_2 absorption. This is because the heat required by the endothermic steam-methane reforming reaction is largely supplied by the exothermic water-gas shift and carbonation reactions. Thus, nearly adiabatic operation of the reactor should be possible when the absorption of CO_2 is taking place via the carbonation of CaO.

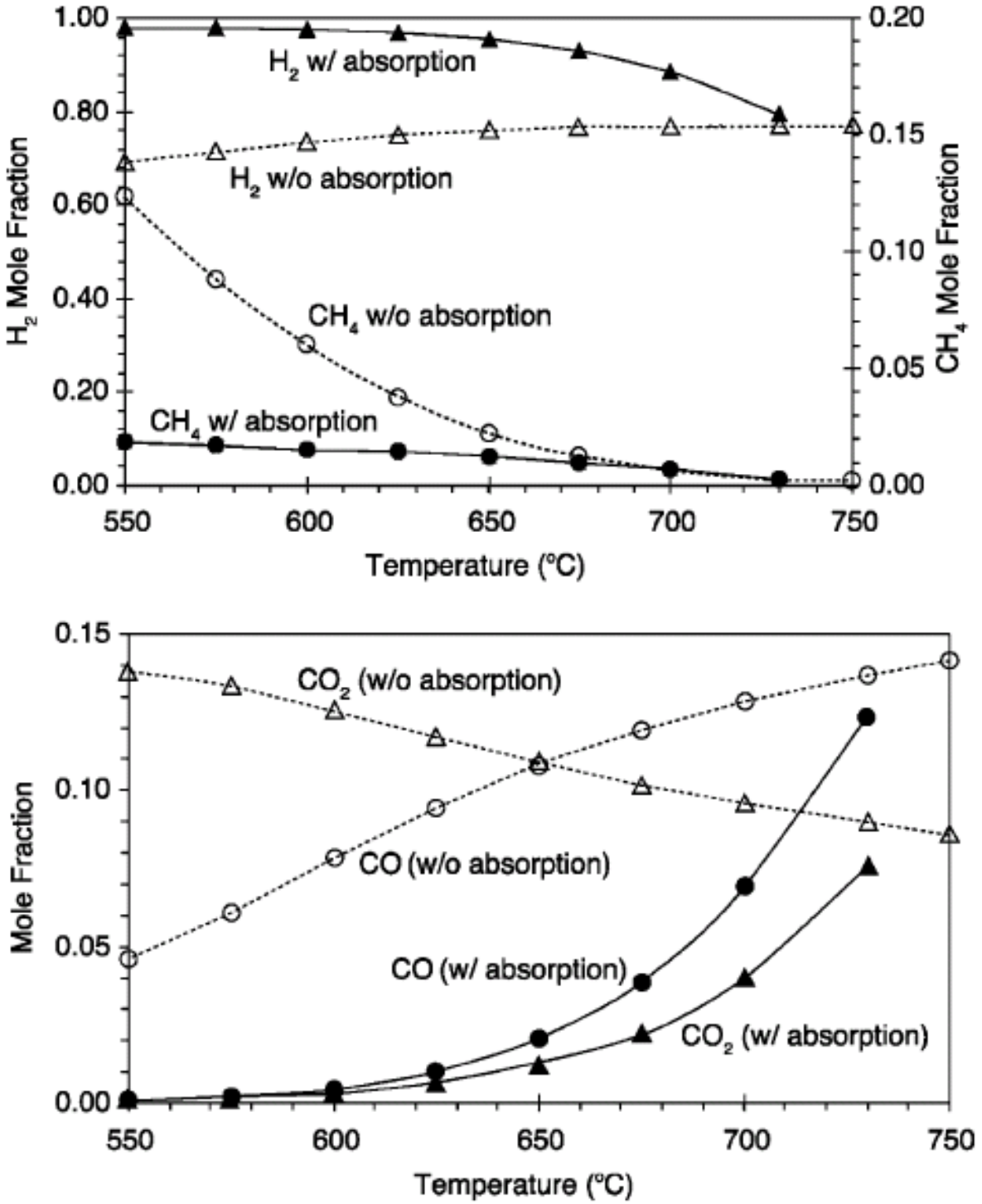

Figure 2. Equilibrium gas concentrations (dry basis) as a function of temperature based on thermodynamic calculations with a 3:1 mole ratio of H_2O:CH_4 at 1.0 atm with and without CO_2 absorption. Taken from Satrio et al.[13]

Materials and Operating Parameters

The production of hydrogen with CO_2 absorption in a fixed bed reactor with a solid sorbent such as CaO is inherently an unsteady state process due to the finite amount of sorbent. Initially, a high concentration of H_2 will be produced as CO_2 is rapidly absorbed. Eventually, the sorbent becomes saturated, resulting in CH_4 and CO conversions similar to those that would be observed without a sorbent present. These different time periods are illustrated in Figure 3, which was taken form Ortiz and Harrison.[7]

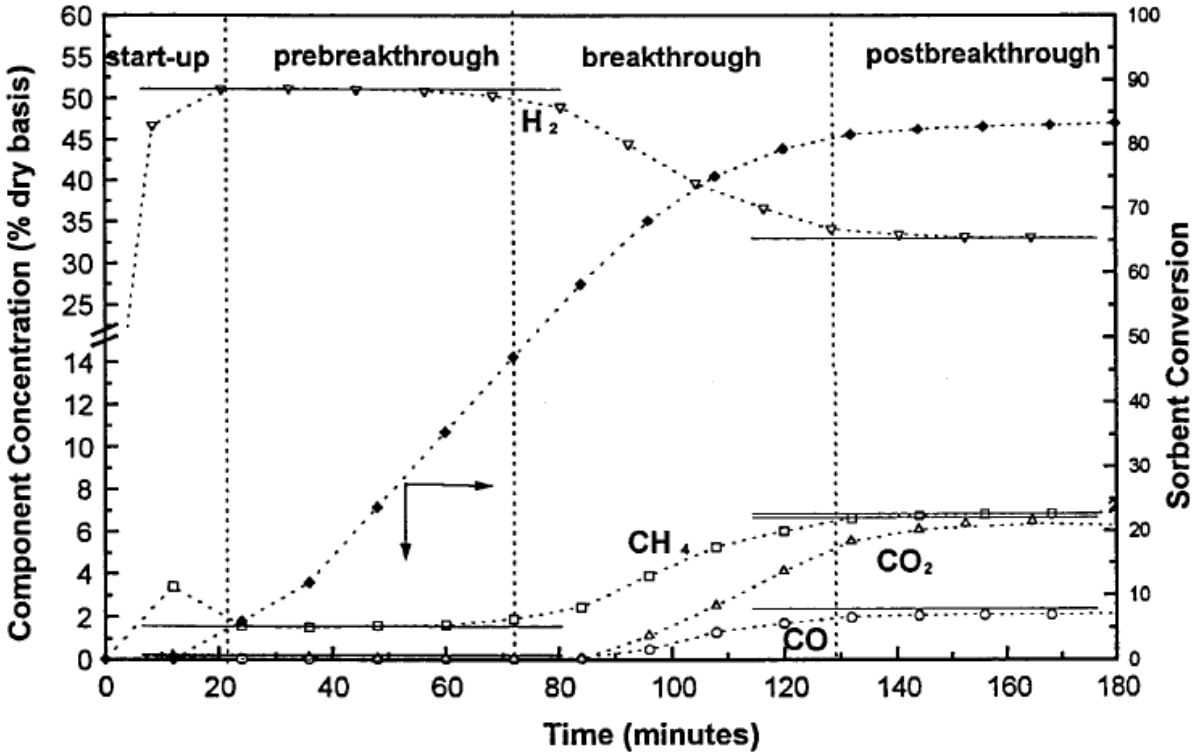

Figure 3. A typical reactor response curve during the sorption enhanced production of H_2. Taken from Ortiz and Harrison.[7]

The results in Figure 3 were obtained with a commercial Ni SMR catalyst and a CaO sorbent derived from dolomite at 650°C and 15.0 atm using a 4:1 mole ratio of H_2O:CH_4.

Thus, once the postbreakthrough period in Figure 3 is achieved, the sorbent would need to be regenerated either through temperature or pressure swing desorption methods.

Hydrotalcite CO_2 Sorbents

The selective separation of CO_2 can be achieved with a variety of different sorbents. One such sorbent is hydrotalcite, which is a Mg-Al hydroxide layered material with interlayers of CO_3^{-2} and water.[19] Hydrotalcite sorbents are typically used at lower temperatures than CaO. Additionally, hydrotalcites will thermally decompose at higher temperatures and effectively lose their ability to remove CO_2 above 600°C.[19]

Ding and Alpay[20, 21] used a K-promoted hydrotalcite to investigate the applicability of the sorbent for sorption enhanced H_2 production. In their work, 7.2 g of a commercial Ni catalyst was used alone or combined with 14.8 g of a commercially available K-promoted hydrotalcite sorbent. The reaction of CH_4 and steam in a 1:6 molar ratio was conducted at 445.7 kPa and 450°C. The addition of the hydrotalcite CO_2 sorbent improved the conversion of CH_4 by 40%. However, the conversion enhancement rapidly decreased after 5 min due to sorbent saturation.

Hufton et al.[22] employed a proprietary KCO_3-promoted hydrotalcite as a sorbent for CO_2 for enhanced H_2 production. The authors reported that a physical mixture of commercial SMR catalyst and the proprietary sorbent resulted in a CH_4 conversion of 82% at 450°C and 4.74 atm using a 6:1 mole ratio of H_2O:CH_4. The purity of the hydrogen in the product stream was 96 mol% H_2 with the primary impurity being CH_4 at 4 mol%. A similar CH_4 conversion level of 82% was achieved when the temperature was increased to 645°C without the CO_2 sorbent. However, the concentration of hydrogen was only 75.5 mol% due to the combined presence of 20.1 mol% CO and CO_2.

Waldron et al.[23] demonstrated sorption enhanced hydrogen production with a hydrotalcite based sorbent using a pilot-scale unit. The same proprietary K_2CO_3-promoted hydrotalcite sorbent employed by Hufton et al.[22] was used in a physical mixture with an industrial SMR catalyst. At a temperature of 490°C and pressure of 1.78 atm with a 6:1 molar ratio of H_2O:CH_4, it was reported that a product stream with 94.4 mol% H_2, 5.6 mol% CH_4, 40 ppm CO_2 and non-detectable amounts of CO could be produced. This reaction step was maintained for between 6 and 18 min before sorbent regeneration became necessary.

While hydrotalcite sorbents are effective for selectively removing CO_2 to enhance H_2 production, they are limited by CO_2 sorption capacity and economics when compared to CaO-based sorbents. Ochoa-Fernández et al.[24] compared CaO and hydrotalcite sorbents for their effectiveness in enhancing hydrogen production through CO_2 sorption. CaO was determined to be a superior sorbent due to favorable thermodynamics and higher reaction rates. However, the authors also suggested that the stability of CaO should be improved to enhance the absorption capacity over many cycles of absorption and regeneration. Hydrotalcite sorbents have a relatively low CO_2 absorption capacity of 0.4 to 0.5 mmol/g sorbent after 15-20 cycles.[22] For comparison, CaO that had been subjected up to 550 cycles maintained an absorption capacity of about 1.2 mmol/g sorbent.[25] Therefore, while it has been demonstrated that hydrotalcite sorbents can effectively enhance hydrogen production through CO_2 separation, more sorbent is required due to a lower sorption capacity. Additionally, CaO-based sorbents that have been subjected to many cycles could have a higher CO_2 sorption capacity than hydrotalcite sorbents that are relatively fresh.

Furthermore, hydrotalcite sorbents are relatively expensive when compared to CaO-based sorbents. An economic study of various methods of absorbing CO_2 found that

hydrotalcites would cost approximately $4.00 per mol of CO_2 removed.[26] The same study determined that crushed $CaCO_3$ (limestone) when used as a CaO-based sorbent precursor would cost approximately $0.0015 per mol of CO_2 removed. Thus, there are economic advantages for using a CaO-based CO_2 sorbents for the enhanced production of hydrogen.

CaO-based CO_2 Sorbents

CaO-based sorbents can be derived from several different precursors through high temperature calcination. Reagent grade materials such as calcium acetate, calcium nitrate, and calcium hydroxide as well as natural minerals such as limestone, dolomite and huntite have all been considered as CaO-based sorbent precursors.[27, 28] However, one major challenge associated with the application of CaO-based sorbents is a decrease in the CO_2 absorption capacity of the sorbent as it repeatedly undergoes absorption and regeneration steps.[29, 30] The loss of CO_2 absorption capacity is due in part to the fact that CO_2 preferentially reacts at or near the surface of a CaO particle. The build up of a carbonate layer at the surface of a CaO particle creates a layer with low porosity, rendering unreacted CaO at the center of the particle more difficult for CO_2 to react with.[31] Additionally, textural changes that result in sintering of the sorbent take place when the material is subjected to several cycles, which further limits the CO_2 absorption capacity.[32] However, the amount of CaO converted during a cycle in a sample that has been subjected to many cycles of absorption and regeneration has been reported to stabilize at 7-8% conversion of CaO, which translates to about 1.2 mmol CO_2 absorbed/g sorbent.[25] Thus, after many cycles, only a small portion of the CaO present is able to absorb CO_2. Further discussion and review of CaO-based sorbents and the decay of CO_2 absorption capacity over many cycles is addressed in the Introduction to Chapter 2.

CaO-based sorbents have been successfully demonstrated to enhance hydrogen production. Han and Harrison[33] utilized a CaO-based sorbent derived from dolomite for enhanced hydrogen production from a mixture of CO and steam via the water-gas shift reaction. The study was conducted without an additional catalyst present. The presence of the CaO sorbent alone was sufficient to produce a high concentration of hydrogen with CO and CO_2 in the 3 and 35 ppm range, respectively, at 500°C and 15 atm. For this study, the optimum CO:H_2O mole ratio was 1:3 with a lower conversion of CO obtained with a CO:H_2O mole ratio of 1:2.

The study by Han and Harrison[33] also investigated a feedstock with compositions similar to syngas. The reactant stream contained H_2, CO_2, H_2O and CO. Carbon-oxide removal of 99.7% was observed during the CO_2 absorption period with the simulated syngas reactant stream. These results were similar to the 99.8% carbon-oxide removal observed during testing by the same authors when CO and steam were used as reactants in a 1:3 mole ratio.

Han and Harrison[33] also claimed dolomite was superior to limestone as a CaO precursor because more of the CaO derived from dolomite was utilized. Dolomite is a natural mineral that ideally contains 50 mol% $Mg(CO_3)$ and 50 mol% $Ca(CO_3)$ while limestone is typically greater than 97 wt% $CaCO_3$.[34] Thus, more of the CaO was converted during the production of a high concentration of H_2 when dolomite was used as the CaO-precursor instead of limestone. The increased utilization of CaO in dolomite compared to limestone has been explained by the excess pore volume created during the initial thermal decomposition of dolomite.[35]

Balasubramanian et al.[8] continued the work of Han and Harrison by mixing a Ni SMR catalyst supported on Al_2O_3 with a CaO-based sorbent to simultaneously perform the SMR, WGS, and CO_2 absorption reactions. This study utilized steam and methane as the reactants. High purity (99.7%) $CaCO_3$ was used for the CaO-precursor. By using a 4:1 molar ratio of H_2O:CH_4 diluted with 70% N_2 at 15 atm, the reaction mixture closely approached thermodynamic equilibrium at temperatures between 550-750°C. The H_2 concentration produced while CO_2 was being absorbed was not strongly dependent on temperature because the heat supplied by the exothermic WGS and carbonation reactions was nearly equal to the heat absorbed by the endothermic SMR reaction. Below 550°C, the concentration of H_2 was below the calculated equilibrium concentration, possibly due to a decrease in the rate of the SMR reaction. The investigators reported a 23.9 mol% H_2 concentration in the reactor effluent at 650°C and 15 atm, which was similar to the H_2 concentration predicted by thermodynamic equilibrium.

Balasubramanian et al.[8] also showed that H_2 in a high concentration could be produced without a N_2 diluent by using a CaO-based sorbent and a Ni SMR catalyst. A test at 650°C and 15 atm with a 4:1 mole ratio of H_2O:CH_4 resulted in nearly equilibrium conversions of CH_4 and CO. This test produced 93 mol% H_2 while CO_2 was being absorbed, which was close to the 96 mol% H_2 predicted by thermodynamic equilibrium. Thus, H_2 in a high concentration was produced without the need for a N_2 diluent.

Ortiz and Harrison[7] tested the durability of a CaO-based sorbent derived from dolomite for the production of high concentration H_2. However, the dolomite contained enough sulfur to warrant a sulfur removal pretreatment step prior to reaction testing in order to avoid poisoning the Ni catalyst. Sulfur removal was accomplished by first heating the

dolomite to 900°C to produce MgS and CaS from $MgSO_4$ and $CaSO_4$. The sulfides were then oxidized with steam to produce H_2S and MgO or CaO.

In order to test the stability of the CaO-based sorbent, Ortiz and Harrison[7] used a hydrogen production step at 650°C and 15 atm with a steam to CH_4 mole ratio of 4:1 combined with 40 mol% inert N_2. Regeneration of the sorbent was performed with either pure N_2, 4% O_2 in 96% N_2, or 100% CO_2 to test the effect of the regeneration atmosphere on the sorbent. Testing over five cycles with regeneration conducted at 800°C in 100% N_2 or at 950°C in 4% O_2 in 96% N_2 had little effect on the sorbent other than to slightly decrease the length of time that H_2 was produced in high concentration. This result was probably due to the decreasing absorption capacity of the CaO as the testing was continued.

Longer lifecycle tests of the CaO sorbent derived from dolomite were also performed by Ortiz and Harrison.[7] For these tests, an atmosphere of 100% N_2 or 100% CO_2 was used for regenerating the sorbent. A pure CO_2 regeneration atmosphere would be ideal for subsequent CO_2 sequestration since no further separation would be required. Regeneration at 950°C in 100% N_2 was detrimental to the sorbent because after the 10^{th} cycle a lower concentration of H_2 was produced. This result was most likely due to a loss in activity of the sorbent. Regeneration performed at 950°C in 100% CO_2 resulted in a diminished absorption capacity after 25 cycles, which shortened the period that high concentration H_2 was produced. However, after 25 cycles of testing using a regeneration temperature of 950°C, the absorption capacity of the CaO sorbent regenerated in 100% CO_2 was greater than the absorption capacity of the sorbent regenerated in 100% N_2. When the same tests were carried out using a regeneration temperature of 800°C, the results achieved with either

regeneration atmosphere were very comparable. After 25 cycles, neither atmosphere produced a large drop in either the H_2 concentration during the period of rapid CO_2 absorption or in the length of time that high concentration H_2 was produced.

Hydrogen that is to be directly utilized in fuel cells for the production of electricity must have a low concentration of CO. Harrison and Peng[36] used a Ni SMR catalyst and high purity $CaCO_3$ at low temperatures to maximize CO conversion in order to produce a 95+ mol% H_2 stream from CH_4 and steam. Results of testing at 480°C and 5 atm with a feed stream of 20% CH_4 and 80% H_2O produced a product stream with 97.8% H_2 and 17 ppmv CO.

Yi and Harrison[37] also demonstrated that H_2 could be produced with a low CO concentration for use in fuel cells. Calcined dolomite was utilized as the CaO sorbent precursor, which was mixed with a commercial Ni SMR catalyst. Pressures between 1 and 5 bars and temperatures between 400-460°C were studied. The authors were able to produce 96 mol% H_2 with a CO concentration of about 50 ppmv at 460°C and 1 bar at a CH_4:H_2O mole ratio of 1:3. Thus, these studies determined that it is indeed possible to produce H_2 with a low CO concentration using sorption-enhanced H_2 production. However, enhancing the conversion of CO at low temperatures requires consideration of the detrimental effect on CH_4 conversion and the formation of $Ca(OH)_2$ by the reaction of CaO and steam.

Sorption enhanced H_2 production has also been studied with feedstocks other than CH_4 and CO. Specht et al.[38] found that steam-reforming methanol with a nickel catalyst and a CaO sorbent derived from dolomite was feasible for the production of hydrogen. At temperatures between 625 and 650°C, a stream of 95 mol% H_2 was produced by employing CO_2 absorption. A variation of the sorption enhanced reaction concept was studied by Lin et

al.[39] who found that mixing coal ground into 0.1 mm sized particles with NaOH as a catalyst and uncalcined $Ca(OH)_2$ as a sorbent in a pressurized autoclave batch reactor produced a product with 85% hydrogen and 15% CH_4. This test was carried out at 650°C and 60 MPa. However, Kuramoto et al.[40] found that calcium-based sorbents undergo deactivation due to solid-solid reaction with silicon and aluminum impurities when used with coal to produce high concentration H_2.

Combining a catalyst and CaO-based sorbent in a fluidized bed reactor for the sorption enhanced production of H_2 has also been investigated. Johnsen et al. [41] demonstrated that at 600°C and 1 atm it is possible to produce 98-99 mol% H_2 using dolomite as the CaO sorbent precursor with a Ni SMR catalyst in a fluidized bed. The 98-99 vol% H_2 product stream was achieved over the course of four cycles. However, the time that the stream was nearly at equilibrium decreased over the four cycles due to the decreasing absorption capacity of the CaO sorbent. The authors also reported that in addition to enhanced mass transfer, axial temperature gradients of only 3-4°C were found, which demonstrated good temperature control.

Core-in-Shell Material

Many of the studies reviewed up to this point were performed with beds packed with a physical mixture of sorbent and catalyst powders. In order to make a material more attractive for scaled up processes, powders have been agglomerated or pelletized to prepare 3-4 mm diameter pellets. Unfortunately, when a CaO precursor such as limestone or dolomite is pelletized, the resulting pellets are friable and do not stand up well to handling. Akiti et al.[9-11] found that it was possible to produce strong pellets of a CaO-based sorbent by a dual step process that first created spherical pellets of the sorbent precursor and then added

a strong porous alumina shell to each pellet. These pellets were calcined at 1100°C for 2 hr to sinter the material, which fused the shell together to create a robust material. The core-in-shell material was originally developed to absorb hot sulfurous gases and was performance tested by absorbing H_2S. It was determined that the shell was sufficiently porous to allow diffusion of H_2S through the shell so that it could be react with the core.

Hasler et al.[42, 43] investigated the core-in-shell concept further. A model of the reaction between H_2S and CaO based on a shrinking-core of CaO was applied to the material with good results. It was found that the rate of reaction between the H_2S and a bare CaO core was limited by the build-up of a product layer within the core. Additionally, the diffusion resistance attributed to the gas film surrounding a pellet without a shell was determined to be significant. When a pellet was coated with an alumina shell, it was found that the shell and the build up of the product layer both contributed to the diffusion resistance of the material. In the case of a core-in-shell pellet, the diffusion resistance attributed to the gas film surrounding the pellet appeared negligible compared to the larger resistances presented by the shell and product layer. Therefore, the rate of H_2S absorption was controlled by the rate of diffusion of H_2S through the shell and layer of reaction product. It was suggested that increasing the porosity of the shell material would decrease the diffusion limitation through the shell.

An extension of the core-in-shell concept to produce a material capable of sorption enhanced H_2 production was developed later. Satrio et al.[13] modified the shell formulation by adding a high surface alumina to make the shell a better support for a Ni catalyst. The addition of the high surface area alumina successfully increased the catalytic activity of the

supported Ni catalyst. However, the addition of the high surface area alumina also had the undesired consequence of decreasing the physical strength of the core-in-shell pellets.

Satrio et al.[13] used the improved core-in-shell pellets to produce H_2 from CH_4 by employing a 3:1 molar ratio of H_2O:CH_4. A 96.3 mol% H_2 stream was produced at 600°C during the CO_2 absorption period while a stream with only 75.5 mol% H_2 was produced without CO_2 absorption. It appeared that the optimum temperature for the production of high concentration H_2 was 600°C when using CH_4 as a feedstock. Steam reforming of CH_4 at temperatures of 650°C and 560°C resulted in product streams with of 84.3 mol% and 90.5 mol% H_2, respectively.

Satrio et al.[13] also successfully produced high concentration H_2 from a mixture of propane and steam with the core-in-shell material. At 560°C using a 3:1 mole ratio of H_2O:C, a 96 mol% H_2 stream was produced during the CO_2 absorption period. However, some CH_4 was also produced while propane was being reformed. While propane was being reformed and CO_2 was being absorbed at 560°C, the CH_4 concentration was 1.5 mol% compared to a level of 8.0 mol% at the same temperature during CH_4 reforming. During propane reforming, the concentration of methane in the product stream increased as the temperature was decreased. This was attributed to either less CH_4 being reformed at the lower temperature or to the exothermic methanation reaction, which is the reverse of the SMR reaction (reaction 1).

Satrio et al.[14] also applied the core-in-shell material with a Ni catalyst to steam reform toluene. Toluene is a compound used to model tars produced during the gasification of coal or biomass. It was determined that at 600°C and 1.0 atm with a H_2O:C molar ratio of 3:1, a

product with 90.5 mol% H_2 could be produced while CO_2 was being absorbed. Without CO_2 absorption the H_2 concentration decreased to 60.8 mol%.

The core-in-shell material impregnated with a Ni catalyst was also used to produce high concentration H_2 from a simulated gasification stream of CH_4, CO and toluene.[14] Results similar to the toluene reforming experiment were found. A H_2 concentration of 90.5 mol% together with a CO concentration of 4.0 mol% was produced at 600°C during the CO_2 absorption period. Thus, the core-in-shell material proved capable of producing H_2 from a variety of different carbonaceous sources.

Conclusion

Sorption enhanced hydrogen production using a CaO-based sorbent is an attractive method for the production of high concentration H_2 in a single step. Furthermore, core-in-shell pellets with a reactive CaO-based core, protective alumina shell and Ni reforming catalyst are a promising material for further development and scale-up for industrial applications. The following chapters focus on meeting some of the challenges associated with the core-in-shell concept. These challenges include the development of a stable CaO-sorbent, development of a strong alumina-based shell material and reaction testing of the material using CH_4 and steam at higher pressures or using CO and steam at atmospheric pressure.

Literature Cited

(1) Stoll, R. E.; Von Linde, F., Hydrogen-what are the costs? *Hydrocarbon Processing, International Edition* **2000,** 79, (12), 42-43, 45-46.

(2) National Research Council Report. *The Hydrogen Economy - Opportunities, Costs, Barriers and R&D Needs*; The National Academies Press: Washington, D.C., 2004.

(3) Bartholomew, C. H.; Farrauto, R. J., *Fundamentals of Industrial Catalytic Processes*. Second ed.; John Wiley & Sons, Inc.: Hoboken, 2006; p 340-486.

(4) Adhikari, S.; Fernando, S., Hydrogen Membrane Separation Techniques. *Industrial & Engineering Chemistry Research* **2006,** 45, (3), 875-881.

(5) Phair, J. W.; Donelson, R., Developments and Design of Novel (Non-Palladium-Based) Metal Membranes for Hydrogen Separation. *Industrial & Engineering Chemistry Research* **2006,** 45, (16), 5657-5674.

(6) Harrison, D. P., Sorption-Enhanced Hydrogen Production: A Review. *Industrial & Engineering Chemistry Research* **2008,** 47, (17), 6486-6501.

(7) Ortiz, A. L.; Harrison, D. P., Hydrogen Production Using Sorption-Enhanced Reaction. *Industrial & Engineering Chemistry Research* **2001,** 40, (23), 5102-5109.

(8) Balasubramanian, B.; Ortiz, A. L.; Kaytakoglu, S.; Harrison, D. P., Hydrogen from methane in a single-step process. *Chemical Engineering Science* **1999,** 54, (15-16), 3543-3552.

(9) Akiti, T. T., Jr.; Constant, K. P.; Doraiswamy, L. K.; Wheelock, T. D., A Regenerable Calcium-Based Core-in-Shell Sorbent for Desulfurizing Hot Coal Gas. *Industrial & Engineering Chemistry Research* **2002,** 41, (3), 587-597.

(10) Akiti, T. T., Jr.; Constant, K. P.; Doraiswamy, L. K.; Wheelock, T. D., Development of an advanced calcium-based sorbent for desulfurizing hot coal gas. *Advances in Environmental Research* **2001,** 5, (1), 31-38.

(11) Akiti, T. T.; Constant, K. P.; Doraiswamy, L. K.; Wheelock, T. D., An improved core-in-shell sorbent for desulfurizing hot coal gas. *Advances in Environmental Research* **2002,** 6, (4), 419-428.

(12) Wheelock, T. D.; Akiti, T. T. Core-in-shell sorbent for hot coal gas desulfurization. Patent:2002103074, 2002.

(13) Satrio, J. A.; Shanks, B. H.; Wheelock, T. D., Development of a Novel Combined Catalyst and Sorbent for Hydrocarbon Reforming. *Industrial & Engineering Chemistry Research* **2005,** 44, (11), 3901-3911.

(14) Satrio, J. A.; Shanks, B. H.; Wheelock, T. D., A Combined Catalyst and Sorbent for Enhancing Hydrogen Production from Coal or Biomass. *Energy & Fuels* **2007,** 21, (1), 322-326.

(15) Wheelock, T. D.; Shanks, B. H. Catalyst and sorbent material for the production of hydrogen. Patent:7176159, 2007.

(16) Baker, E. H., CaO-CO2 system in the pressure range 1-300 atm. *Journal of the Chemical Society* **1962**, 464-70.

(17) Babushkin, V. I.; Matveyev, G. M.; Mchedlov-Petrossyan, O. P., *Thermodynamics of Silicates*. Fourth Edition ed.; Springer-Verlag Berlin Heidelberg: Berlin, 1985.

(18) Czuppon, T. A.; Knez, S. A.; Newsome, D. S., Hydrogen. In *Encyclopedia of Chemical Technology*, J. I. Kroschwitz, M. H.-G., Ed. John Wiley & Sons: New York, 1995; Vol. 13, pp 852-859.

(19) Cobden, P. D.; van Beurden, P.; Reijers, H. T. J.; Elzinga, G. D.; Kluiters, S. C. A.; Dijkstra, J. W.; Jansen, D.; van den Brink, R. W., Sorption-enhanced hydrogen production for pre-combustion CO2 capture: thermodynamic analysis and experimental results. *International Journal of Greenhouse Gas Control* **2007,** 1, (2), 170-179.

(20) Ding, Y.; Alpay, E., Adsorption-enhanced steam-methane reforming. *Chemical Engineering Science* **2000,** 55, (18), 3929-3940.

(21) Ding, Y.; Alpay, E., Equilibria and kinetics of CO2 adsorption on hydrotalcite adsorbent. *Chemical Engineering Science* **2000,** 55, (17), 3461-3474.

(22) Hufton, J. R.; Mayorga, S.; Sircar, S., Sorption-enhanced reaction process for hydrogen production. *AIChE Journal* **1999,** 45, (2), 248-256.

(23) Waldron, W. E.; Hufton, J. R.; Sircar, S., Production of hydrogen by cyclic sorption enhanced reaction process. *AIChE Journal* **2001,** 47, (6), 1477-1479.

(24) Ochoa-Fernandez, E.; Haugen, G.; Zhao, T.; Ronning, M.; Aartun, I.; Borresen, B.; Rytter, E.; Ronnekleiv, M.; Chen, D., Process design simulation of H2 production by sorption enhanced steam methane reforming: evaluation of potential CO2 acceptors. *Green Chemistry* **2007,** 9, (6), 654-662.

(25) Grasa, G. S.; Abanades, J. C., CO2 Capture Capacity of CaO in Long Series of Carbonation/Calcination Cycles. *Industrial & Engineering Chemistry Research* **2006,** 45, (26), 8846-8851.

(26) Abanades, J. C.; Rubin, E. S.; Anthony, E. J., Sorbent Cost and Performance in CO2 Capture Systems. *Industrial & Engineering Chemistry Research* **2004,** 43, (13), 3462-3466.

(27) Lu, H.; Reddy, E. P.; Smirniotis, P. G., Calcium Oxide Based Sorbents for Capture of Carbon Dioxide at High Temperatures. *Industrial & Engineering Chemistry Research* **2006,** 45, (11), 3944-3949.

(28) Bandi, A.; Specht, M.; Sichler, P.; Nicoloso, N. *In situ Gas Conditioning in Fuel Reforming for Hydrogen Generation*; Center for Solar Energy and Hydrogen Research, ZSW: Stuttgart, Germany.

(29) Barker, R., Reversibility of the reaction of calcium carbonate to give calcium oxide and carbon dioxide. *Journal of Applied Chemistry & Biotechnology* **1973,** 23, (10), 733-42.

(30) Silaban, A.; Harrison, D. P., High temperature capture of carbon dioxide: characteristics of the reversible reaction between CaO(s) and CO2(g). *Chemical Engineering Communications* **1995,** 137, 177-90.

(31) Abanades, J. C.; Alvarez, D., Conversion Limits in the Reaction of CO2 with Lime. *Energy & Fuels* **2003,** 17, (2), 308-315.

(32) Alvarez, D.; Abanades, J. C., Pore-Size and Shape Effects on the Recarbonation Performance of Calcium Oxide Submitted to Repeated Calcination/Recarbonation Cycles. *Energy & Fuels* **2005,** 19, (1), 270-278.

(33) Han, C.; Harrison, D. P., Simultaneous shift reaction and carbon dioxide separation for the direct production of hydrogen. *Chemical Engineering Science* **1994,** 49, (24B), 5875-83.

(34) Readman, J. E.; Blom, R., The use of in situ powder X-ray diffraction in the investigation of dolomite as a potential reversible high-temperature CO2 sorbent. *Physical Chemistry Chemical Physics* **2005,** 7, (6), 1214-1219.

(35) Silaban, A.; Narcida, M.; Harrison, D. P., Characteristics of the reversible reaction between CO2(g) and calcined dolomite. *Chemical Engineering Communications* **1996,** 146, 149-162.

(36) Harrison, D. P.; Peng, Z., Low carbon monoxide hydrogen by sorption-enhanced reaction. *International Journal of Chemical Reactor Engineering* **2003,** 1, No pp. given.

(37) Yi, K. B.; Harrison, D. P., Low-Pressure Sorption-Enhanced Hydrogen Production. *Industrial & Engineering Chemistry Research* **2005,** 44, (6), 1665-1669.

(38) M. Specht, A. B., F. Baumgart, T. Moellenstedt, O. Textor, Enhanced Reforming Reaction for Hydrogen Production from Carbonaceous Feestock. In *Hydrogen Energy Progress XIII*, Z. Q. Mao, T. N. V., Ed. 2000; p 1203.

(39) Lin, S.-Y.; Suzuki, Y.; Hatano, H.; Harada, M., Hydrogen Production from Hydrocarbon by Integration of Water-Carbon Reaction and Carbon Dioxide Removal (HyPr-RING Method). *Energy & Fuels* **2001,** 15, (2), 339-343.

(40) Kuramoto, K.; Shibano, S.; Fujimoto, S.; Kimura, T.; Suzuki, Y.; Hatano, H.; Lin, S.-Y.; Harada, M.; Morishita, K.; Takarada, T., Deactivation of Ca-Based Sorbents by Coal-Derived Minerals during Multicycle CO2 Sorption under Elevated Pressure and Temperature. *Industrial & Engineering Chemistry Research* **2003,** 42, (15), 3566-3570.

(41) Johnsen, K.; Ryu, H. J.; Grace, J. R.; Lim, C. J., Sorption-enhanced steam reforming of methane in a fluidized bed reactor with dolomite as CO2-acceptor. *Chemical Engineering Science* **2006,** 61, (4), 1195-1202.

(42) Hasler, D. J. L.; Doraiswamy, L. K.; Wheelock, T. D., A Plausible Model for the Sulfidation of a Calcium-Based Core-in-Shell Sorbent. *Industrial & Engineering Chemistry Research* **2003,** 42, (12), 2644-2653.

(43) Hasler, D. J.; Wheelock, T. D.; Doraiswamy, L. K.; Constant, K. P., Physical Properties and Composition Effects on the Reactivity of Calcium-Based Sulfur Sorbents. *Industrial & Engineering Chemistry Research* **2007,** 46, (18), 5913-5921.

Chapter 2. Development of a CaO-based Sorbent with Improved Cyclic Stability

A paper published in *Industrial & Engineering Chemistry Research* 2008, 47, (20), 7841-7848[a]

Karl O. Albrecht,[b] Kyle S. Wagenbach,[b] Justinus A. Satrio,[c] Brent H. Shanks,[b] and Thomas D. Wheelock[b,*]

Abstract

The carbonation of CaO is an attractive method for removing CO_2 from hot gas mixtures. However, regeneration and reuse of a CaO-based sorbent causes a gradual decline in absorption capacity, which ultimately limits the life of the material. Various methods have been proposed for increasing the life cycle performance of a CaO-based sorbent. Two of these methods were selected for further investigation. One method incorporates an "inert" material in the sorbent, while a second method stabilizes the sorbent through controlled sintering. Promising results were achieved with both methods when they were applied separately to a sorbent derived from a natural limestone. In one case MgO was finely dispersed within the sorbent where it served as an "inert" material in the sense that it did not absorb CO_2. A concentration of approximately 20 wt % appeared to be nearly optimal. In a second case the sorbent was stabilized by calcining the material at 1100°C for 5 hr. Although neither method produced a completely stable material, the stability of the sorbents was improved sufficiently so that by the end of a 1200 cycle test the absorption capacity of

[b]Dept. of Chemical and Biological Engineering, 2114 Sweeney Hall, Iowa State University, Ames, IA 50011

[c]Center for Sustainable Environmental Technologies, 0411 Marston Hall, Iowa State University, Ames, IA 50011

*Corresponding Author: wheel@iastate.edu

either of the treated sorbents was 45% greater than that of an untreated sorbent and their rate of decline was very small.

Keywords: Limestone, Dolomite, Absorption capacity, Magnesium Oxide, Lanthanum Oxide, Sorbent, Calcium oxide, Carbon dioxide

Introduction

The carbonation of CaO is a reversible reaction with several potential applications.

$$CaO + CO_2 \leftrightarrow CaCO_3 \qquad \Delta H_{25^\circ C} = -175 \text{ kJ/mol} \qquad (1)$$

Reaction 1 may be used in the future to absorb CO_2 from hot process streams for subsequent disposal in order to alleviate global climate change.[1, 2] CaO has also been demonstrated for selective, in-situ CO_2 separation from other reaction products produced in a combined methane reforming/water-gas shift reactor resulting in improved feedstock conversion.[3-9] Energy storage systems based on reaction 1 have also been investigated because of the high exothermicity of the carbonation reaction.[10-12] The major challenge associated with some practical applications of reaction 1 is a lack of total reversibility. At any temperature above the equilibrium decomposition temperature, $CaCO_3$ will completely decompose to form CaO. However, upon recarbonation, the reaction will not proceed to completion within a reasonable time. Therefore, upon subsequent regeneration and carbonation less CO_2 is absorbed and the fraction of CaO recarbonated declines from cycle to cycle.[13, 14] When it is impractical to continuously purge and replenish the CaO, such as when it is combined with a catalyst for steam reforming methane, the absorption capacity of the CaO must be maintained over an industrially relevant lifetime.[8, 9] Consequently, there is need for a CaO-based sorbent such that its absorption capacity declines only very gradually as it is loaded and regenerated.

One possibility for enhancing the cyclic stability of CaO-based sorbents is through the incorporation of inert materials. MgO has been proposed for this application since it is inert under some conditions where CaO may be used for absorbing CO_2. Dolomite, a mineral which nominally has a 1:1 ratio of $MgCO_3$ to $CaCO_3$, with the Ca and Mg ions interspersed in layers in the naturally occurring crystal, decomposes into separate MgO and CaO phases.[15] The CaO derived from dolomite was found to be more stable than CaO derived from limestone when subjected repeatedly to CO_2 absorption and regeneration.[16, 18] Huntite, which has a 1:3 molar ratio of $CaCO_3$ to $MgCO_3$, provided CaO with even greater stability.[17] However, the presence of a large amount of inert material in an industrial sorbent is undesirable since it would increase capital and operating costs. Therefore, in the present investigation consideration was given to the use of smaller concentrations of MgO applied by a doping method.

Other materials have been added to CaO to improve its stability for repeated CO_2 absorption/desorption. Salvador et al.[18] subjected limestone impregnated with 0.5 wt % NaCl to thermogravimetric analysis (TGA) using a temperature of 700°C for absorption and 850°C for regeneration. The CaO conversion achieved with a NaCl-doped sample was lower than the conversion achieved with an undoped sample during the first CO_2 absorption cycle. However, after 14 carbonation/calcination cycles, the conversion achieved with a NaCl-doped sample was 40% compared to a CaO conversion of only 30% achieved by an undoped sample after 11 cycles. Aihara et al.[10] doped CaO with inert $CaTiO_3$ either by using an alkoxide method or by physically mixing $CaTiO_3$ with $CaCO_3$. The doped CaO was then tested by employing thermogravimetric analysis at 750°C. The presence of $CaTiO_3$ was reported to enhance the cyclic stability of the CaO-based sorbent over 10 cycles when

compared to CaO without $CaTiO_3$ present. Li et al.[19] investigated the effect of adding an inert phase consisting of $Ca_{12}Al_{14}O_{33}$ to CaO. The $Ca_{12}Al_{14}O_{33}$ phase was created by adding $Al(NO_3)_3 \cdot 9H_2O$ to the sorbent and then calcining the material. Sorbents with the $Ca_{12}Al_{14}O_{33}$ phase present exhibited enhanced stability over 13 cycles. Later work showed that a 25/75 weight ratio of $Ca_{12}Al_{14}O_{33}$ to CaO followed by calcination at 900°C for 1.5 hr was optimal for preparing this sorbent.[20] TGA tests performed with carbonation at 650°C and calcination at 850°C showed that after 50 cycles the sorbent was still capable of achieving a CaO conversion of 65%.

Some additives have been shown to be ineffective or even detrimental to the stability of CaO. Lu et al.[21] found no enhancement in CaO stability by the addition of 10 to 50 wt % silica when the sorbent was tested at 700°C. The material was prepared by adding silica to a solution of calcium acetate followed by evaporation at 70°C to precipitate the salt and then calcination at 750°C. Another investigation showed that the addition of $SrCO_3$ to limestone had a detrimental effect regardless of whether the dry powders were mixed together or co-precipitated from solution.[22] TGA testing showed after 8 cycles a CaO conversion of 44% was achieved with the sorbent prepared from pure limestone, whereas a conversion of only 17 to 20% was achieved with the sorbent containing strontium. Scanning electron micrographs of the samples with strontium present showed increased sintering and rounding of the particles after eight cycles.

Enhancing the ability of CaO to absorb CO_2 over many cycles can also be achieved through modification of the pore structure.[24] It is well known that subjecting a microporous material to sintering conditions will coalesce smaller pores into larger pores. Although this will reduce the pore surface area, it can also improve the stability of the material, and it can

make the central core of a particle more accessible to the CO_2. Without such treatment the micropores near the surface of a sorbent particle can become plugged by the reaction product before the CO_2 reaches the core. The process is exacerbated by the increase in molar volume which accompanies the conversion of CaO into $CaCO_3$. With the proper balance of micropores and mesopores, more of a sorbent particle should be capable of participating in the absorption process.

Altered pore structures of CaO sorbents have been previously reported. In CO_2 absorption tests conducted by Silaban, et al.,[16] higher conversions of CaO in dolomitic lime were attributed in part to excess pore volume created by the initial decomposition of the $MgCO_3$. Hughes et al.[23] increased the pore volume and pore surface area of two different limestone samples by a process of steam hydration conducted at 150°C and 475 kPa. When the hydrated limestones were subjected to a cyclic absorption test conducted at 750°C, a CaO conversion of 52% was achieved after 20 cycles. Gupta and Fan[1] reported precipitating $CaCO_3$ by reacting Ca^{2+} ions with CO_3^{2-} ions in water to create a sorbent with pores predominately in the mesoporous region of 5-20 nm. When the CaO derived from the precipitated calcium carbonate was subjected to an absorption test at 700°C, a CaO conversion of 95% was obtained after 2 cycles. The authors claimed that the larger pores that formed were less susceptible to pore plugging than the micropores produced by calcining limestone or dolomite.

Information about the life of a CaO-based sorbent material is difficult to evaluate on the basis of a few initial absorption and regeneration cycles. Grasa and Abanades[24] investigated sorbents derived from different sources of limestone that were then carbonated and regenerated at different process conditions. They discovered that the conversion of CaO

during the first 10-25 cycles varied widely depending on the limestone source, regeneration temperature, and partial pressure of CO_2. However, sorbent testing for more than 100 cycles revealed that regardless of process conditions or limestone type, the absorption capacity of all the samples approached 7.5-8.0 wt %, and the capacity remained constant for up to 500 cycles. For some industrial applications, sorbent capacity must remain in a useful range for thousands of absorption and regeneration cycles. Sorbents with a high initial absorption capacity acquired by a costly treatment process would be of little use if the benefit of the treatment was lost after a few hundred cycles. Many CaO-based sorbents reported in the literature are tested over only tens of cycles, which may not be sufficient to determine whether the sorbent will have a useful life.

Although many methods have been proposed for extending the life cycle performance of a CaO-based sorbent, only a few seem well suited for an economical, industrial process. Among these methods, two were selected for further study. One method makes use of an inert material, which is incorporated in the sorbent while a second method stabilizes the sorbent through controlled sintering. To demonstrate the first method, MgO was selected as an inert material, since it would not absorb CO_2 under the conditions being considered for applying the sorbent. Numerous sorbent samples were prepared subsequently by impregnating ultrafine size limestone particles with $Mg(NO_3)_2$ in various concentrations followed by calcination to decompose the nitrate. To demonstrate the second method samples of the ultrafine size limestone were calcined under conditions that became increasingly severe resulting in progressively greater stability. The prepared sorbents were then subjected to a life cycle performance test in which the material was repeatedly loaded with CO_2 and regenerated under carefully controlled conditions.

Experimental Methods and Materials

Materials

Different sources of CaO were used in this study. Limestone was obtained from two sources. Columbia River Carbonates in Washington State provided Microna 3 limestone with a mean particle size of 3.2 μm and with a $CaCO_3$ content greater than 97 wt % according to the producer. Coarser limestone with 97 wt % $CaCO_3$ according to the producer was obtained from the Ames, Iowa, quarry of Martin Marietta Aggregates. This limestone was ground and screened to a size of -212/+63 μm.

Dolomitic limestone, or dolomite, was received from Graymont Dolime (OH), Inc. in Ohio. The dolomite was also ground and screened to a size of -212/+63 □m. Fisher Scientific was the source of the calcium acetate, calcium carbonate and calcium hydroxide used in sorbent studies. These materials were reagent grade and were used as received.

Lanthanum nitrate [$La(NO_3)_3 \cdot xH_2O$] and magnesium nitrate [$Mg(NO_3)_2 \cdot 6H_2O$] were purchased from Sigma Aldrich. The magnesium nitrate was reagent grade. Due to the indeterminate nature of the hydrate in the lanthanum nitrate, a stock solution was prepared. The molarity of the stock solution was then determined gravimetrically by heating samples of a known volume of the stock solution in air to at least 900°C for 12 hr or more to convert the lanthanum nitrate to lanthanum oxide, La_2O_3, which could be weighed.

Preparation Methods

Most sorbents were calcined before undergoing cyclic tests of absorption and regeneration unless otherwise noted as “uncalcined” in which case the material was tested unaltered. For the initial calcination of a sorbent material a thin layer consisting of about 6 g material was calcined in a quartz boat in a horizontal tube oven. Calcination at 900°C began

with a 2 hr temperature ramp from room temperature to 900°C followed by an isothermal step at 900°C for the appropriate time. The calcined material was then cooled to room temperature using a 2 hr temperature ramp. For materials calcined at 1100°C, a 3 hr ramp from room temperature was employed followed by an isothermal step for the appropriate time at 1100°C. The calcined material was then cooled to room temperature using a 2 hr ramp. All initial calcinations were performed under flowing air.

For some studies, magnesium nitrate or lanthanum nitrate was added to Microna 3 limestone in an amount designed to provide an appropriate concentration of either oxide in the calcined sorbent. Both limestones were conservatively assumed to contain 97 wt % $CaCO_3$. The nitrate salt was dissolved in THF and an appropriate amount of this solution was added to the Microna 3 to form a thick paste when mixed in a mortar. After mixing, the THF was evaporated, and the resulting powder was dried in the mortar at 120°C for at least 5 hr. The powder was then reground in the mortar and calcined at the appropriate temperatures using the ramping procedures described above. Some sorbent tests were performed using Microna 3 limestone, which had been calcined prior to adding one of the nitrates. The procedure was the same as the preceding one except that the Microna 3 limestone was calcined in flowing air at 750°C for 5 hr before adding the nitrate. All samples were stored in a desiccator for the time between preparation and characterization.

Characterization Methods

The absorption capacity and the effect of multiple absorption and desorption cycles on the life of the sorbent were determined with a thermogravimetric analysis (TGA) system which utilized a Cahn 2000 electrobalance. The sorbent was tested as a powder contained in

a small ceramic, cylindrical cup, which had a diameter of 6 mm and height of 6 mm. The cup was half filled with sorbent material, which typically provided a sample mass of 20-40 mg. However, the mass would vary depending on the density of the material. For calcium acetate only 11.2 mg would half fill the cup. For testing the sample was suspended in a vertical quartz tubular reactor having an inside diameter of 25 mm and was subjected to a series of absorption and desorption cycles conducted isothermally at 750°C and at 1.0 atm. During an absorption step a gas stream composed of 25 vol % CO_2 and 75 vol % N_2 was supplied to the reactor at a rate of 3.72 mmol/min for 20 min. This was followed by a desorption step in which only N_2 was supplied for 30 min at a flow rate of 2.79 mmol/min. The two steps constituted a complete cycle. While these conditions did not produce the high concentration of CO_2 required for an industrial application, they were well suited for experimentally conducting a large number of absorption and regeneration cycles because they did not require varying the temperature throughout each cycle which would have been very time consuming overall.

Scanning electron microscope (SEM) images of the sorbent were collected by using a JEOL 840A SEM. Images were collected using an accelerating voltage of 20 kV and secondary electron imaging. The fresh sorbent samples were imaged after initial calcination at 900°C for 3 hr and tested sorbent samples were imaged following recarbonation of the samples after the 30^{th} cycle.

The pore volume distribution of selected samples of sorbent material was determined with a Micromeritics ASAP 2020 instrument. The BJH method of desorption analysis was employed in which nitrogen was adsorbed at -196°C. This method required a larger sample of material than could be treated with the TGA system. Therefore, samples of sorbent

material were treated in a heated, horizontal tubular reactor that could accommodate a quartz boat holding about 8 g of material. The samples were treated isothermally at 750°C by a cyclic process consisting of a 20 min. absorption step followed by a 30 min. desorption step. A gas mixture consisting of 25 vol % CO_2 and 75 vol % N_2 was supplied at a rate of 9.24 mmol/min for absorption while only nitrogen was supplied at a rate of 6.93 mmol/min for desorption. The process was interrupted periodically to remove a 0.5 g sample of material for analysis. This was timed so that the sample was collected 5 min. before the end of a desorption step.

Experimental Results and Discussion

Calcium oxide can be prepared from various precursors such as limestone and dolomite. An alternative precursor which has been shown to produce somewhat more stable CaO is calcium acetate.[21] These and several other precursors were utilized to prepare sorbents for evaluation in the present study. After each material had been calcined at 900°C for 3 hr, it was subjected to a multicycle test of absorption and regeneration conducted at 750°C. The results of a preliminary series of tests are presented in Figure 1. In this and subsequent figures the CO_2 apparent absorption capacity of the calcined material is indicated. Figure 1 shows that the absorption capacity of each material decreased with usage. The theoretical maximum absorption capacity of the limestone with 97 wt % $CaCO_3$ and 3 wt % inert material is 16.9 mmol CO_2/g calcined sorbent. Although CaO derived from calcium acetate displayed the highest absorption capacity, the material was not completely stable.

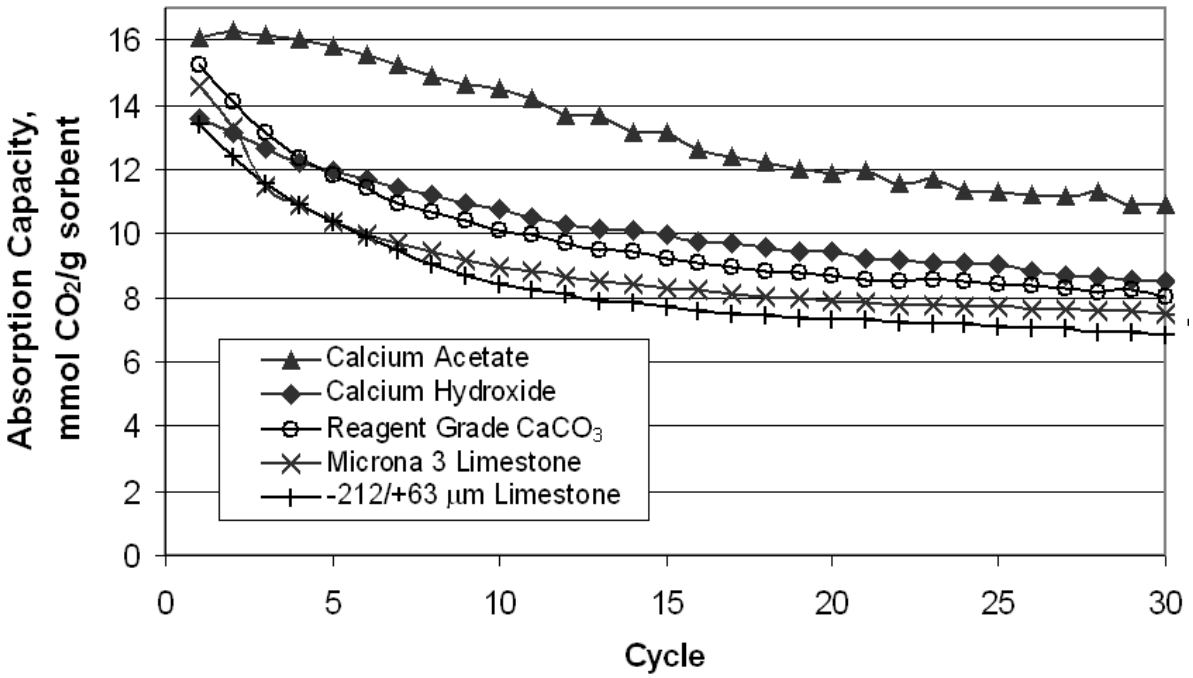

Figure 1. The apparent absorption capacity of CaO prepared by calcining various source materials at 900°C for 3 hr.

Because of their higher purity, reagent grade calcium hydroxide and calcium carbonate provided sorbents with a slightly greater absorption capacity than those provided by either limestone. However, the reagent grade materials were not chosen for further investigation because of their higher cost.

Since Bandi et al.[17] had shown previously that the absorption capacity of CaO was more stable when derived from dolomite or huntite than from limestone, the possibility of stabilizing CaO with smaller concentrations of MgO was investigated by impregnating Microna 3 limestone with $Mg(NO_3)_2$ followed by calcination at 900°C for 3 hr to decompose the nitrate. Sorbents with different levels of MgO were then subjected to 30-cycle tests of absorption and regeneration. The results presented in Figure 2a indicate the variation in absorption capacity of each material identified by the mass ratio of MgO to CaO.

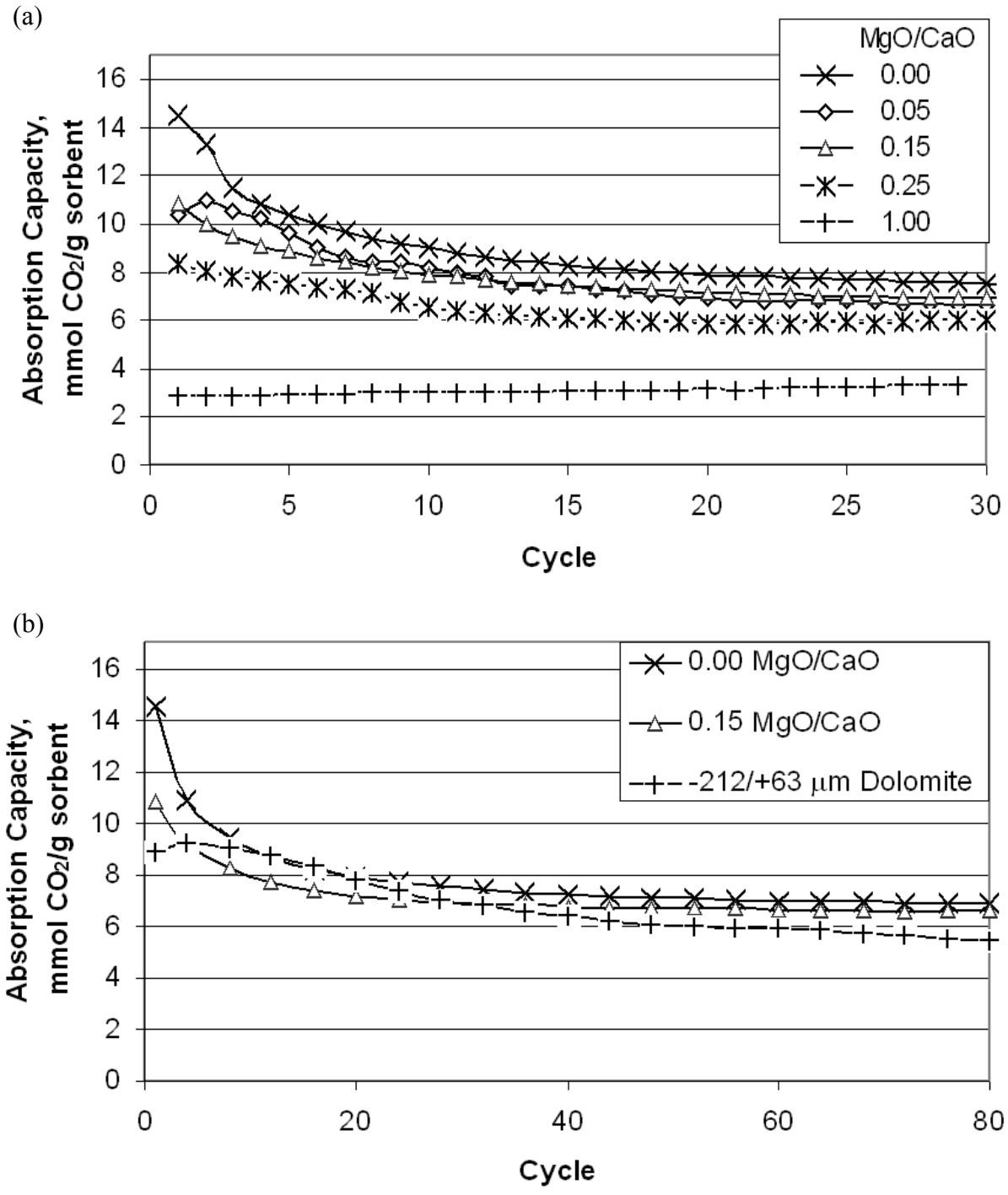

Figure 2. Effect of MgO expressed as g MgO/g CaO on the apparent absorption characteristics of CaO derived from Microna 3 limestone or dolomite. All samples were initially calcined at 900°C for 3 hr before testing. (a) Effect of different MgO loading levels; (b) Effect of extended life cycle testing.

The indicated values of the mass ratio of MgO to CaO encompass that of dolomitic lime (0.72 g MgO/g CaO). It is apparent that the initial absorption capacity decreased as the MgO content increased, but at the same time the sorbent became more stable so that its capacity decreased less with usage. The decrease in absorption capacity was largely due to the decrease in CaO content of a given sample as the MgO content was increased. The absorption capacity may also have declined because MgO covered the CaO particles. Of special interest is the increase in absorption capacity with usage of the sorbent with 1.0 g MgO/g CaO. Such an increase is not well understood although it was likely due to rearrangement of the pore structure or crystal structure. Another interesting feature suggested by Figure 2a was the apparent activation of the sorbent with 0.05 g MgO/g CaO between the first and second cycles. This phenomenon was not observed with any of the other samples doped with MgO.

A longer life cycle test was conducted with several samples, and the results are presented in Figure 2b. Although the initial absorption capacity of the sorbent without MgO present was greater than that of the sorbent with 0.15g MgO/g CaO, both materials absorbed about the same amount of CO_2 at the end of 80 cycles. This result indicates that more of the CaO in the sorbent containing MgO was available for absorption of CO_2. The dolomitic lime absorbed the same amount of CO_2 as the Microna 3 lime between 10 and 20 cycles even though the dolomitic lime was equivalent to a sorbent with 0.72 g MgO/g CaO. Thus, more of the CaO in dolomitic lime was available for reaction. Others have attributed such behavior to the increased porosity of the dolomitic lime formed upon calcination.[16]

Another material considered as a potential stabilizing agent for the CaO sorbent was La_2O_3. This material had been shown previously to stabilize alumina when alumina had been

used as a catalyst support.[25, 26] However, unlike MgO, La_2O_3 cannot be considered completely inert for the conditions used in the present investigation. Shirsat et al.[27] reported that lanthanum dioxycarbonate, $La_2O_2CO_3$, is a stable intermediate in the decomposition of lanthanum carbonate, $La(CO_3)_3$. $La_2O_2CO_3$ decomposes above 720°C via the reaction:

$$La_2O_2CO_3 \leftrightarrow La_2O_3 + CO_2 \quad (2)$$

However, the equilibrium partial pressure of CO_2 for reaction 2 at 750°C is 0.06 atm. Therefore, the carbonation of La_2O_3 appeared likely. To investigate this possibility, a sorbent derived from Microna 3 limestone was impregnated with lanthanum to provide a mixture with 0.10 g La_2O_3/g CaO. After this material was subjected to a 30-cycle test of CO_2 absorption and regeneration in the TGA, it was analyzed by x-ray diffraction and was found to contain a small amount of crystalline $La_2O_2CO_3$. In order to determine the amount of CO_2 that could be absorbed by La_2O_3, a pure La_2O_3 sample was prepared by calcining $La(NO_3)_3$ at 900°C for 3 hr, and then it was subjected to a four-cycle absorption/regeneration test at 750°C. It was found that after four cycles less than 0.1 mmol CO_2/g sorbent was being absorbed. Therefore, La_2O_3 was not absorbing a large amount of CO_2, but was also not completely inert.

To see what effect La_2O_3 would have on the stability of the sorbent, samples were prepared with different ratios of La_2O_3 to CaO, based on Microna 3 limestone. After the samples had been calcined for 3 hr at 900°C, some were treated to 30 cycles of absorption and regeneration at 750°C. The results presented in Figure 3a show that the samples containing small amounts of La_2O_3 had a higher absorption capacity through 30 cycles than the sample of untreated limestone.

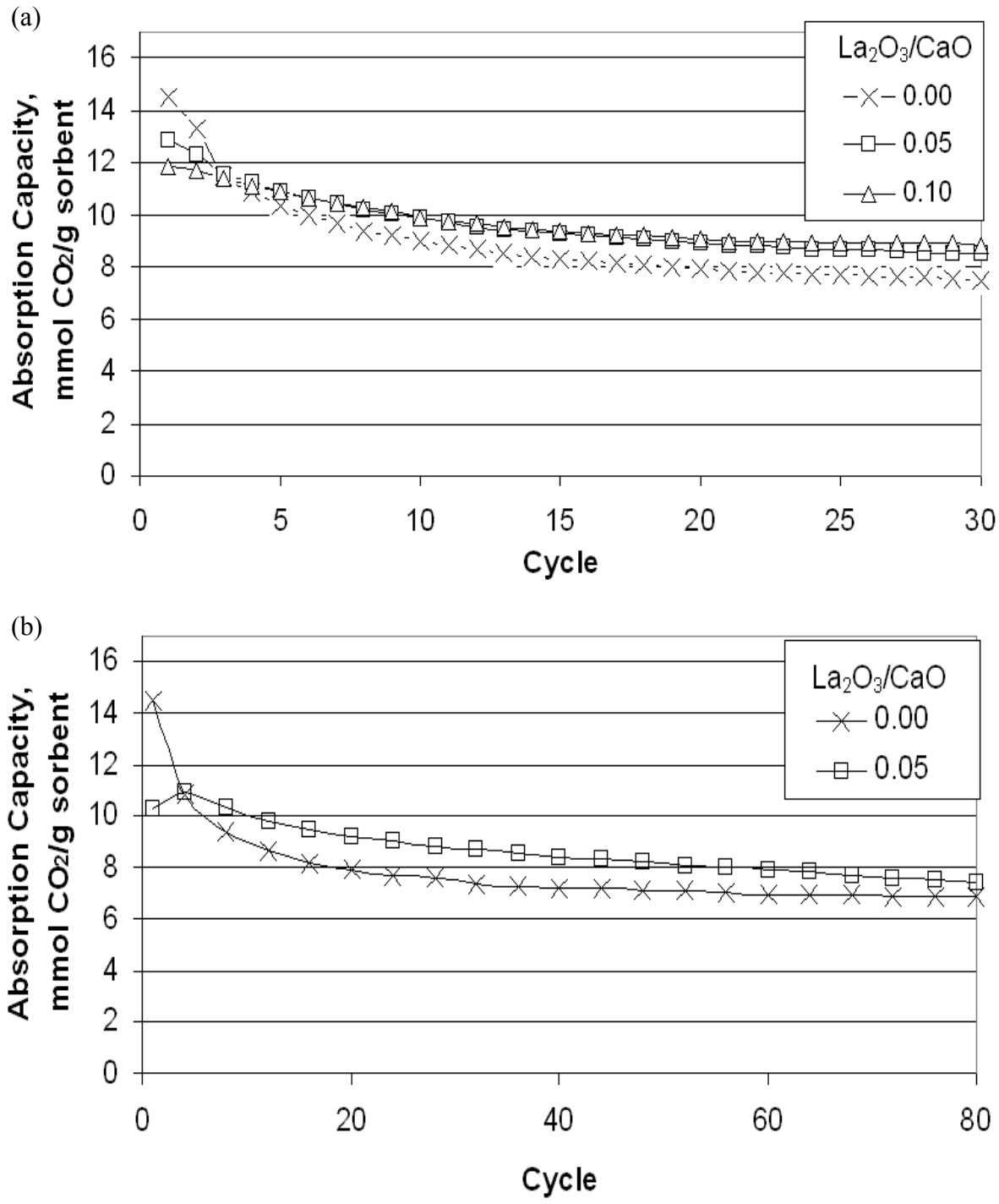

Figure 3. Effect of La_2O_3 expressed as g La_2O_3/g CaO on the apparent absorption characteristics of CaO derived from Microna 3 limestone. The samples were initially calcined at 900°C for 3 hr before testing. (a) Effect of different La_2O_3 loading levels; (b) Effect of extended life cycle testing.

On the other hand, different levels of La_2O_3 had little effect. Extending the sorbent performance to 80 cycles produced the results shown in Figure 3b.It can be seen that as the number of cycles was extended beyond 30, the absorption capacity advantage of the sorbent with La_2O_3 gradually faded and almost disappeared entirely after 80 cycles. Consequently, this is an excellent example of the need for extended testing of CaO sorbents. While it could reasonably be assumed from Figure 3a that the addition of lanthanum is indeed beneficial, further testing showed that the benefit gradually disappeared after many more cycles.

An alternative method of preparing the sorbents with added MgO or La_2O_3 was also investigated. Microna 3 limestone with little initial porosity was calcined at 750°C for 5 hr in air before adding the nitrates. This increased the porosity of the sorbent and presumably allowed more of the dissolved nitrates to penetrate the particles. The nitrate-impregnated samples were subsequently calcined at 900°C for 3 hr and then tested, which produced the results shown in Figure 4. A comparison of the results in Figure 4 with results presented in Figures 2 and 3 shows that the initial absorption capacity of the sorbents produced by the alternative method was less than that produced before. However, after 80 cycles the absorption capacities of the sorbents prepared by the alternative method were not significantly different from those prepared by the first method. On the other hand, the sorbents prepared by the alternative method were more stable, at least for 30 cycles.

The purpose of adding MgO to the Microna 3 limestone was to improve the stability of the sorbent by inhibiting sintering. SEM images were obtained of Mg-free samples and of samples with a 0.05 g MgO/g CaO both before and after being subjected to a 30-cycle test. The samples were calcined initially at 900°C for 3 hr. Figure 5a is an image of the calcined limestone before testing, while Figure 5b is an image after testing. Although Figure 5a

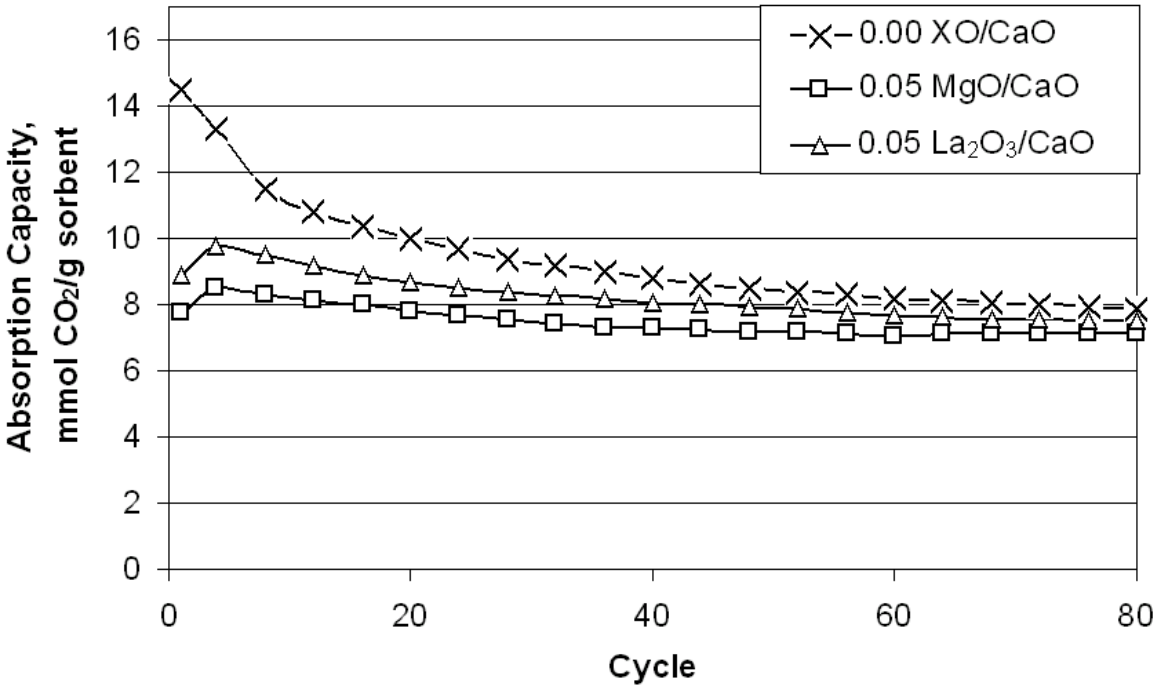

Figure 4. A comparison of the effects of MgO and La_2O_3 expressed as g XO/g CaO on the apparent absorption characteristics of CaO derived from Microna 3 limestone. The limestone was calcined at 750°C for 5 hr before adding $Mg(NO_3)_2$ or $La(NO_3)_3$. The mixture was then calcined at 900°C for 3 hr.

shows that the pure limestone experienced some sintering during initial calcination, it experienced more severe sintering during the 30 cycle test (Figure 5b). By comparison, the samples with MgO may have undergone slightly more sintering during initial calcination (Figure 5c) but much less sintering during the 30-cycle test (Figure 5d). Overall, it appeared that a small amount of MgO was beneficial.

The effects of initial calcination conditions on Microna 3 limestone prior to cyclic testing were also studied, and the results are shown in Figure 6. It was hypothesized that increasing the severity of the initial calcination conditions would produce larger pores in the mesoporous region, which would then allow CO_2 to penetrate deeper into a CaO particle because of reduced mass transfer limitations. However, this could also reduce the surface

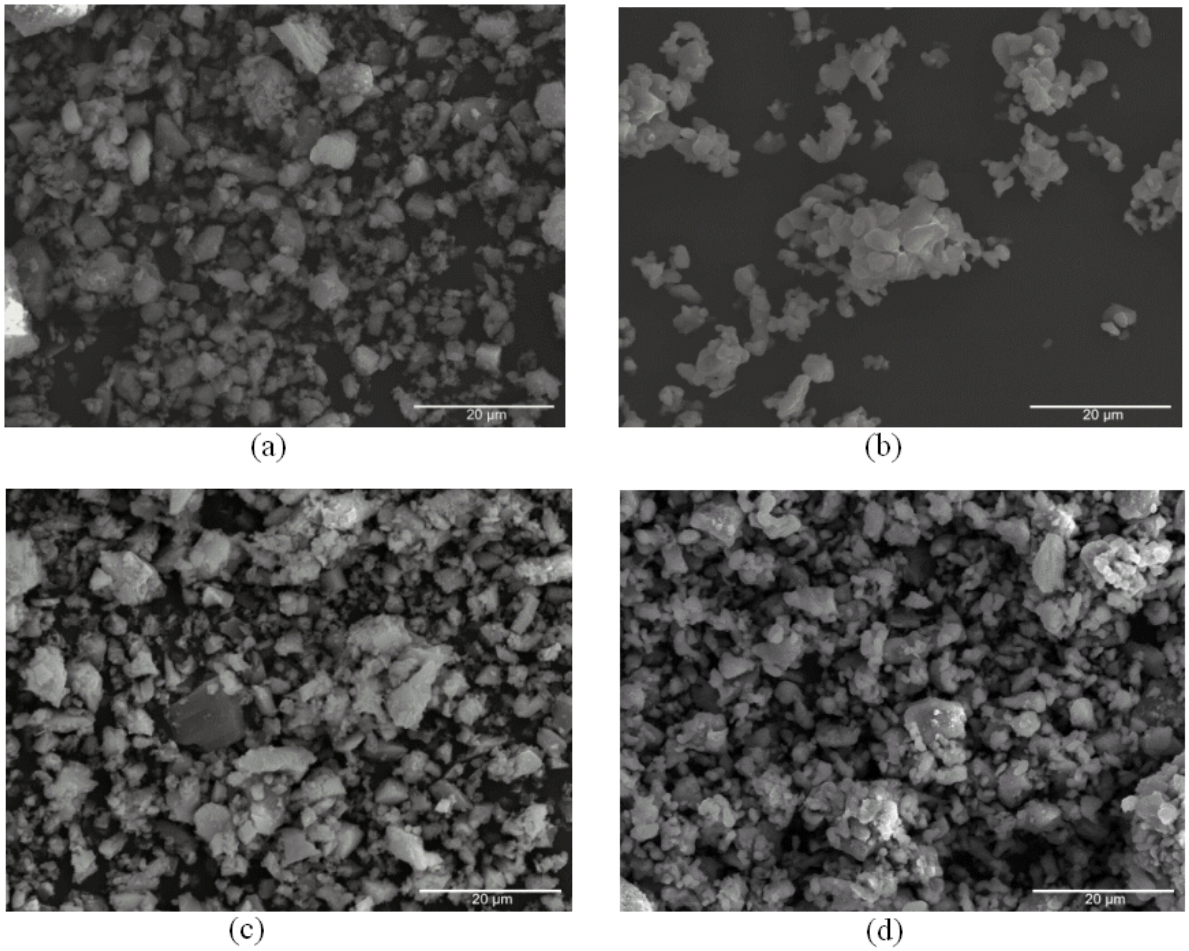

Figure 5. SEM micrographs of Microna 3 limestone samples after initial calcination at 900°C for 3 hr and after 30 cycles of CO2 absorption and desorption at 750°C. (a) After initial calcination without MgO; (b) After 30 cycles without MgO; (c) After initial calcination with 0.05 g MgO/g CaO; (d) After 30 cycles with 0.05 g MgO/g CaO.

area available for sorption and reduce the absorption capacity. On the other hand, it could also result in a more stable material. Figure 6 shows that calcining the Microna 3 limestone at 1100°C for 2 hr produced a somewhat more stable sorbent than that produced by calcining the material at 900°C for 3 hr. Increasing the calcination time to 5 hr while maintaining the 1100°C temperature produced a more stable sorbent but with less capacity. Also, the sample that was calcined at 1100°C for 5 hr exhibited the interesting property of becoming slightly

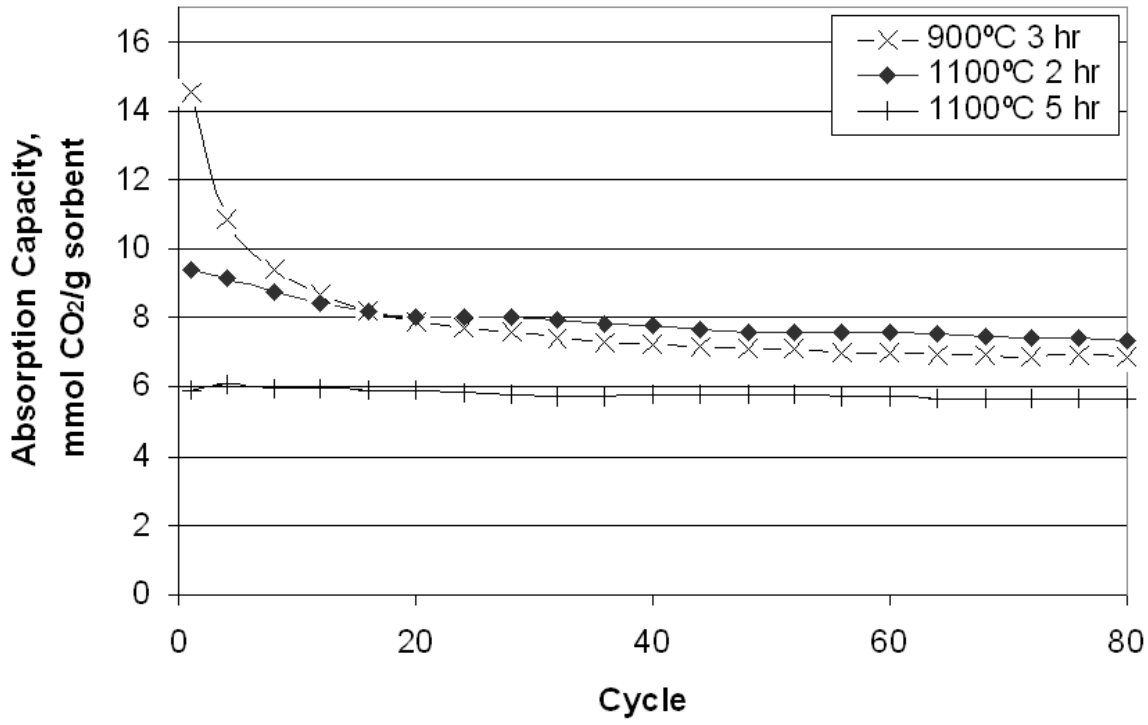

Figure 6. Effect of initial calcination conditions on the apparent absorption capacity of CaO derived from Microna 3 limestone.

more active between the first and second cycles. This increase in activity may have been due to the development of new pores and cracks during the initial cycle of carbonation and regeneration of the CaO.

To provide greater insight into the effects of initial calcination conditions and repeated absorption and regeneration on the physical properties of the sorbent, samples of Microna 3 limestone were calcined initially either at 900°C for 3 hr or 1100°C for 5 hr and then subjected to a 30-cycle test of absorption and regeneration at 750°C. The pore volume distribution of the samples was then determined after the initial calcination and after the 30-cycle test. Figure 7 shows on a logarithmic scale the cumulative pore volume of the samples that had received the different treatments. The sample calcined initially at 900°C for 3 hr

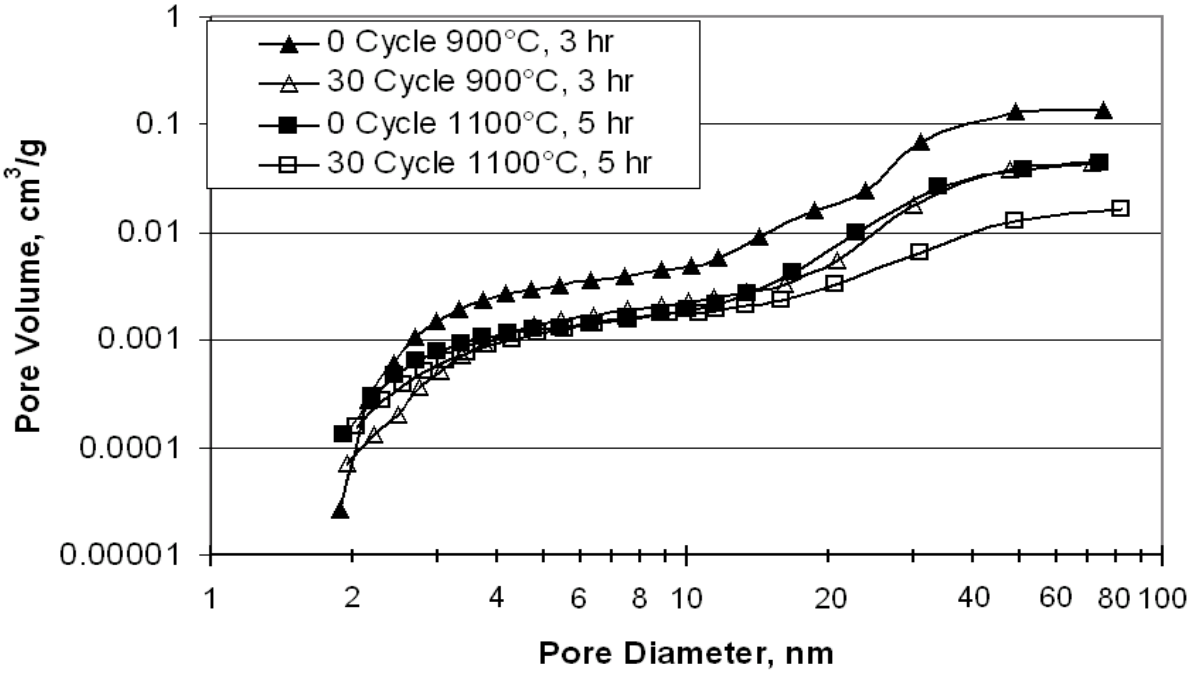

Figure 7. Cumulative pore volume distribution of Microna 3 limestone after it had been subjected to various treatments.

had the largest cumulative pore volume whereas the sample that had been calcined initially at 1100°C for 5 hr had less cumulative pore volume. Therefore, the more severe calcination conditions reduced both the pore volume and absorption capacity of the material, which was not desirable. However, these conditions did produce a more stable material. This increase in stability was not only reflected by the cyclic results in Figure 6 but also by the porosity results which are reported in Figure 7. The results of this test showed that after 30 absorption cycles the cumulative pore volume of the pores smaller than 10 nm was reduced only 6% for the sorbent calcined at 1100°C for 5 hr compared to a reduction of 54% for the sorbent calcined at 900°C for 3 hr.

Since it appeared that the life cycle performance of a sorbent could be better determined by extended testing, several sorbent samples were subjected to a 200 cycle test

and three samples were even subjected to a test of 1100 cycles or more. The results are presented in Figures 8 and 9, respectively. In Figure 8, it can be seen that pre-calcining the sorbent had some effect initially, as did the calcination temperature. However, after 50-60 cycles there was little difference in the absorption capacity. It is also apparent that while a small amount of La_2O_3 was beneficial initially, any benefit disappeared after 120-130 cycles. These results again bring out the importance of extended life cycle testing of any proposed sorbent.

Further confirmation of this observation are provided by the results of the most prolonged testing presented in Figure 9. Two of the sorbents tested were based on Microna 3 limestone initially calcined either at 900°C for 3 hr or 1100°C for 5 hr. The third sorbent was composed of Microna 3 impregnated with $Mg(NO_3)_2$ to provide a material with 0.25 g MgO/g CaO after calcining at 900°C for 3 hr. The sorbents calcined at 900°C for 3 hr were tested for 1250 cycles while the sample calcined at 1100°C for 5 hr was tested for 1124 cycles. The results presented in Figure 9 indicate that the absorption capacity of the modified sorbents started with absorption capacities lower than that of the Microna 3 sample calcined at 900°C for 3 hr. However, as the number of cycles increased, the modified sorbents proved to be more stable than the Microna 3 sorbent calcined at 900°C for 3 hr. Consequently the absorption capacity of this material was surpassed by that of the material calcined at 1100°C for 5 hr after 500 cycles and by that of the sorbent with 0.25 g MgO/g CaO after 700 cycles. Whether a truly stable state had been achieved with the two modified sorbents could only have been determined by extending the test even further. Nevertheless, the results indicate that the modified sorbents were likely to retain their absorption capacity longer than the Microna 3 sample calcined at 900°C for 3 hr.

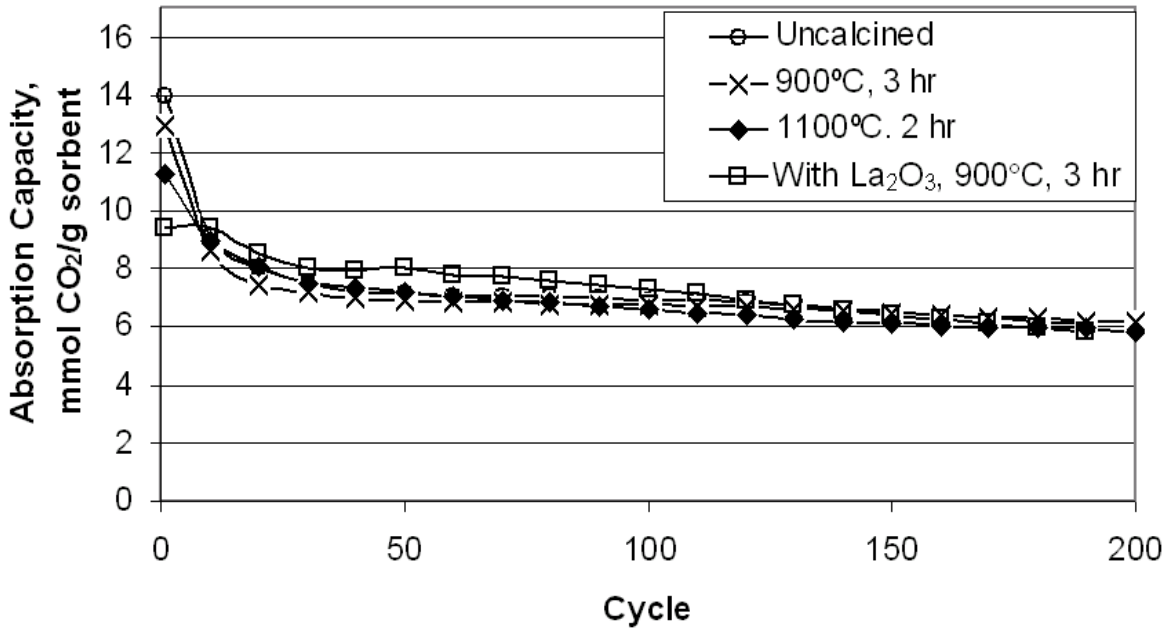

Figure 8. Various sorbents derived from Microna 3 limestone were tested after being initially calcined at the indicated conditions. One sorbent contained 0.05 g La_2O_3/g CaO.

Another interesting result displayed by Figure 9 was the difference in absorption capacity of the CaO by the end of the test. At the end of the 1250 cycle test, the Microna 3 sample initially calcined at 900°C for 3 hr absorbed 2.68 mmol CO_2/g sorbent, which corresponded to a 15.8% conversion of CaO. However, the sorbent with 0.25 g MgO/ g CaO absorbed 3.85 mmol CO_2/g sorbent, which corresponded to a 28.1% conversion of CaO. Thus, the presence of the inert MgO increased the absorption capacity of the CaO.

The results in Figure 9 are important because they show that the life cycle performance of the sorbent was improved significantly either by the addition of MgO or by the use of a higher initial calcination temperature.

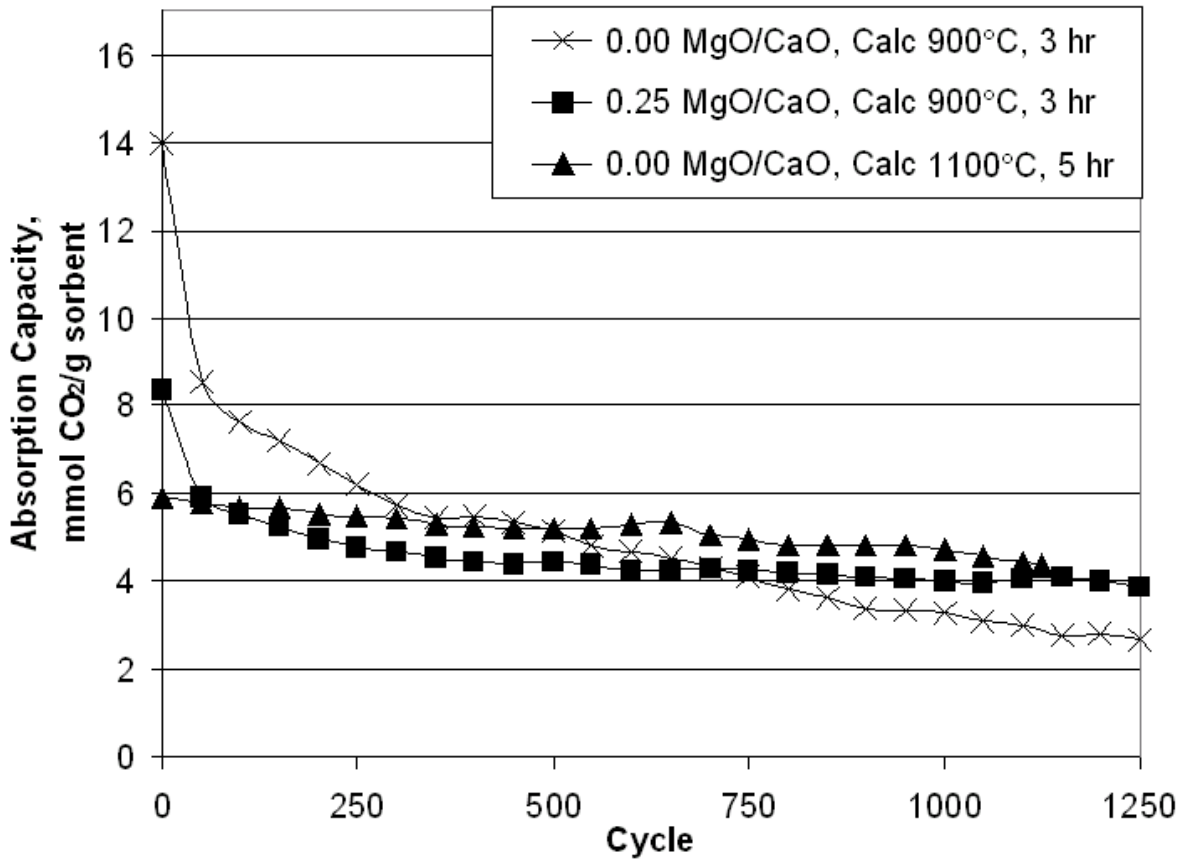

Figure 9. Absorption capacity of CaO derived from Microna 3 limestone. One sorbent contained 0.25 g MgO/g CaO. The sorbents had been initially calcined at either 900°C for 3 hr or 1100°C for 5 hr.

Conclusions

The carbonation of CaO is an attractive method for removing CO_2 from hot gas mixtures such as are produced for example by steam reforming methane. However, to be economical the sorbent must be regenerated and reused for many cycles which requires maintaining the activity of the sorbent. A sorbent performance test of CaO derived from natural limestones and several pure materials showed that in every case the absorption capacity declined as the material was subjected repeatedly to a cycle of CO_2 absorption and regeneration. However, the rate of decline and the initial absorption capacity did vary

somewhat depending on the source of the CaO such that CaO derived from pure calcium acetate had the highest absorption capacity after 30 cycles, and CaO derived from an Iowa limestone had the lowest.

Subsequent investigation showed that the rate of decline in CaO activity can be reduced by incorporating finely dispersed MgO in the sorbent. But this also reduces the absorption capacity of the sorbent, since MgO does not absorb CO_2 under the proposed conditions of usage. Because of these competing effects, a long life-cycle performance test was required to show the advantage of incorporating MgO in the sorbent. When such a test was conducted for 1250 cycles, the absorption capacity of a limestone-based sorbent with 20 wt % MgO was 45% greater than that of a similar material without MgO by the end of the test, and the rate of decline in absorption capacity was very small.

Further investigation showed that the stability of a CaO-based sorbent derived from limestone is also greatly affected by the initial calcinations conditions. Therefore, a material calcined at 1100°C for 5 hr is more stable than one calcined at 1100°C for 2 hr, which is more stable than one calcined at 900°C for 3 hr. Although the initial CO_2 absorption capacity of the material is inversely proportional to the severity of the calcination conditions, extended life-cycle performance tests have shown that the material subjected to the more severe initial calcination condition can have the higher absorption capacity after many cycles. Consequently, the absorption capacity of a limestone sample calcined at 1100°C for 5 hr was 45% greater than that of a limestone sample calcined at 900°C for 3 hr by the end of a 1200 cycle test.

Acknowledgement

This report was prepared with the support of the U.S. Department of Energy, under Award No. DE-FG26-04NT 42182. However, any opinions, findings, conclusions, or recommendations expressed herein are those of the authors and do not necessarily reflect the views of DOE.

Literature Cited

(1) Gupta, H.; Fan, L.-S., Carbonation-Calcination Cycle Using High Reactivity Calcium Oxide for Carbon Dioxide Separation from Flue Gas. *Industrial & Engineering Chemistry Research* **2002,** 41, (16), 4035-4042.

(2) Hughes, R. W.; Lu, D. Y.; Anthony, E. J.; Macchi, A., Design, process simulation and construction of an atmospheric dual fluidized bed combustion system for in situ CO2 capture using high-temperature sorbents. *Fuel Processing Technology* **2005,** 86, (14-15), 1523-1531.

(3) Balasubramanian, B.; Ortiz, A. L.; Kaytakoglu, S.; Harrison, D. P., Hydrogen from methane in a single-step process. *Chemical Engineering Science* **1999,** 54, (15-16), 3543-3552.

(4) Han, C.; Harrison, D. P., Simultaneous shift reaction and carbon dioxide separation for the direct production of hydrogen. *Chemical Engineering Science* **1994,** 49, (24B), 5875-83.

(5) Harrison, D. P.; Peng, Z., Low carbon monoxide hydrogen by sorption-enhanced reaction. *International Journal of Chemical Reactor Engineering* **2003,** 1, No pp. given.

(6) Ortiz, A. L.; Harrison, D. P., Hydrogen Production Using Sorption-Enhanced Reaction. *Industrial & Engineering Chemistry Research* **2001,** 40, (23), 5102-5109.

(7) Yi, K. B.; Harrison, D. P., Low-Pressure Sorption-Enhanced Hydrogen Production. *Industrial & Engineering Chemistry Research* **2005,** 44, (6), 1665-1669.

(8) Satrio, J. A.; Shanks, B. H.; Wheelock, T. D., Development of a Novel Combined Catalyst and Sorbent for Hydrocarbon Reforming. *Industrial & Engineering Chemistry Research* **2005,** 44, (11), 3901-3911.

(9) Satrio, J. A.; Shanks, B. H.; Wheelock, T. D., A Combined Catalyst and Sorbent for Enhancing Hydrogen Production from Coal or Biomass. *Energy & Fuels* **2007,** 21, (1), 322-326.

(10) Aihara, M.; Nagai, T.; Matsushita, J.; Negishi, Y.; Ohya, H., Development of porous solid reactant for thermal-energy storage and temperature upgrade using carbonation/decarbonation reaction. *Applied Energy* **2001,** 69, (3), 225-238.

(11) Barker, R., Reversibility of the reaction of calcium carbonate to give calcium oxide and carbon dioxide. *Journal of Applied Chemistry & Biotechnology* **1973,** 23, (10), 733-42.

(12) Barker, R., Reactivity of calcium oxide towards carbon dioxide and its use for energy storage. *Journal of Applied Chemistry & Biotechnology* **1974,** 24, (4/5), 221-7.

(13) Silaban, A.; Harrison, D. P., High temperature capture of carbon dioxide: characteristics of the reversible reaction between CaO(s) and CO2(g). *Chemical Engineering Communications* **1995,** 137, 177-90.

(14) Bhatia, S. K.; Perlmutter, D. D., Effect of the product layer on the kinetics of the carbon dioxide-lime reaction. *AIChE Journal* **1983,** 29, (1), 79-86.

(15) Readman, J. E.; Blom, R., The use of in situ powder X-ray diffraction in the investigation of dolomite as a potential reversible high-temperature CO2 sorbent. *Physical Chemistry Chemical Physics* **2005,** 7, (6), 1214-1219.

(16) Silaban, A.; Narcida, M.; Harrison, D. P., Characteristics of the reversible reaction between CO2(g) and calcined dolomite. *Chemical Engineering Communications* **1996,** 146, 149-162.

(17) Bandi, A.; Specht, M.; Sichler, P.; Nicoloso, N. *In situ Gas Conditioning in Fuel Reforming for Hydrogen Generation*; Center for Solar Energy and Hydrogen Research, ZSW: Stuttgart, Germany. Available at: http://www.netl.doe.gov/publications/proceedings/02/GasCleaning/gas_clean02.html.

(18) Salvador, C.; Lu, D.; Anthony, E. J.; Abanades, J. C., Enhancement of CaO for CO2 capture in an FBC environment. *Chemical Engineering Journal (Amsterdam, Netherlands)* **2003,** 96, (1-3), 187-195.

(19) Li, Z.-s.; Cai, N.-s.; Huang, Y.-y.; Han, H.-j., Synthesis, Experimental Studies, and Analysis of a New Calcium-Based Carbon Dioxide Absorbent. *Energy & Fuels* **2005,** 19, (4), 1447-1452.

(20) Li, Z.-s.; Cai, N.-s.; Huang, Y.-y., Effect of Preparation Temperature on Cyclic CO2 Capture and Multiple Carbonation-Calcination Cycles for a New Ca-Based CO2 Sorbent. *Industrial & Engineering Chemistry Research* **2006,** 45, (6), 1911-1917.

(21) Lu, H.; Reddy, E. P.; Smirniotis, P. G., Calcium Oxide Based Sorbents for Capture of Carbon Dioxide at High Temperatures. *Industrial & Engineering Chemistry Research* **2006,** 45, (11), 3944-3949.

(22) Hasler, D. J. L.; Franck, B. J.; Wheelock, T. D., A reusable calcium-based sorbent for hot gas cleaning. *American Institute of Chemical Engineers, [Spring National Meeting], New Orleans, LA, United States, Mar. 30-Apr. 3, 2003* **2003**, 2554-2568.

(23) Hughes, R. W.; Lu, D.; Anthony, E. J.; Wu, Y., Improved Long-Term Conversion of Limestone-Derived Sorbents for In Situ Capture of CO2 in a Fluidized Bed Combustor. *Industrial & Engineering Chemistry Research* **2004,** 43, (18), 5529-5539.

(24) Grasa, G. S.; Abanades, J. C., CO_2 Capture Capacity of CaO in Long Series of Carbonation/Calcination Cycles. *Industrial & Engineering Chemistry Research* **2006,** 45, (26), 8846-8851.

(25) Yamamoto, T.; Hatsui, T.; Matsuyama, T.; Tanaka, T.; Funabiki, T., Structures and Acid-Base Properties of La/Al2O3 - Role of La Addition to Enhance Thermal Stability of g-Al2O3. *Chemistry of Materials* **2003,** 15, (25), 4830-4840.

(26) Koryabkina, N. A.; Shkrabina, R. A.; Ushakov, V. A.; Ismagilov, Z. R., Synthesis of a mechanically strong and thermally stable alumina support for catalysts used in combustion processes. *Catalysis Today* **1996,** 29, (1-4), 427-431.

(27) Shirsat, A. N.; Ali, M.; Kaimal, K. N. G.; Bharadwaj, S. R.; Das, D., Thermochemistry of La2O2CO3 decomposition. *Thermochimica Acta* **2003,** 399, (1-2), 167-170.

Chapter 3. Development of an Alumina-Based Material for Use as the Shell of a Combined Catalyst/Sorbent Core-in-Shell Material

A paper to be submitted to *Industrial & Engineering Chemistry Research*

Karl O. Albrecht,[a] Justinus A. Satrio,[b] Brent H. Shanks,[a] and Thomas D. Wheelock[a,*]

Abstract

A novel material in the form of spherical core-in-shell pellets is being developed that can be used to produce hydrogen in high concentration via simultaneous application of the steam-methane reforming reaction, the water-gas shift reaction and CO_2 absorption. The core of a core-in-shell pellet is composed of a CaO-based material for *in-situ* sorption of CO_2. The shell of the pellet is largely an alumina-based material that has the dual function of protecting the friable CaO core and supporting a Ni catalyst for catalyzing the steam-methane reforming reaction. The shell material must be porous to conduct CO_2 into the core. This investigation focused on developing a shell formulation with enhanced strength and a high surface area. In order to produce samples of shell material rapidly and efficiently for testing, alumina formulations were cast into cylindrical tablets that were then calcined. The force required to break the tablets and surface area were determined. X-ray diffraction was also performed to determine the presence of crystalline phases.

The first part of the investigation focused on the addition of fine particle limestone to the alumina formulation in order to produce a calcium aluminate phase with a lower melting

[a]Dept. of Chemical and Biological Engineering, 2114 Sweeney Hall, Iowa State University, Ames, IA 50011

[b]Center for Sustainable Environmental Technologies, 0411 Marston Hall, Iowa State University, Ames, IA 50011

*Corresponding Author: wheel@iastate.edu

point than either Al_2O_3 or CaO. The calcium aluminate would ideally act as a binder for the material. The second part of the investigation focused on the addition of calcium, lanthanum, zinc or barium nitrate salts to the alumina formulation to create a well-dispersed binder. The addition of lanthanum nitrate proved to be beneficial as it greatly increased the compressive force required to break the calcined cast tablets. The increase in tablet strength was directly proportional to the amount of lanthanum nitrate that was added. Finally, core-in-shell pellets with lanthanum nitrate added to the shell formulation were prepared, calcined and tested. Compared to the cast tablets, the core-in-shell pellets required a larger concentration of lanthanum to achieve a comparable increase in compressive strength.

Introduction

The recent development of a combined catalyst and sorbent material for use in reforming hydrocarbons has created a need for a porous but strong catalyst support that can be combined with a sorbent for CO_2, which is one of the reaction products. It has been proposed to produce this material in the form of core-in-shell pellets where the cores are made of friable limestone and the shells are made largely of sintered alumina, a known catalyst support. After calcination, the cores selectively absorb CO_2 formed sequentially by the steam-methane reforming and water-gas shift reactions. Due to the fragile nature of the limestone core, an alumina shell is applied around the material to serve both as a support for a Ni catalyst and as a container for the friable sorbent. The desired product is a robust material capable of withstanding repeated loading and regeneration of the sorbent over many cycles. The shell must be porous to allow CO_2 diffusion to the core, have high surface area to support the nickel catalyst and be relatively strong. Although core-in-shell pellets can be

prepared by pan rolling of the powders, the method imparts minimal physical strength. Therefore, some means of enhancing the strength was the focus of this investigation.

Initially, the core-in-shell concept provided a basis for the development of a reusable long-life sorbent for desulfurizing hot coal gas.[1-7] The shell had to be porous and strong but did not require a large surface area. During development of the shell formulation, it was determined that the addition of 20 wt% limestone to alumina powder of varying particle sizes increased the mechanical strength of the core-in-shell material.[1] The strength increase was thought to be due to the formation of a calcium aluminate phase by the reaction between CaO and α-Al_2O_3 during calcination at 1100°C. Later, the alumina formulation of the shell was modified by substitution of a high surface area amorphous alumina for some of the α-alumina in order to make the shell a viable catalyst support.[8] However, the addition of the high surface area alumina greatly decreased the mechanical strength of the pellets. The limestone used in the previous investigations was screened to a particle size of –212/+48 μm. If the hypothesis that a calcium aluminate phase enhanced the strength was correct, decreasing the size of the limestone particles would further enhance the strength because the kinetics of powder reactions depends on the particle size of the reactants.[9]

The toughening effect of *in-situ* reaction sintered calcium aluminate systems has been studied in the case of a calcium aluminate phase with the stoichiometry of $CaAl_{12}O_{19}$. By starting with a mixture of alumina and calcium carbonate powders, $CaAl_{12}O_{19}$ was produced with a plate-like morphology that could bridge cracks and increase the toughness of ceramic composites.[10] $CaAl_{12}O_{19}$ has also been shown to be a suitable support for a nickel catalyst with high stability against steam treatment when prepared via a combustion reaction.[11] A study of the grain morphology of $CaAl_{12}O_{19}$ found that beginning with Al_2O_3 and either

$CaCO_3$ or CaO with or without the presence of a sintering aid (anorthite glass) and followed by calcination at 1200°C for 12 hr, the material passed through several stages of development.[12] First, $CaAl_2O_4$ is formed between 1000°C and 1200°C; $CaAl_2O_4$ then undergoes further reaction with Al_2O_3 to form $CaAl_4O_7$, which then undergoes even further reaction with four moles of Al_2O_3 to form $CaAl_{12}O_{19}$ at temperatures higher than 1200°C.[13] Thus, $CaAl_{12}O_{19}$ seemed unlikely to be present in the core-in-shell pelletized material developed by Akiti et al.[1] for hot gas desulfurization since this material was not calcined above 1100°C. It was more likely that the increased strength of this material was due to the formation of the phases $CaAl_2O_4$ or $CaAl_4O_7$. Since $CaAl_2O_4$ and $CaAl_4O_7$ respectively melt at 1602°C and 1762°C,[14] these phases will sinter more readily at 1100°C than Al_2O_3 or CaO, which have melting points of 2054°C and 2613°C, respectively.[15] Also, due to the high temperature needed to form $CaAl_{12}O_{19}$, it was not possible in the present investigation to form $CaAl_{12}O_{19}$ where calcination was limited to 900°C for 3 hr and 1100°C for 2 hr.

Assuming that the formation of a calcium aluminate phase acted as a binder to increase the mechanical strength of the core-in-shell pellets, it was hypothesized that creating more of an aluminate phase via reaction sintering with a doped oxide would further strengthen the pellets. Furthermore, since alumina is classified as an acidic oxide,[16] increasing the basicity of the doping oxide should cause more of an aluminate phase to form, thus creating a stronger material. The use of basicity differences as a driving force for reaction was demonstrated by Balta,[17] who showed that the number of stable binary silicate compounds increased with an increase in the basicity difference. The measure of basicity used in this study was optical basicity, which is a numerical expression of the average

electron donor power of an oxide and thus provides a measure of the acid-base properties of an oxide.[18] In order to achieve maximum dispersion of the dopant, the basic oxides were added as nitrates in solution to the alumina powder mixture. The basic oxides tested in order of increasing basicity were CaO, La_2O_3, ZnO and BaO with optical basicities of 1.00,[16] 1.07,[18] 1.08,[16] and 1.21,[16] respectively.

While calcium nitrate was utilized as a source of one of the basic oxides used to investigate the aluminate phase formation it also acted as a point of reference for comparison with the results achieved when limestone was the calcium oxide source. Calcium nitrate incorporated in the alumina mixture would ideally create well-dispersed CaO, enhancing the formation of calcium aluminate. Bulk calcium nitrate has been shown to melt prior to decomposition at 562°C.[19] While the decomposition of calcium nitrate was dependent on the heating rate observed by Ettarh and Galwey,[19] the decomposition was complete between 659°C-679°C. Thus, bulk calcium nitrate would be expected to melt and then decompose during calcination at either 900°C for 3 hr or 1100°C for 2 hr.

Lanthanum oxide was the second basic oxide considered for addition to the alumina mixture via addition as a nitrate in solution. The addition of lanthanum oxide to alumina has been studied for a variety of applications. Lanthanum nitrate impregnation of γ-alumina has been shown to stabilize the surface area of the alumina during subsequent high temperature heat treatment.[20, 21] Of course, this was also the initial reason for adding lanthanum nitrate in the present investigation. Preliminary results yielded a dramatic compressive force increase in pellets doped with lanthanum nitrate so further investigation was deemed warranted.

In-situ reinforcing of alumina composites by adding lanthanum nitrate has been studied by others.[22] La_2O_3 reacts with alumina to first form two moles of $LaAlO_3$ that then

react further with Al_2O_3 to form $LaAl_{11}O_{18}$.[23] An increase in strength through lanthanum nitrate addition was shown to be due to the formation of $LaAl_{11}O_{18}$, which grew in a needle-like fashion and bridged cracks in the composite. However, inducing $LaAl_{11}O_{18}$ to grow as needles depended on the preparation method. Pressing and impregnation of the sample yielded the beneficial needle-like growth of the $LaAl_{11}O_{18}$ phase, whereas slip casting the samples did not. Also, like the calcium compound $CaAl_{12}O_{19}$, the lanthanum compound $LaAl_{11}O_{18}$ is formed at too high a temperature to be of use in the current investigation. Interestingly, $LaAlO_3$ melts between 2031°C-2049°C.[24] Thus, the sintering of $LaAlO_3$ would not be expected to be as severe as the sintering of $CaAl_2O_4$, which melts at 1602°C.[15]

Zinc oxide was chosen for this study because its optical basicity of 1.08 is similar to that of La_2O_3.[16] ZnO has been shown to react with Al_2O_3 to form $ZnAl_2O_4$ at temperatures of 900°C and above.[25] The density of $ZnAl_2O_4$ is 4.68 g/cm^3,[26] which is also close to the reported density of $LaAlO_3$, which is 4.89 g/cm^3.[27] Since the densities of $ZnAl_2O_4$ and $LaAlO_3$ are both relatively high, the materials are similar in this respect. Also, zinc would be an attractive substitute for lanthanum due to the higher cost of lanthanum.

Barium oxide was the most basic oxide investigated via nitrate addition to the alumina formulation. When utilizing a system of powdered oxides, it has been reported that $BaAl_2O_4$ will form by the interaction of BaO and Al_2O_3.[28] The formation of $BaAl_2O_4$ was reported to be faster than the formation of $CaAl_2O_4$. However, the formation of $BaAl_2O_4$ required a higher temperature to form compared to $CaAl_2O_4$. The increased temperature was due to the fact that the Ba^{+2} ion is larger than the Ca^{+2} ion and ion transport is involved in the formation of these phases.

The purpose of the present investigation was to develop an alumina-based material with high compressive strength and enhanced surface area for use as a shell material in core-in-shell pellets. In order to test a wide variety of formulations, cylindrical tablets were produced by mixing the formulation and casting the tablets. Preparation of cast tablets required less material than the preparation of core-in-shell pellets made by pan-rolling. Also, a large batch of cast tablets could be made relatively quickly. Two hypotheses were tested in this investigation. The first was that the addition of fine limestone particles would increase the compressive strength of the cast tablets due to the formation of calcium aluminate. The second was that better results would be achieved by doping the alumina with a solution of $Ca(NO_3)_2$ or other nitrate that would decompose when calcined to form a basic oxide capable of reacting with alumina to form an aluminate phase. Tablets were subjected to compressive force testing to determine the force required to break the tablets, N_2 adsorption to determine the surface area of the samples by the BET method, and X-ray diffraction (XRD) to determine the presence of any crystalline phases. Certain samples were also selected for mercury porosimetry measurements in order to elucidate the effects of additives on interparticle pore size distribution as well as cumulative pore volume. Finally, core-in-shell pellets were prepared with lanthanum nitrate in the alumina shell mixture to see whether this additive had the same effect on core-in-shell pellets as it had on cast pellets.

Experimental Methods and Materials

Materials

Table 1 shows the properties of the alumina and limestone used for preparing the shell material formulations. Three different types of alumina were utilized in this study. One was a tabular α-alumina consisting of -325 mesh particles supplied by Almatis and designated as T-64 alumina. A second α-alumina, also supplied by Almatis and designated as A16-SG, had a mean particle size of 0.4 μm. A third designated as DD-290 was an amorphous form of alumina with a high surface area and a mean particle size of 9.8 μm that was supplied by the Engelhard Corporation. This material was claimed to be identical to CP-7 alumina formerly supplied by Almatis and used in previous studies.[8, 29]

Table 1. Properties of materials used for preparing sorbent and shell formulations.

Material	I.D. Source	Particle Size, μm	Surface Area, m^2/g	Supplier
Al_2O_3[a]	DD-290	8	275	Engelhard
α-Al_2O_3	T64	-44[b]		Almatis
α-Al_2O_3	A16-SG	0.4	8.9	Almatis
Limestone	Microna 3	3.2		Columbia River Carbonates
Limestone	Iowa	-212/+63[c]		Martin Marietta Aggregates

[a]Amorphous
[b]Based on sieving by supplier
[c]Based on sieving in laboratory

Limestone was obtained from two sources. Columbia River Carbonates in Washington provided Microna 3 limestone with a mean particle size of 3.2 μm. Microna 3 was greater than 97 wt% $CaCO_3$ according to the producer. Coarser limestone with 97 wt% $CaCO_3$ was obtained from the Ames, Iowa, quarry of Martin Marietta Aggregates. This limestone was ground and screened to a size of -212/+63 μm.

Fisher Scientific was the source of reagent grade calcium nitrate [$Ca(NO_3)_2 \bullet 4H_2O$], barium nitrate [$Ba(NO_3)_2$] and zinc nitrate [$Zn(NO_3)_2 \bullet 6H_2O$]. Reagent grade lanthanum nitrate [$La(NO_3)_3 \bullet xH_2O$] was obtained from Sigma Aldrich. Due to the indeterminate nature of the hydrate present in the lanthanum nitrate, a stock solution of lanthanum nitrate in tetrahydrofuran (THF) was prepared. The molarity of the lanthanum nitrate stock solution was determined gravimetrically by evaporation and then calcination at 900°C for several hours to convert the lanthanum nitrate to lanthanum oxide, La_2O_3, which could be weighed.

Preparation of the Shell Material

The shell material formulation was composed largely of alumina together with a small amount of an additive such as limestone. Akiti et al.[1] had found previously that a 3:2 mass ratio of T-64 α-alumina to A16-SG α-alumina was optimum. For the present study, half of the T-64 α-alumina was replaced with DD-290 amorphous alumina to provide a larger surface area for supporting a nickel catalyst. This resulted in a specific mixture of alumina particles consisting of 30 wt% DD-290, 30 wt% T-64, and 40 wt% A16-SG that was employed throughout the present study. For part of the study this mixture was combined with either limestone or another additive. If limestone was used, the proportions were such that the overall mixture contained either 5 or 10 wt.% limestone which provided a Ca:Al

molar ratio of 0.026 or 0.055. These values are based on the assumption that the limestone contained 97 wt% $CaCO_3$. The same molar ratios were employed when calcium was replaced with lanthanum, zinc or barium. This procedure resulted in the equivalent concentrations of the various oxides reported in Table 2.

Table 2. Equivalent concentrations of different oxides in two-component mixtures with Al_2O_3.

Limestone Conc., wt%	Ca:Al Atomic Ratio	Equivalent Oxide Concentration, wt%			
		CaO	La_2O_3	BaO	ZnO
3	0.015	1.6	4.6	4.3	2.3
5	0.026	2.7	7.7	7.2	3.9
10	0.055	5.7	14.9	14.2	8.1

The majority of the samples in this study were prepared for testing as cylindrical tablets having a diameter of 6 mm and thickness of 6 mm. A 20 g batch of tablets was prepared by first weighing out appropriate amounts of alumina and limestone and mixing the powders. The dry mixture was then combined with 5 to 7 ml of a 5 wt% lignin in deionized water solution to prepare a viscous, well-mixed suspension, which was poured into a plastic mold coated with a mold releasing agent. The tablets were allowed to dry overnight at atmospheric conditions prior to removal from the mold. This method produced about 45 tablets per batch.

In some cases limestone was replaced with calcium, lanthanum, zinc or barium nitrate. In these cases 20 g of the alumina mixture was weighed and an appropriate amount of the nitrate salt dissolved in solution was mixed with the alumina using a mortar and pestle to produce a thick paste. After the paste had been mixed thoroughly and allowed to dry at

room temperature, it was placed in a drying oven at 110°C for at least 5 hr. After drying, the resulting powder was reground if necessary and used to make tablets by first adding a 5 wt% lignin solution to produce a viscous, well mixed suspension that was then placed in a mold with a mold releasing agent. When calcium, lanthanum or zinc nitrate was mixed with alumina, tetrahydrofuran (THF) was used as the solvent. However, barium nitrate required using water as the solvent because of its low solubility in THF. This method also produced about 45 cast tablets.

Preparation of Core-in-Shell Pellets

In addition to cylindrical cast tablets, spherical core-in-shell pellets were tested. These were prepared by using a rotating drum that had a maximum diameter of 25 cm and was operated at 30 rpm. The cores of the spherical pellets were prepared first by placing Microna 3 limestone powder in the rotating drum and spraying it with water intermittently so that it balled up. Cores were built up in this way until about 20 g of pellets ranging between 5 and 6 mesh, or between 3.96 mm and 3.35 mm in diameter, were produced. The cores were then hardened by operating the drum at the following speed and time settings: 10 rpm for 10 min., 30 rpm for 20 min., 60 rpm for 30 min., and 90 rpm for 30 min.

Shell material was prepared by weighing out 600 g of the alumina mixture followed by the addition of lanthanum nitrate in THF. The materials were mixed well by using a mortar to prepare a slurry. The THF was evaporated and the mixture dried for at least 5 hr at 110°C. The resulting powder was then reground in the mortar and used to make the shells by coating the previously prepared cores as they were tumbled in the rotating drum pelletizer. The powder was added gradually and the pellets were sprayed intermittently with a 5 wt% lignin solution in water to build up the shells until the pellets were between 4 and 5 mesh in

size. When about 30 g of pellets were produced between 4 and 5 mesh, or between 4.76 and 3.96 mm in diameter, they were hardened by using the same procedure described above for the cores.

Calcination of Tablets and Pellets

All the samples were calcined at high temperature in an atmosphere of flowing air to increase the physical integrity of the tablets and pellets. Some samples were calcined at 900°C for 3 hr after being heated gradually from room temperature over a two-hour period. Other samples were calcined at 1100°C for 2 hr following a 3 hr heating ramp to 1100°C. All of the calcined materials were cooled using a 2 hr ramp back to room temperature.

Calcined tablets or pellets that subsequently were stored or exposed to air for some time before testing were recalcined to destroy any hydroxides or carbonates that could have formed on exposure to the atmosphere. The re-calcination was conducted at 750°C for 0.5 hr, and then the calcined materials were cooled immediately before conducting breaking force tests.

Physical Characterization of Shell Material

The force required to break tablets or pellets was determined with an Accuforce EZ 250 instrument. A single pellet or tablet was placed between two flat plates, and the top plate was lowered at a rate of 10 mm/min. Cylindrical tablets were placed with their flat surfaces facing the plates. A small piece of cardboard was placed on either side of a tablet to distribute the force evenly over the sample; cardboard was not used in compressive force measurements of spherical core-in-shell pellets. The force that caused the pellet or tablet to break was taken to be the breaking force. In the case of a cylindrical tablet, the breaking force was divided by the flat surface area to provide the compressive strength that was

recorded as the pressure required to break a sample in MPa. The average breaking force of 40 tablets with fine limestone particles was calculated. The average breaking force of 20 tablets was calculated for samples with nitrates added. The compressive strength averages are presented with 95% confidence intervals.

Surface area analysis was performed using a Micromeritics ASAP 2020 instrument. The BET method was employed using nitrogen at -196°C. Five intact cast pellets were utilized for these tests. The five cast pellets weighed about 1.5 g.

Powder X-ray diffraction (XRD) was conducted with a Siemens D-500 Diffractometer using Cu Kα radiation with a graphite monochromator. Samples, which had previously been used for measuring breaking force, were ground with an agate mortar and pestle and back-loaded into a holder. A voltage of 50 kV and a current of 27 mA were employed. The divergence slits used were 1.0°, and the detector slit used was 0.15°. A counting time of 4 sec was engaged while rotating the sample at 54 rpm.

A semi-quantitative analysis of relevant crystalline phases was performed on results obtained from XRD measurements. The height of the most intense peak, or I_{100}, of the reported phase and the height of I_{100} of the α-Al_2O_3 phase were determined. The ratio of I_{100} (reported phase)/I_{100}(α-Al_2O_3 is reported in order to relay the relative amount of the reported phase present. Powder diffraction files (PDF's) provided by The International Centre for Diffraction Data were consulted for the location of I_{100} in the measured diffractograms.

Mercury intrusion porosimetry measurements were conducted with a Quantachrome PoreMaster mercury porosimeter on three intact cylindrical cast tablets. The mass of the samples was about 0.9 g. The cumulative mercury intrusion curve was recorded and the volume/pressure relationship was calculated using the Washburn equation. The Washburn

equation used a mercury contact angle of 140° and a surface tension of 480 erg/cm^2. The pore size distribution was calculated as the derivative of the volume of the mercury intrusion curve with respect to the log of the pore diameter, or dV/d(log d).

Experimental Results and Discussion

Addition of Limestone

Cast tablets made of the specific mixture of alumina particles and different concentrations of limestone particles of different sizes were prepared and calcined at either 900°C for 3 hr or 1100°C for 2 hr and then tested. Figure 1 shows the recorded compressive strength of the pure alumina tablets as well as tablets made with limestone of different sizes. The concentration of the limestone added was less than the optimum 20 wt% determined previously.[1] This change was made because it was believed that by using smaller particles of limestone less material would be required to achieve the strength obtained with larger particles. In other words, a lesser amount of the smaller limestone particles would provide as much contact area as a greater amount of the coarser limestone. A smaller concentration of limestone also increased the alumina surface area by a small amount.

Figure 1 shows that a 5 wt% concentration of limestone had little effect on the compressive strength of tablets calcined at 900°C for 3 hr. However, a 10% concentration did increase the compressive strength of tablets calcined at this temperature compared to that of pure alumina tablets. Also it can be seen that the compressive strength of tablets calcined at 1100°C for 2 hr increased in direct proportion to the concentration of Microna 3 limestone.

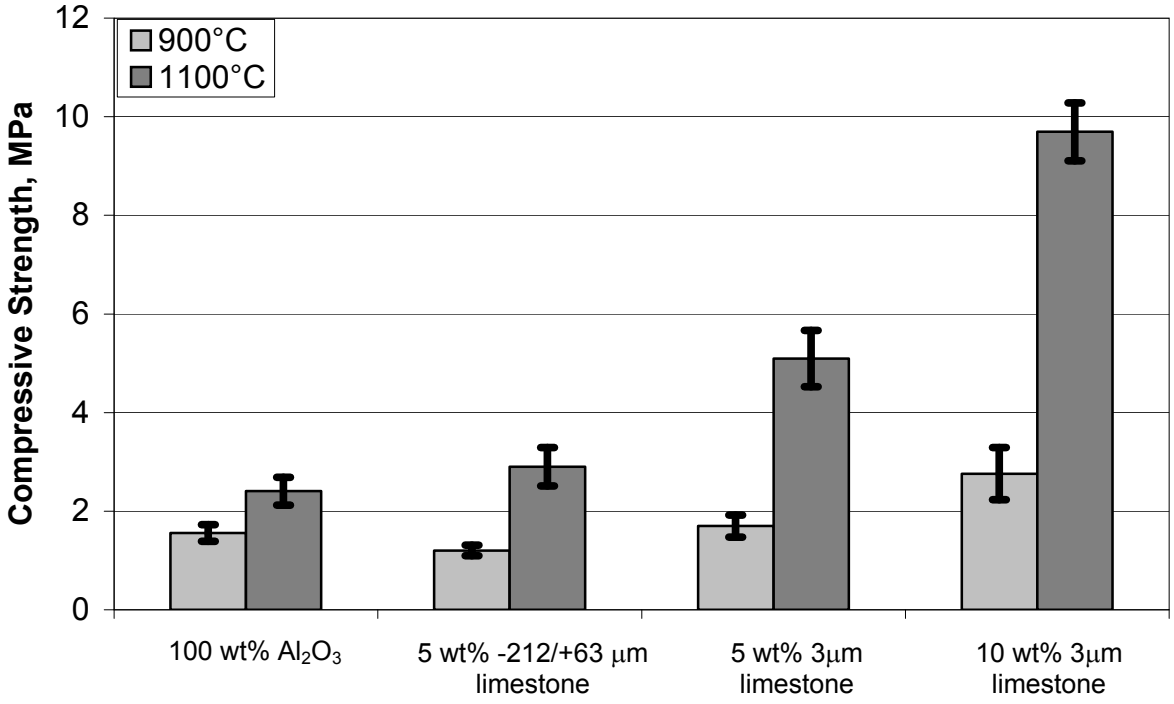

Figure 1. Compressive strength of cast alumina tablets made limestone with various concentrations and particle sizes and calcined at either 900°C for 3 hr or 1100°C for 2 hr.

Furthermore, it is apparent that 5 wt% concentration of Microna 3 limestone was much more effective than a similar concentration of –212/+63 μm limestone, especially at the higher calcination temperature.

Selected samples of tablets that gave the results displayed in Figure 1 were analyzed by X-ray diffraction and the results are shown in Table 3. In all samples with limestone present and calcined at 900°C for 3 hr, no calcium aluminate phases were detected. However, in the samples calcined at 1100°C for 2 hr, the first expected calcium aluminate phase, $CaAl_2O_4$ was detected. The second calcium aluminate phase, $CaAl_4O_7$, formed by the reaction of $CaAl_2O_4$ with Al_2O_3, was also detected. The phase $CaAl_4O_7$ was weakly observed in the 2.7 wt% CaO sample calcined at 1100°C for 2 hr even though a minor

Table 3. The ratio of the height of the most intense peak (I_{100}) of the reported phase to the I_{100} α-Al_2O_3 peak obtained from XRD measurements of cast tablets made of Al_2O_3 and Microna 3 limestone after calcination at different temperatures.

Additive Material	Temperature, °C	I_{100} (Reported Phase)/I_{100}(α-Al_2O_3)		
		CaO	$CaAl_2O_4$	$CaAl_4O_7$
2.7 wt% CaO	900	0.17	0.00	0.00
	1100	0.07	0.05	Observed[a]
5.7 wt% CaO	900	0.27	0.00	0.00
	1100	0.05	0.18	0.56

[a]$CaAl_4O_7$ was observed but the major peak was obscured under a minor α-Al_2O_3 peak

α-Al_2O_3 peak obscured the strongest XRD peak. The trend in the appearance of the calcium aluminate phases appeared to correlate with the increase in the compressive strength of the tablets demonstrated in Figure 1. Also of interest is the decrease in the amount of crystalline CaO present in the XRD results in samples calcined at 1100°C.

The appearance of the calcium aluminate phases could account for the increase in compressive strength of tablets with Microna 3 limestone that were calcined at 1100°C. The melting points of $CaAl_2O_4$ and $CaAl_4O_7$ are 1602°C and 1762°C,[14] respectivley, whereas melting points of Al_2O_3 and CaO are 2054°C and 2613°C, respectively.[15] Thus, at 1100°C the sintering of the calcium aluminate phases is more likely to take place than the sintering of either CaO or Al_2O_3. The formation of calcium aluminate in the CaO-Al_2O_3 system occurs by ionic Ca^{2+} diffusion into Al_2O_3,[28] which would account for the decrease in the quantity of the crystalline CaO phase present. Since the Tamman temperature for CaO is about 1000-1250°C,[30] calcination at 1100°C would facilitate sintering of CaO, which presumably would enhance the diffusion of Ca^{2+} ions to form calcium aluminate.

Surface area measurements of the tablets made with limestone are presented in Figure 2. As expected, the surface area decreased in samples calcined at 1100°C for 2 hr when compared with similar samples calcined at 900°C for 3 hr. This was most likely due to sintering of small pores in the high surface area DD-290 alumina. Samples calcined at 900°C appeared to retain a surface area of nearly 40 m^2/g, whereas most samples calcined at 1100°C for 2 hr retained a surface area of only 22 m^2/g. In addition, the sample with 10 wt% Microna 3 limestone calcined at 1100°C retained a surface area of only 15 m^2/g.

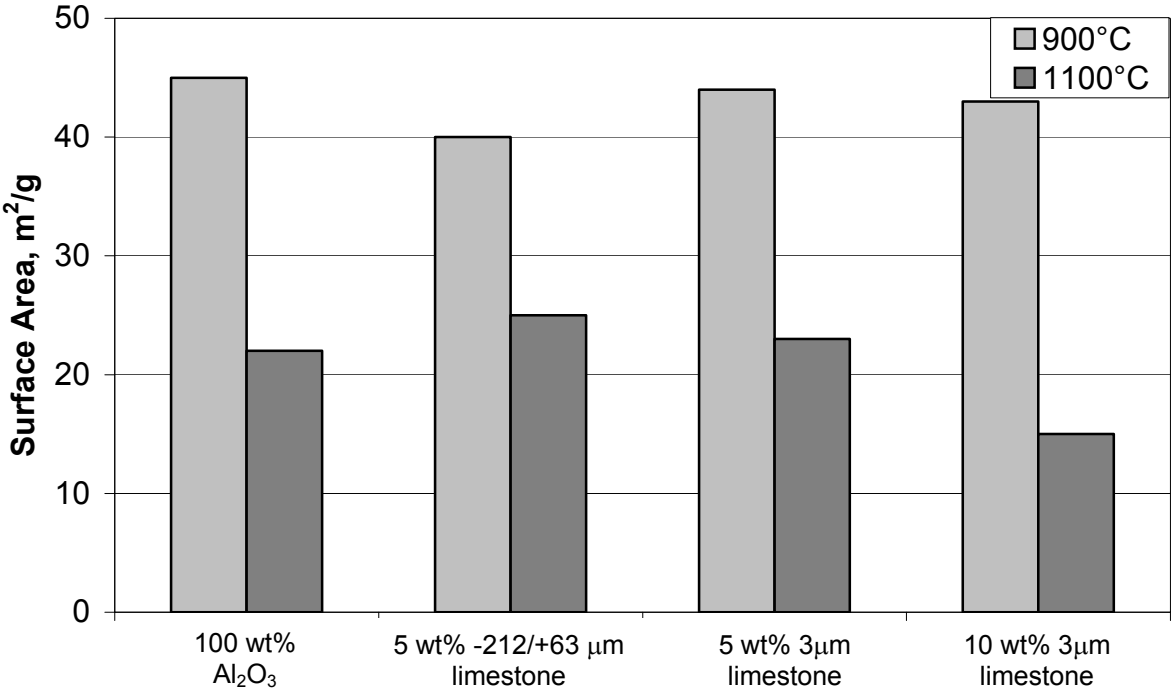

Figure 2. BET surface area of cast alumina tablets made with various limestone concentrations and particle sizes and calcined at either 900°C for 3 hr or 1100°C for 2 hr. Pure alumina tablets and tablets with 10 wt% Microna 3 limestone present were calcined at either 900°C for 3 hr or 1100°C for 2 hr.

In order to obtain further insight into the nature of the interaction between particles during sintering, intact cast tablets were subjected to mercury intrusion porosimetry. This

technique provides the means for determining the pore size distribution between particles. The intact calcined tablets were then subjected to the mercury intrusion technique, and the results are shown in Figure 3 parts (a) and (b).

Figure 3 (a) illustrates the pore size distribution curves for pure alumina cast tablets, which appear as a broad distribution that reaches a maximum at pore diameter of 0.15 μm for tablets calcined at 900°C for 3 hr and at a pore diameter of 0.20 μm for tablets calcined at 1100°C for 2 hr. The small peak in the pore size distribution curve centered around a pore diameter of 0.015 μm in the sample calcined at 1100°C for 2 hr is believed to represent an increase in the size of pores within particles of amorphous DD-290 alumina as smaller pores within particles coalesce into larger pores. The shift in the distribution curves above a pore diameter of 0.06 μm was probably due to particle sintering as the temperature was increased, resulting in a wider interstitial pore size distribution with a larger mean pore diameter. As smaller particles fused together through sintering, the smaller spaces between particles would be closed, changing the pore size distribution observed in Figure 3 (a). Figure 3 (b) shows the pore size distribution curves obtained by testing cast tablets with 10 wt% Microna 3 limestone in the alumina mixture. Above a pore diameter of 0.10 μm there was a shift from a unimodal distribution to a bimodal distribution with addition of the Microna 3 limestone. Instead of a single broad peak, two sharper peaks appeared in each curve. Both curves displayed a smaller peak centered on a pore diameter of 0.15 μm and a larger peak centered around a pore diameter of 0.57 μm in one case (900°C) and 0.9 μm in a second case (1100°C). Interestingly, the smaller peak in each curve appeared to be largely independent of the calcination temperature, which suggests that it was due to the change in the particle size

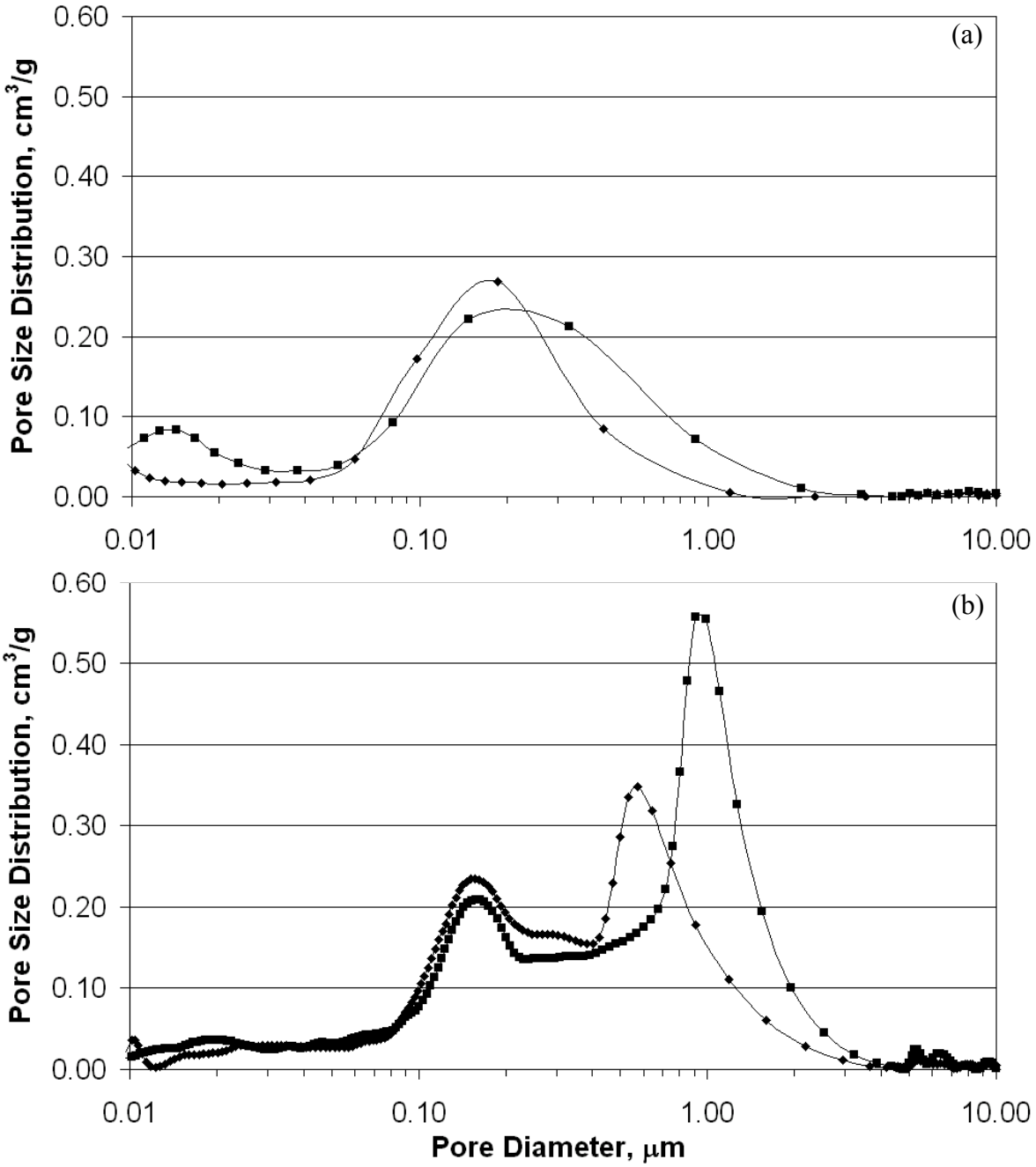

Figure 3. Pore size distributions obtained by mercury intrusion porosimetry of (a) 100% Al_2O_3 tablets and (b)10 wt% Microna 3 limestone tablets. Samples were calcined at 900°C for 3 hr (◆) or 1100 °C for 2 hr (■).

distribution of the physical mixture. In direct contrast, the larger peak in each curve was highly temperature dependent so that an increase in calcination temperature produced a taller peak. The limestone particles, which became CaO particles upon calcination, could have reacted with alumina particles directly adjacent to them at high temperature resulting in the formation of calcium aluminate with a lower melting point than either Al_2O_3 or CaO. Thus, enhanced sintering could have taken place at the interface between CaO and Al_2O_3 particles due to the formation of calcium aluminate. Table 4, which shows selected physical properties of the compounds CaO, Al_2O_3, and $CaAl_2O_4$ among others, demonstrates that sintering of $CaAl_2O_4$ would be likely at 900°C and 1100°C due to a Tamman temperature of about 801°C.

Table 4. Selected properties of various phases present during the preparation and testing of cast tablets and core-in-shell pellets.

Phase	Density, g/ml	Melting Point, °C	Tamman Temperature, °C[a]
α-Al_2O_3	3.99[15]	2054[15]	1027
CaO	3.34[15]	2613[15]	1000-1250[30]
$CaAl_2O_4$	2.51[31]	1602[14]	801
$LaAlO_3$	4.89[27]	2031-2049[24]	1015-1024
$ZnAl_2O_4$	4.68[26]	1950[32]	975
$BaAl_2O_4$	4.04[33]	1829[34]	914.5

[a]Taken as half the melting point unless otherwise noted

Although crystalline calcium aluminate was not observed with XRD in samples calcined at 900°C for 3 hr, amorphous calcium aluminate could still have been present. Thus, the pore size distributions with maxima located at pore sizes of 0.57 μm and 0.90μm for samples calcined at 900°C for 3 hr or 1100°C for 2 hr, respectively, could have been due to neck growth and grain coarsening of the particles as the particles fused together by the formation of calcium aluminate. Some alumina particles may not have had limestone particles adjacent to them, causing sintering that also may have led to the smaller peak in each distribution curve centered around a pore diameter of 0.15 μm.

The sintering mechanism that appeared to take place during calcination with the addition of Microna 3 limestone was probably a non-densifying mechanism produced by surface diffusion or lattice diffusion from the surface that forms necks.[35] The cumulative pore volume between particles was measured in the pore range from 0.05 μm to 10.0 μm for all samples. The cumulative pore volume for the pure alumina tablets calcined at 900°C for 3 hr was 0.20 cm^3/g and for tablets calcined at 1100°C for 2 hr it was 0.23 cm^3/g. When Microna 3 limestone was present in 10 wt% concentration in the cast tablets, the pore volume for samples calcined at 900°C for 3 hr was 0.26 cm^3/g and for samples calcined at 1100°C for 2 hr was 0.32 cm^3/g. Thus, the interstitial pore volume increased with the addition of Microna 3 limestone. Therefore, the increase in compressive strength of the material was most likely due to the formation of a binding calcium aluminate phase that resulted in neck growth between CaO and Al_2O_3 particles, but did not result in densifying of the particle mixture. The lack of densification is a beneficial result since decreased pore volume could impede the diffusion of CO_2 to the core of a core-in-shell pellet.

Addition of Metal Oxides

An alternative method for introducing various metal oxides into the alumina particle mixture was also investigated. This method involved doping the alumina with a solution of the nitrate salt of the metal that upon calcination was converted to the oxide. The metal oxides were chosen to provide a range of optical basicity. Alumina is classified as an acidic oxide.[16] It was hypothesized that the difference between the optical acidity of the alumina and optical basicity of the additive would act as a driving force to produce an aluminate phase. The aluminate phase produced during sintering would ideally act as a binder for the material, thus increasing the compressive strength of the tablets.

In order to produce comparable results to tablets made with added limestone, tablets with other oxides were made for testing with the same atomic ratio of each metallic element to that of aluminum as the atomic ratio of Ca:Al indicated in Table 2. The tablets were created by first mixing the alumina powders with a solution of a metal nitrate, which was then dried. The dried mixture was then mixed with a 5 wt% lignin solution and cast. After drying at room temperature, the tablets were calcined at 900°C for 3 hr or 1100°C for 2 hr.

The compressive strength of tablets made with equivalent concentrations of different metal oxides and subsequently calcined at either 900°C for 3 hr or 1100°C for 2 hr is indicated in Figure 4. All of the results in Figure 4 that were obtained with added basic oxides that employed the same atomic ratio of 0.026 mol X/mol Al, where X is the basic oxide atom. While results are presented in order of increasing basicity, the compressive strength does not increase in a similar manner. However, the incorporation of lanthanum oxide in the material greatly increased the compressive strength of the samples and the

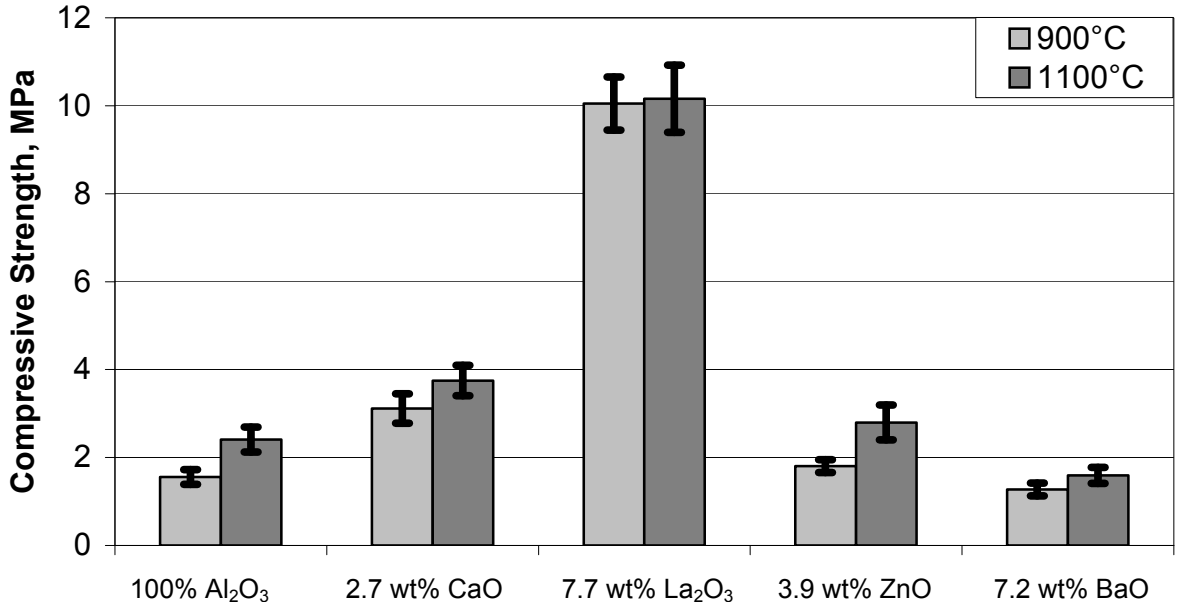

Figure 4. Compressive strength of cast tablets made with equivalent concentrations of basic oxides derived from nitrate salts and calcined at 900°C for 3 hr or 1100°C for 2 hr. All of the samples with basic oxides had an atomic ratio X/Al of 0.026 where X was Ca, La, Zn, or Ba.

increase in compressive strength was the same for both calcination temperatures. The fact that a large compressive strength could be achieved at the lower calcination temperature is highly beneficial since it would permit calcining core-in-shell pellets at a temperature where less of the high surface area alumina would be degraded.

X-ray diffraction (XRD) measurements were also performed on tablets containing metal oxides derived from the corresponding nitrates. The XRD results are presented in Table 5. While increasing the basicity of the metal oxide incorporated in the tablets did not produce an increase in the compressive strength of cast tablets, it can be seen from Table 5 that in general an increase in basicity of the metal oxide did increase the amount of the aluminate phase formed. The addition of CaO derived from heat treating cast tablets with

Table 5. The ratio of the height of the most intense peak (I_{100}) of the reported phase to the I_{100} α-Al_2O_3 peak obtained from XRD measurements of cast tablets made of Al_2O_3 and added metal nitrates after calcination at different temperatures.

Additive Material	Temperature, °C	I_{100} (Reported Phase)/I_{100} (α-Al_2O_3)			
		$CaAl_2O_4$	$LaAlO_3$	$ZnAl_2O_4$	$BaAl_2O_4$
2.7 wt% CaO	900	0.00			
	1100	0.00			
7.7 wt% La_2O_3	900		0.02		
	1100		0.17		
3.9 wt% ZnO	900			0.07	
	1100			0.10	
7.2 wt% BaO	900				0.08
	1100				0.28

calcium nitrate present did not produce an observable calcium aluminate phase, which contrasted sharply with the results achieved by incorporating limestone in the tablets (see Table 3). However, lanthanum, zinc and barium oxides all produced crystalline aluminate phases in tablets calcined at 900°C for 3 hr or 1100°C for 2 hr. Thus, the large increase in compressive strength achieved by adding La_2O_3 could not be explained by the presence of the amount of the aluminate phases observed.

The addition of lanthanum nitrate to the alumina mixture prior to casting and calcination resulted in an increase in compressive strength that was statistically similar for tablets calcined at 900°C for 3 hr or 1100°C for 2 hr. Thus, the strength of the samples could be increased sufficiently by the addition of lanthanum nitrate even at the lower calcination temperature. The advantage of using the lower calcination temperature is that it had less effect on the BET surface area of the shell material as indicated by Figure 5. This surface area was determined by nitrogen adsorption measurements carried out on alumina tablets

made by the same procedure as that employed to make the tablets used for measuring the breaking force. These measurements showed that the samples calcined at 900°C for 3 hr did retain a higher surface area compared to similar samples calcined at 1100°C for 2 hr. More than likely, the large loss in surface area experienced by the tablets calcined at 1100°C was due to sintering of the amorphous DD-290 alumina, which had a large surface area initially.

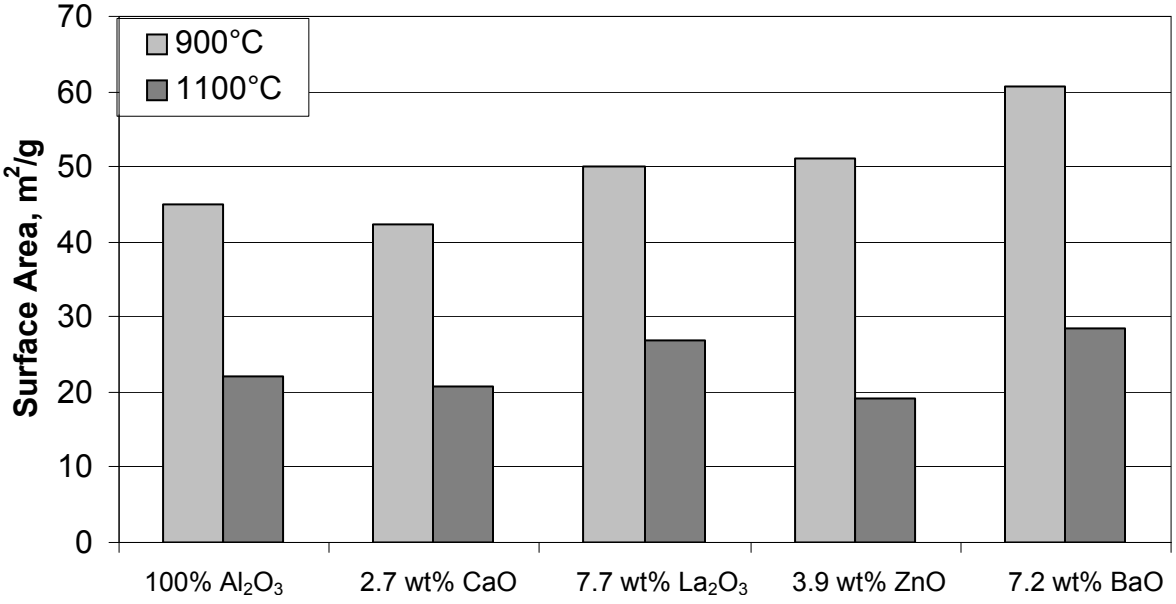

Figure 5. BET surface areas of cast tablets made with equivalent concentrations of basic oxides derived from nitrate salts and calcined at 900°C for 3 hr or 1100°C for 2 hr. All of the samples with basic oxides had an atomic ratio X/Al of 0.026 where X was Ca, La, Zn, or Ba.

Further Testing of Lanthanum Nitrate Addition

Since the incorporation of La_2O_3 in the shell material produced a dramatic increase in the compressive strength of the cast tablets, further consideration was given to the effect of La_2O_3 concentration in the tablets. When a lower concentration corresponding to a molar ratio of 0.15 La:Ca or a mass concentration of 4.7 wt% La_2O_3 was used, the results presented in Figures 6 and 7 were achieved. Figure 6 shows that the increase in compressive strength

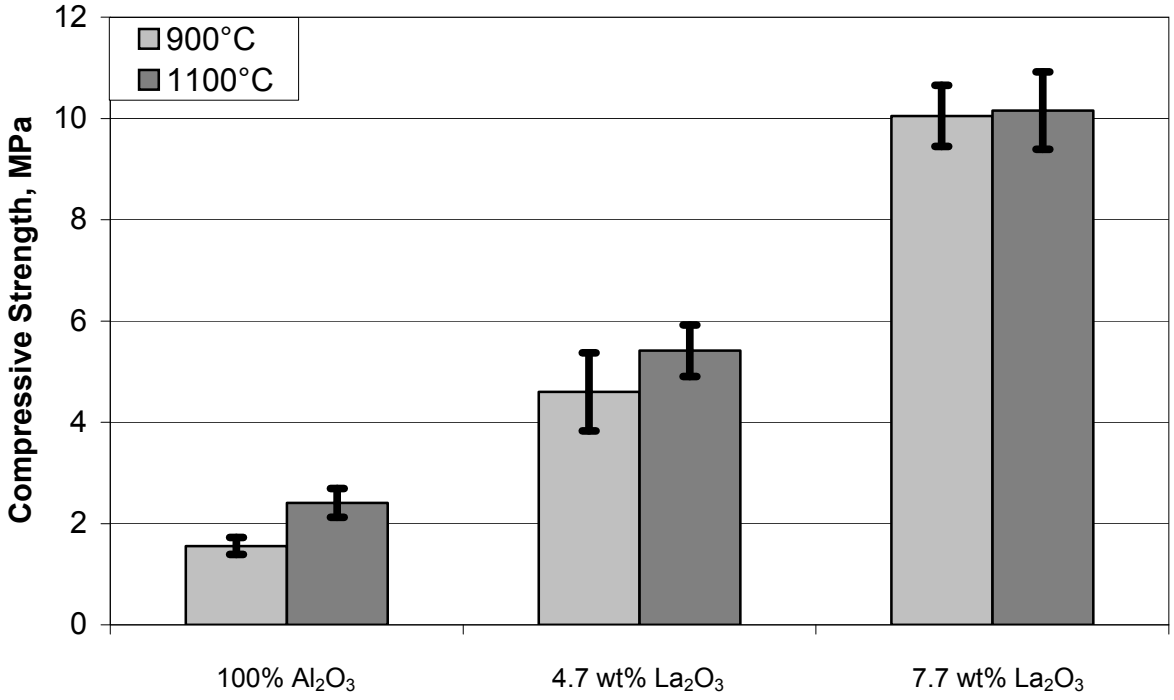

Figure 6. Compressive strength of cast tablets made with various concentrations of La_2O_3 derived from nitrate salts and calcined at 900°C for 3 hr or 1100°C for 2 hr.

of the tablets due to the addition of La_2O_3 is directly proportional to its concentration. Furthermore, the results show that at either La_2O_3 concentration, the effect of calcination temperature on the compression strength was not statistically significant.

As shown in Figure 7, the BET surface of the tablets calcined at 900°C was slightly greater for tablets with La_2O_3 than for pure Al_2O_3 tablets, but the surface area was not affected by the concentration of La_2O_3. The apparently greater surface area of tablets with lanthanum compared to pure alumina tablets agrees with earlier results that showed that lanthanum oxide has a stabilizing effect on the area of alumina at high temperatures.[20] This effect may also have accounted for the slightly greater surface area of tablets calcined at 1100°C that contained 7.7 wt% La_2O_3.

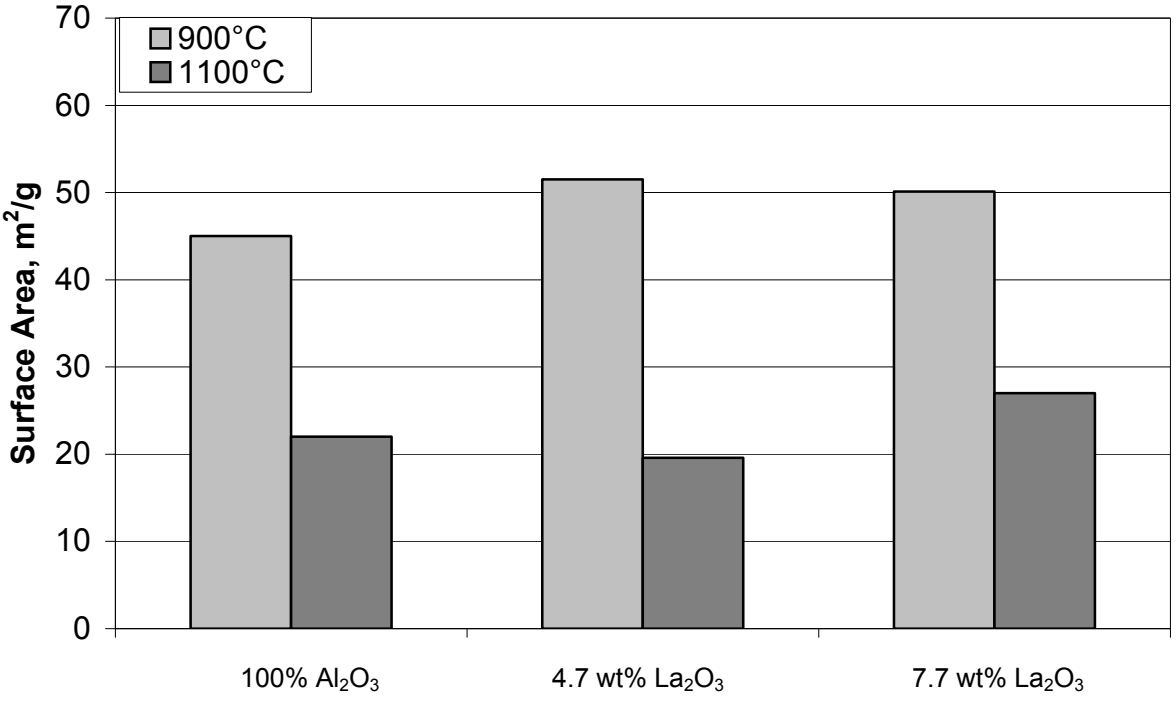

Figure 7. BET surface area measurements of cast tablets made with various concentrations of La_2O_3 derived from nitrate salts and calcined at 900°C for 3 hr or 1100°C for 2 hr.

To determine the effects of La_2O_3 on the porosity of intact cast tablets, mercury intrusion porosimetry was applied to selected samples that contained 7.7 wt% La_2O_3 and had been calcined at either 900°C or 1100°C (Figure 8). For ease of comparison the porosity of pure Al_2O_3 tablets presented in Figure 3 (a) are reproduced in Figure 8 (a). Figure 8 (b) shows the pore size distribution within tablets containing 7.7 wt% La_2O_3 and calcined at 900°C for 3 hr or 1100°C for 2 hr. The two large peaks centered around a pore diameter of 0.35 μm are most likely to account for the pore space between particles or interparticle porosity while the smaller peak centered around a pore diameter of 0.015 μm probably accounts for the pore space within particles of amorphous DD-290 alumina. Figure 8 indicates that the addition of La_2O_3 shifts the pore size distribution so that the interparticle

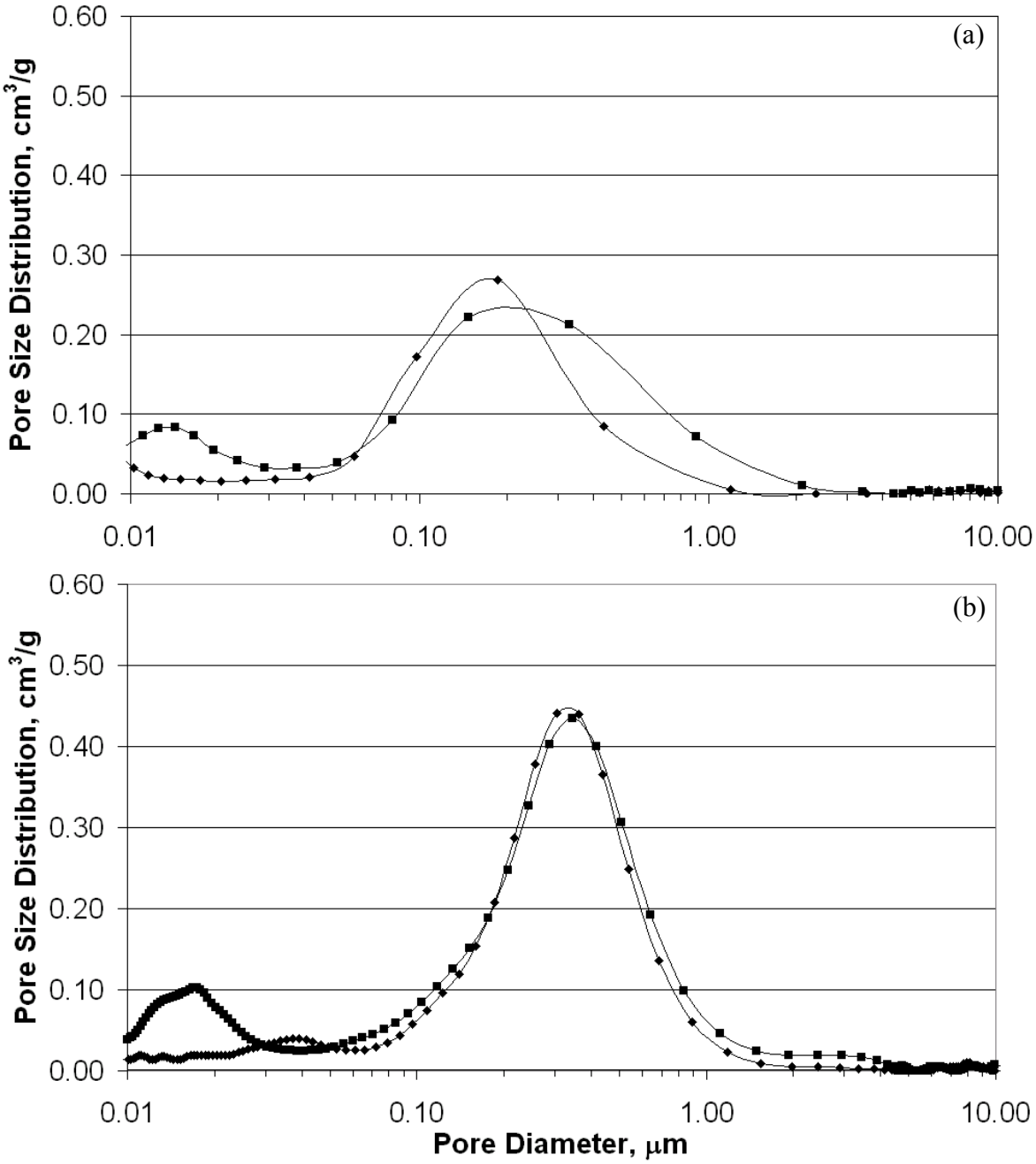

Figure 8. Pore size distribution obtained by mercury intrusion porosimetry of (a) 100% Al2O3 tablets and (b) tablets with 7.7 wt% La_2O_3. Samples were calcined at 900°C for 3 hr (◆) or 1100 °C for 2 hr (■).

porosity is more narrowly focused about a larger mean size. It also indicates that the pore size distribution is essentially independent of the calcination temperature between 900°C and 1100°C, which correlates with the effect of calcination temperature over this range on the compressive strength.

Further insight into the effect of adding lanthanum nitrate to the alumina mixture, tablet casting and subsequent calcination can be gained from consideration of the thermal decomposition of bulk lanthanum nitrate hexahydrate and the phase diagram of lanthanum oxide and aluminum oxide. The phase expected to form from reaction between lanthanum oxide and aluminum oxide, $LaAlO_3$, was observed by XRD. The formation of this material by the solid state reaction between La_2O_3 and Al_2O_3 at a temperature as low as 900°C seems unlikely considering the high melting points and sintering temperatures of all three compounds (see Table 4). A more likely explanation is that an intermediate thermal decomposition product of the lanthanum nitrate hydrate interacts with the alumina as the materials are heated from room temperature to calcination temperature. The series of decomposition products that can result from heating the lanthanum nitrate hexahydrate is indicated in Table 6. Also shown for comparison are the thermal decomposition products resulting from heating calcium nitrate tetrahydrate. It is conceivable that any of the lanthanum nitrate decomposition products, especially those formed at higher temperatures, could react with Al_2O_3 to form $LaAlO_3$. For example, Gobichon et al.[36] claimed that one of the decomposition products, i.e. $LaO(NO_3)$, which is formed at 440°C, is unstable and will react with CO_2 in air to form $La_2O_2CO_3$. The demonstrated reactivity of $LaO(NO_3)$ suggests that it may also react with Al_2O_3. From these and other considerations it appears that the interaction between Al_2O_3 and a decomposition product of lanthanum nitrate hydrate is most

Table 6. Analysis thermal effects upon heating bulk $La(NO_3)_3$•6 H_2O and $Ca(NO_3)_2$•4 H_2O.

$La(NO_3)_3$•6 H_2O Decomposition[a]		**$Ca(NO_3)_2$•4 H_2O Decomposition**	
Temp, °C	**Occurrence**	**Temp, °C**	**Occurrence**
54	$La(NO_3)_3$•6 H_2O melts	40	$Ca(NO_3)_2$•4 H_2O melts[b]
90	Decomposes to $La(NO_3)_3$•5 H_2O	40	Decomposes to $Ca(NO_3)_2$•3 H_2O[b]
105	Decomposes to $La(NO_3)_3$•4 H_2O	40-140	Decomposes to a mixture of $Ca(NO_3)_2$•3 H_2O and α-$Ca(NO_3)_2$•2H_2O[b]
150	Decomposes to $La(NO_3)_3$•3 H_2O	140-225	Decomposes to $Ca(NO_3)_2$[b]
175	Decomposes to $La(NO_3)_3$•2 H_2O	563	$Ca(NO_3)_2$ melts[c]
215	Decomposes to $La(NO_3)_3$•H_2O	659-679	Decomposes to CaO[c]
410	Decomposes to $La(OH)(NO_3)_2$	2613	CaO melts[e]
440	Decomposes to $LaO(NO_3)$[d]		
570	Decomposes to $La_4O_5(NO_3)_2$		
640	Decomposes to La_2O_3		
2304	La_2O_3 melts[e]		

[a]Taken from Mekhemer and Balboul.[37]
[b]Taken from Nirsha, et al.[38]
[c]Taken from Ettarh and Galwey.[19]
[d]Claimed to react with CO_2 in air to form $La_2O_2CO_3$.[36]
[e]Taken from CRC Handbook of Chemistry and Physics.[15]

likely responsible for the increase in strength of the cast tablets. This interaction most likely occurs while the material is being heated gradually to the final calcination temperature of either 900°C or 1100°C, which accounts for the apparent lack of dependence on the final calcination temperature. Additionally, since XRD analysis revealed the presence of crystalline $LaAlO_3$, which has a high melting point, a stable material was made with a high crushing strength and an interstitial pore size distribution that was not affected by temperature over the 900°C to 1100°C range.

The dramatic increase in compressive force required to break the cast tablets made with lanthanum nitrate appeared to be due to local bonding and not due to densification of the cast tablets while being calcined. The lack of densification was based on the interstitial pore volume between particles in the cast tablets determined by mercury porosimetry. The interstitial pore volume of the cast tablets was determined over a range of pore diameters from 0.05 μm to 10.0 μm. Pure alumina cast tablets calcined at 900°C for 3 hr had a pore volume of 0.20 cm^3/g while similar tablets calcined 1100°C for 2h had a pore volume of 0.23 cm^3/g. In contrast, cast tablets made with added lanthanum and calcined under similar conditions exhibited pore volumes of 0.27 cm^3/g and 0.28 cm^3/g, respectively. Thus, local binding of the alumina particles and not an overall densification of the cast tablets took place. The same trend was observed when Microna 3 limestone was introduced to strengthen the tablets. The lack of densification is beneficial because it permits gas to diffuse through the material when it is used as a shell around a core of sorbent material.

Core-in-Shell Pellets

Since the addition of lanthanum had greatly increased the compressive strength of cast alumina tablets, further tests were conducted to see if lanthanum would have a similar

effect on the compressive strength of core-in-shell pellets when lanthanum was added to the shell material. The breaking force of spherical core-in-shell pellets and cylindrical tablets would likely have different modes of fracture and the compressive strengths are not directly comparable. Therefore, spherical core-in-shell pellets with and without lanthanum were produced in order to compare compressive strength testing results. To control the amount of La_2O_3 present in the alumina shell, lanthanum was added to the shell mixture prior to pelletization. Measured quantities of the specific alumina mixture used previously and a lanthanum nitrate solution were mixed and then allowed to dry. The resulting material was reground and applied as a shell material to spherical pellets made of Microna 3 limestone. The core-in-shell pellets were subsequently calcined at either 900°C for 3 hr or 1100°C for 2 hr. A compressive strength test of the calcined pellets produced the results presented in Figure 9. Since the spherical pellets did not have a flat surface over which a force could be applied, the results are presented in terms of the breaking force in Newtons divided by the pellet diameter in millimeters. The pellets that were produced with only alumina present in the shell composition were weak, which was expected. Surprisingly, the addition of 4.7 wt% La_2O_3 to the shell material seemed to have no effect on the compressive strength, whereas the addition of 7.7 wt% La_2O_3 improved the compressive strength significantly. However the improvement in compressive strength was not as large as that observed with the cast tablets. On the other hand, as with the cast tablets, the calcination temperature over the 900°C to 1100°C range did not have a significant effect on the compressive strength.

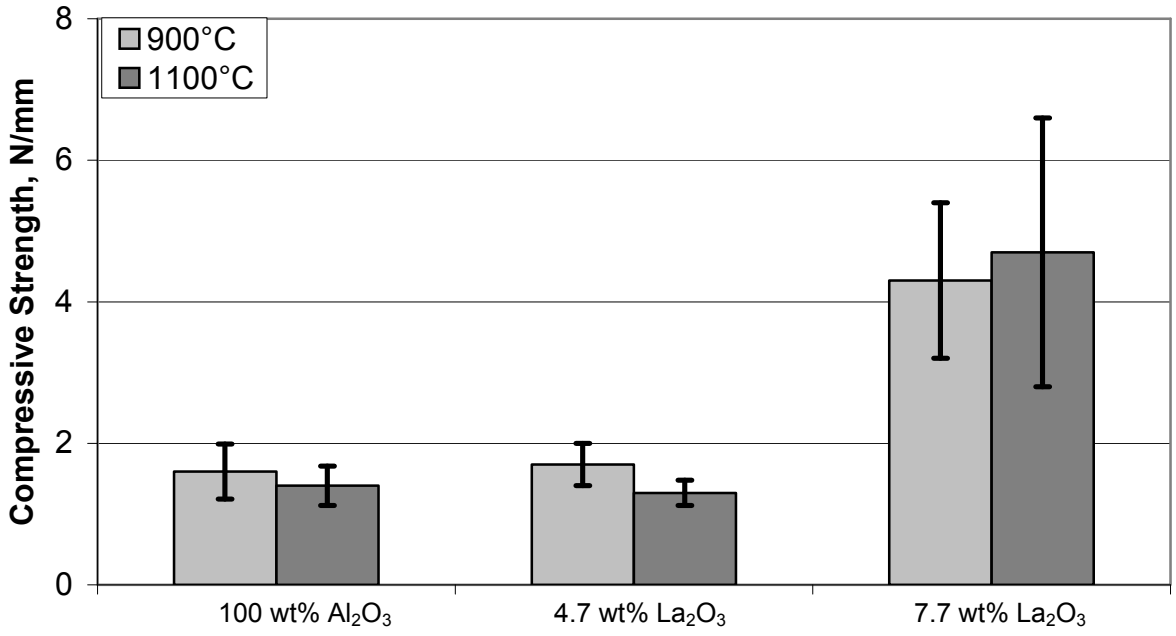

Figure 9. Compressive strength of core-in-shell spherical pellets with lanthanum nitrate added to the Al_2O_3 shell mixture prior to pelletization. The cores were made of Microna 3 limestone. The samples were calcined at 900°C for 3 hr or 1100°C for 2 hr.

Conclusions

An improved alumina-based material has been developed for use in the shell of spherical core-in-shell pellets such that each pellet combines a sorbent core of CaO surrounded by a porous but strong shell of alumina that can support a nickel catalyst. Increasing the strength while preserving the surface area of the alumina-based material was the goal of this research. To achieve this goal, different formulations of the alumina-based material were used in the preparation of cast tablets that were calcined and subsequently subjected to a compression test and surface area determination. Additional insight was gained by subjecting some calcined tablets to X-ray diffraction analysis. The alumina formulations included substances such as limestone or calcium nitrate, which decomposed on

heating to form CaO, which reacted with Al_2O_3 to form calcium aluminate. Among the additives tested only Microna 3 limestone, calcium nitrate, and lanthanum nitrate produced a significant increase in the compressive strength of cast tablets. In the case of limestone, a significant increase in tablet strength was achieved by calcining the tablets at 1100°C but not at 900°C. The presence of $CaAl_2O_4$ in tablets calcined at the higher temperature indicated that $CaAl_2O_4$ acted as a binder and accounted for the increased strength of the tablets.

The addition of limestone to the tablet formulation only seemed to have an effect on the surface area when it was applied at the higher concentration (10 wt%), and the tablets were calcined at the higher temperature (1100°C). With all of the formulations tested, the surface area of the tablets calcined at 1100°C was much lower than that of tablets calcined at 900°C, and the difference was nearly the same in all cases. The drop in surface area was probably due to increased pore sintering of the DD-290 alumina, which had a large surface area initially.

A large increase in compressive strength was achieved by incorporating lanthanum nitrate in the tablet material. The results achieved by calcining the pellets at 900°C are of particular interest because they showed that the compressive strength of the tablets to be equal to that of tablets calcined at 1100°C. Therefore, by employing lanthanum nitrate and a calcination temperature of 900°C, it is possible to produce a strong alumina-based material with a large surface area.

The excellent results achieved with lanthanum were extended to core-in-shell pellets in which the shell formulation included lanthanum nitrate that decomposed when the pellets were calcined and the product reacted with the alumina present. However, the results

differed from the previous ones in that a larger concentration of La_2O_3 was required to achieve a similar increase in the relative compressive strength of the material. The need for a larger concentration of La_2O_3 in the pelletized material may have been due to differences in either the density or the structure of the two materials.

Acknowledgement

This report was prepared with the support of the U.S. Department of Energy, under Award No. DE-FG26-04NT 42182. However, any opinions, findings, conclusions, or recommendations expressed herein are those of the authors and do not necessarily reflect the views of DOE.

Literature Cited

(1) Akiti, T. T., Jr.; Constant, K. P.; Doraiswamy, L. K.; Wheelock, T. D., A Regenerable Calcium-Based Core-in-Shell Sorbent for Desulfurizing Hot Coal Gas. *Industrial & Engineering Chemistry Research* **2002,** 41, (3), 587-597.

(2) Hasler, D. J. L.; Doraiswamy, L. K.; Wheelock, T. D., A Plausible Model for the Sulfidation of a Calcium-Based Core-in-Shell Sorbent. *Industrial & Engineering Chemistry Research* **2003,** 42, (12), 2644-2653.

(3) Hasler, D. J. L.; Franck, B. J.; Wheelock, T. D., A reusable calcium-based sorbent for hot gas cleaning. *American Institute of Chemical Engineers, [Spring National Meeting], New Orleans, LA, United States, Mar. 30-Apr. 3, 2003* **2003**, 2554-2568.

(4) Hasler, D. J.; Wheelock, T. D.; Doraiswamy, L. K.; Constant, K. P., Physical Properties and Composition Effects on the Reactivity of Calcium-Based Sulfur Sorbents. *Industrial & Engineering Chemistry Research* **2007,** 46, (18), 5913-5921.

(5) Akiti, T. T., Jr.; Constant, K. P.; Doraiswamy, L. K.; Wheelock, T. D., Development of an advanced calcium-based sorbent for desulfurizing hot coal gas. *Advances in Environmental Research* **2001,** 5, (1), 31-38.

(6) Akiti, T. T.; Constant, K. P.; Doraiswamy, L. K.; Wheelock, T. D., An improved core-in-shell sorbent for desulfurizing hot coal gas. *Advances in Environmental Research* **2002,** 6, (4), 419-428.

(7) Wheelock, T. D.; Akiti, T. T. Core-in-shell sorbent for hot coal gas desulfurization. Patent:2002103074, 2002.

(8) Satrio, J. A.; Shanks, B. H.; Wheelock, T. D., Development of a Novel Combined Catalyst and Sorbent for Hydrocarbon Reforming. *Industrial & Engineering Chemistry Research* **2005,** 44, (11), 3901-3911.

(9) Schmalzried, H., *Chemical Kinetics of Solids*. VCH Verlagsgesellschaft: Weinheim, Germany, 1995; p 433.

(10) An, L.; Chan, H. M., R-curve behavior of in-situ-toughened Al2O3:CaAl12O19 ceramic composites. *Journal of the American Ceramic Society* **1996,** 79, (12), 3142-3148.

(11) Zhao, S. J.; Hu, X. D.; Born, M.; Ladebeck, J. *A New Class of High Temperature Support of H_2 and Snthesis Gas Generation -- Alumina-Rich Pure Calcium Aluminate*; Sud-Chemie Inc.: Louisville, KY 40210 (USA).

(12) An, L.; Chan, H. M.; Soni, K. K., Control of calcium hexaluminate grain morphology in in-situ toughened ceramic composites. *Journal of Materials Science* **1996,** 31, (12), 3223-3229.

(13) Asmi, D.; Low, I. M., Physical and mechanical characteristics of in-situ alumina/calcium hexaaluminate composites. *Journal of Materials Science Letters* **1998,** 17, (20), 1735-1738.

(14) Nurse, R. W.; Welch, J. H.; Majumdar, A. J., The CaO-Al2O3 system in a moisture-free atmosphere. *Transactions of the British Ceramic Society* **1965,** 64, (9), 409-18.

(15) *CRC Handbook of Chemistry and Physics*. 87th Edition ed.; Taylor & Francis Group: Boca Raton, Fl, 2006-2007.

(16) Dimitrov, V.; Komatsu, T., Classification of Simple Oxides: A Polarizability Approach. *Journal of Solid State Chemistry* **2002,** 163, (1), 100-112.

(17) Balta, P., The chemical reactivity of oxides and basicity. *Materiale de Constructii (Bucharest)* **2000,** 30, (3), 179-183.

(18) Honma, T.; Benino, Y.; Fujiwara, T.; Komatsu, T.; Sato, R.; Dimitrov, V., Electronic polarizability, optical basicity, and interaction parameter of La2O3 and related glasses. *Journal of Applied Physics* **2002,** 91, (5), 2942-2950.

(19) Ettarh, C.; Galwey, A. K., A kinetic and mechanistic study of the thermal decomposition of calcium nitrate. *Thermochimica Acta* **1996,** 288, (1-2), 203-219.

(20) Yamamoto, T.; Hatsui, T.; Matsuyama, T.; Tanaka, T.; Funabiki, T., Structures and Acid-Base Properties of La/Al2O3 - Role of La Addition to Enhance Thermal Stability of g-Al2O3. *Chemistry of Materials* **2003,** 15, (25), 4830-4840.

(21) Chen, X.; Liu, Y.; Niu, G.; Yang, Z.; Bian, M.; He, A., High temperature thermal stabilization of alumina modified by lanthanum species. *Applied Catalysis, A: General* **2001,** 205, (1,2), 159-172.

(22) Gorter, H.; Bos, B.; Dortmans, L. J. M. G., Processing of in situ reinforced alumina composites. *Ceramic Engineering and Science Proceedings* **2003,** 24, (4, 27th International Cocoa Beach Conference on Advanced Ceramics and Composites, 2003, Part B), 127-133.

(23) Ropp, R. C.; Carroll, B., Solid-state kinetics of lanthanum aluminum oxide (LaAl11O18). *Journal of the American Ceramic Society* **1980,** 63, (7-8), 416-19.

(24) Guo, R.; Ravindranathan, P.; Selvaraj, U.; Bhalla, A. S.; Cross, L. E.; Roy, R., Modified mixed oxide perovskites 0.7Sr(Al1/2B12) O3.03LaAlO3 and 0.7Sr(Al1.2B1/2) O3.0.3NdGaO3 (B = Ta5+ or Nb5+) for high-Tc superconductor substrate applications. *Journal of Materials Science* **1994,** 29, (19), 5054-8.

(25) Anseau, M. R.; Cambier, F.; Leblud, C., Some comments on ceramic solid-state reaction kinetics using results obtained on the zinc oxide-alumina system. *Journal of Materials Science* **1981,** 16, (4), 1121-6.

(26) Chen, Z.-Z.; Shi, E.-W.; Zheng, Y.-Q.; Li, W.-J.; Xiao, B.; Zhuang, J.-Y.; Tang, L.-A., Particle size control and dependence on precursor pH: synthesis uniform submicrometer zinc aluminate particles. *Journal of the American Ceramic Society* **2005,** 88, (1), 127-133.

(27) Kingsley, J. J.; Suresh, K.; Patil, K. C., Combustion synthesis of fine particle rare earth orthoaluminates and yttrium aluminum garnet. *Journal of Solid State Chemistry* **1990,** 88, (2), 435-42.

(28) Ali, M. M.; Agarwal, S. K.; Handoo, S. K., Diffusion studies in formation and sintering of CaAl2O4 and BaAl2O4: a comparative evaluation. *Cement and Concrete Research* **1997,** 27, (7), 979-982.

(29) Satrio, J. A.; Shanks, B. H.; Wheelock, T. D., A Combined Catalyst and Sorbent for Enhancing Hydrogen Production from Coal or Biomass. *Energy & Fuels* **2007,** 21, (1), 322-326.

(30) Cheng, J.; Zhou, J.; Liu, J.; Zhou, Z.; Huang, Z.; Cao, X.; Zhao, X.; Cen, K., Sulfur removal at high temperature during coal combustion in furnaces: A review. *Progress in Energy and Combustion Science* **2003,** 29, (5), 381-405.

(31) Fumo, D. A.; Morelli, M. R.; Segadaes, A. M., Combustion synthesis of calcium aluminates. *Materials Research Bulletin* **1996,** 31, (10), 1243-1255.

(32) Bunting, E. N., Phase equilibria in the system: SiO2-ZnO-Al2O3. *Bur. Standards J. Research* **1932,** 8, 279-87.

(33) Kadyrova, Z. R.; Sirazhiddinov, N. A., Barium aluminate gallate (BaAl2(1-x)Ga2xO4). *Zhurnal Neorganicheskoi Khimii* **1986,** 31, (6), 1530-2.

(34) Udalov, Y. P., Calculated fusibility diagrams of MO-Ln2O3-Al2O3 systems (M = magnesium, strontium, or barium). *Zhurnal Neorganicheskoi Khimii* **1977,** 22, (2), 483-9.

(35) *Handbook of Advanced Ceramics*. 1st ed.; Elsevier: London, England, 2003; Vol. 1: Materials Science, p 787.

(36) Gobichon, A.-E.; Auffredic, J.-P.; Loueer, D., Thermal decomposition of neutral and basic lanthanum nitrates studied with temperature-dependent powder diffraction and thermogravimetric analysis. *Solid State Ionics* **1996,** 93, (1,2), 51-64.

(37) Mekhemer, G. A. H.; Balboul, B. A. A., Thermal genesis course and characterization of lanthanum oxide. *Colloids and Surfaces, A: Physicochemical and Engineering Aspects* **2001,** 181, (1-3), 19-29.

(38) Nirsha, B. M.; Obozenko, Y. V.; Fakeev, A. A., Study of the thermal dehydration of calcium nitrate tetrahydrate. *Izvestiya Akademii Nauk SSSR, Neorganicheskie Materialy* **1981,** 17, (8), 1435-7.

Chapter 4. High Concentration H_2 Production via the Steam-Methane Reforming Reaction Utilizing a Combined Catalyst/Sorbent Core-in-Shell Material

A paper to be submitted to *Industrial & Engineering Chemistry Research*

Karl O. Albrecht,[a] Justinus A. Satrio,[b] Brent H. Shanks[a] and Thomas D. Wheelock[a,*]

Abstract

The ability of a novel combined catalyst and sorbent material to produce H_2 by reacting a mixture of CH_4 and steam was investigated by employing a reactor packed with the material. The combined catalyst and sorbent was in the form of multi-layered spherical pellets, each having an inner core and outer shell. The core of a core-in-shell pellet was composed of CaO derived from limestone. The shell of the pellet was composed of an alumina formulation that served the dual function of protecting the friable CaO core while also supporting a Ni catalyst that was required to catalyze the steam-methane reforming reaction. Based on the results of previous investigations, two core-in-shell formulations were chosen for study. One formulation had 10 wt% limestone added to the shell mixture. The other formulation added lanthanum oxide to the shell composition by first doping the alumina mixture with a solution of lanthanum nitrate. Both formulations utilized 3.2 μm mean diameter particles of limestone in the core as a CaO precursor. Reaction testing in the range of 550-650°C and 1.0-10.0 atm showed that both core-in-shell formulations were capable of producing H_2 at or near equilibrium levels during a period when CO_2 was being

[a]Dept. of Chemical and Biological Engineering, 2114 Sweeney Hall, Iowa State University, Ames, IA 50011

[b]Center for Sustainable Environmental Technologies, 0411 Marston Hall, Iowa State University, Ames, IA 50011

*Corresponding Author: wheel@iastate.edu

rapidly absorbed by the CaO sorbent. Lifecycle testing of the core-in-shell pellets was also performed at 650°C and 1.0 atm over 10 cycles of H_2 production and sorbent regeneration. A product stream with 98 mol% H_2 (dry basis) was produced with either core-in-shell formulation during each cycle of the lifecycle testing. However, the length of time high concentration H_2 was produced during each cycle decreased as the number of cycles increased because of a decrease in the sorbent absorption capacity. Sintering of the Ni catalyst and fracturing of the core-in-shell pellets was also shown to occur during lifecycle testing.

Introduction

Hydrogen is an important chemical with a wide variety of industrial uses. For example, it is used in the synthesis of methanol and ammonia as well for the hydrogenation of various materials used in the production of chemicals, petroleum, food and pharmecueticals.[1] In addition, if fuel cells in automobiles become commercially available, the amount of hydrogen consumed will increase dramatically.[2] Therefore, efficient means for the production of H_2 is an active research area with the potential for large economic and societal benefits

The most widely used industrial method for the production of H_2 is the steam reforming of methane or other hydrocarbons.[1] The steam-methane reforming reaction is conducted over a supported Ni catalyst, and it is represented by the following reaction:

$$CH_4 + H_2O \leftrightarrow 3H_2 + CO \qquad \Delta H_{25°C} = 206 \text{ kJ/mol} \qquad (1)$$

This reaction is highly endothermic. In order to achieve maximum conversion of CH_4, industrial reformers operate with an exit temperature of 900-1100°C.[1] A byproduct of steam-

methane reforming is CO. Thus, the gas produced by the steam-methane reforming step is further treated by the water-gas shift reaction, which is given by:

$$CO + H_2O \leftrightarrow CO_2 + H_2O \qquad \Delta H_{25°C} = -41 \text{ kJ/mol} \tag{2}$$

In order to maximize the conversion of CO by the exothermic water-gas shift reaction, a two-step reaction scheme is industrially employed. First, the process stream is cooled from the CH_4 reformer and then treated in a high temperature shift reactor over a Fe_3O_4/Cr_2O_3 catalyst at 350-500°C. The product of this reactor is then treated in a low temperature shift reactor, which operates at about 200°C and contains a $Cu/ZnO/Al_2O_3$ catalyst. The stream leaving the low temperature shift reactor will have a dry basis composition of 2-3% CO, 20% CO_2, and 77-78% H_2. The mixture is subsequently treated with an amine scrubber to remove most of the CO_2 and any residual CO_2 and CO can be removed by methanation over another Ni catalyst.

The industrial method of H_2 production is a complicated, multi-step process. Several recent investigations have attempted to simplify this process by mixing a CO_2 sorbent with the CH_4 reforming catalyst so as to remove the CO_2 as it is produced.[3] By combining the catalyst and sorbent, the methane reforming and water-gas shift reactions can be conducted simultaneously with CO_2 separation. Selective removal of CO_2 also allows for the equilibrium conversion limitations of the steam-methane reforming and water-gas shift reactions to be overcome, resulting in CH_4 and CO conversions that are much higher than would be possible otherwise. Therefore, by combining the catalyst and CO_2 sorbent, it should be possible to replace a complicated multi-step process with a more efficient single-step method.

Different CO_2 sorbents are capable of selectively absorbing CO_2 in order to produce H_2 in a single step. Recently, Harrison[3] documented several different sorbents that could be used to produce high concentration H_2 through sorption enhanced reactions. Two of the more promising sorbents that have received a large amount of investigation are potassium promoted hydrotalcite sorbents and CaO.

A proprietary KCO_3-promoted hydrotalcite sorbent was utilized by Hufton et al.[4] to produce a stream with 95 mol% H_2 and 5 mol% CH_4 that contained less than 50 ppm carbon oxide impurities. The process was conducted at 450°C and 4.7 atm while utilizing a 6:1 steam to CH_4 feed ratio. Likewise, Ding and Alpay[5] used an industrial K-promoted hydrotalcite sorbent to selectively remove CO_2 at a reaction temperature of 450°C . These authors determined that a lower steam to methane ratio could be utilized than in normal steam-methane reforming operations. However, Cobden et al.[6] studied hydrotalcite sorbents for steam-methane reforming at 400°C and suggested increasing the temperature of the process in order to reduce the amount of catalyst required because of low reaction rates. Hydrotalcite based sorbents are typically used at lower temperatures than CaO sorbents. Additionally, hydrotalcite thermally decomposes to a solid solution of MgO and Al_2O_3 above 600°C, which limits the effective range of CO_2 sorption to between 400-600°C.[6]

Calcium oxide is also an attractive CO_2 sorbent that has been the focus of recent investigations. CaO reacts with CO_2 to form a carbonate, as shown in reaction 3:

$$CaO + CO_2 \leftrightarrow CaCO_3 \qquad \Delta H_{25°C} = -175 \text{ kJ/mol} \qquad (3)$$

Ochoa-Fernández et al.[7] studied several CO_2 sorbents including CaO for use in sorption enhanced steam-methane reforming and determined that CaO was a superior CO_2 acceptor based on the favorable thermodynamic properties of CaO to absorb CO_2 as well as the rapid

kinetics of absorption and regeneration. However, it was also determined that the ability of CaO to absorb CO_2 over numerous absorption and sorbent regeneration cycles needed enhancement. The amount of CO_2 that CaO can absorb decreases as the number of absorption and regeneration cycles increases. On the other hand, CaO has been shown recently to absorb 2.7 mmol of CO_2/g CaO after 1250 cycles CO_2 absorption and regeneration,[8] whereas some fresh hydrotalcite based sorbents have an initial CO_2 capture capacity of less than 1 mmol CO_2/g sorbent.[6, 9] Thus, CaO that has experienced a substantial number of absorption and regeneration cycles could have a larger absorption capacity than fresh hydrotalcite based sorbents. Additionally, Abanades et al.[10] reported that the price of hydrotalcite sorbents is approximately 1000 times greater than crushed $CaCO_3$. Therefore, CaO is an economical CO_2 sorbent with an absorption capacity that could be superior to other sorbents even after numerous cycles of absorption and regeneration.

Sorption enhanced steam-methane reforming utilizing CaO as the CO_2 sorbent has been the focus of several investigations in recent years. Balasubramanian et al.[11] studied simultaneous application of reactions 1-3 using high concentration $CaCO_3$ as the sorbent precursor and a Ni-supported Al_2O_3 catalyst. Under process conditions of 550-750°C and 15 atm with a 1:4 mole ratio of CH_4:H_2O in 70% inert N_2, H_2 was produced within 1% of calculated equilibrium values. Additionally, a stream with 95 mol% H_2 was produced in a single reactor at 650°C and 15 atm using a 1:4 mole ratio of CH_4:H_2O with no N_2 dilution.

Ortiz and Harrison[12] tested dolomite as a CaO precursor for use with a Ni catalyst for the production of high concentration H_2. The dolomite required a sulfur removal pretreatment to avoid poisoning the Ni catalyst. The durability of the dolomite based sorbent was tested through several cycles of absorption and regeneration conducted in the 800-950°C

range while supplying either pure CO_2 or pure N_2. The absorption capacity of the CaO sorbent decreased with an increasing number of cycles regardless of regeneration conditions. However, when the sorbent was regenerated at 950°C in N_2, the H_2 concentration produced also decreased substantially after 6 cycles. This was explained as a reduction in sorbent activity as the number of cycles increased. Thus, sorbent activity can affect the overall concentration of H_2 produced.

Yi and Harrison[13] investigated sorption enhanced steam-methane reforming as a method for producing H_2 with a low CO concentration for use in an atmospheric PEM fuel cell. Since H_2 production was to be integrated with the PEM fuel cell, the sorption-enhanced reaction was studied at 1 bar. To produce a product stream with a very low CO concentration at atmospheric pressure, a reaction temperature of 460°C was chosen to maximize the CO conversion via the exothermic water-gas shift reaction. A product gas with 96 mol% H_2 and only 50 ppmv CO was produced at 460°C and 1 bar with a 3:1 mole ratio of H_2O:CH_4. An even lower CO concentration of 11 ppmv was obtained by increasing the pressure to 3 bar and decreasing the temperature to 440°C. However, the H_2 concentration fell to 92 mol% because less CH_4 was converted.

The combination of the steam-methane reforming and water-gas shift reactions coupled with CO_2 absorption by a CaO sorbent has been demonstrated as an attractive method of producing high concentration H_2 in a single step. However, most previous studies have employed a physical mixture of powdered catalyst and sorbent in a fixed bed reactor. Industrial scale-up of powder bed reactors is subject to special challenges such as gas channeling through the powdered bed and a large pressure drop. Increasing the particle size of the material through pelletization could address some of these challenges. However,

pelletized CaO is friable and easily broken during handling and reactor loading. To over come this deficiency, a method of encapsulating the sorbent in a strong but porous protective shell was conceived.[14-17] By making the shell of powdered alumina, it could be strengthened by high temperature calcination, thus creating a core-in-shell pellet. After the application of the alumina-basis shell, the material was subjected to high temperature heat treatment in order to sinter the shell, which created a core-in-shell pellet with a reactive CaO core and a strong alumina-based shell.

The core-in-shell concept was originally developed for the absorption of sulfurous gases in hot coal.[14-19] The core-in-shell material utilized a reactive CaO core and a shell that was composed mainly of low surface area α-Al_2O_3. Initial development of the core-in-shell concept for sulfur removal determined that the addition of limestone to the alumina shell mixture increased the physical strength of the core-in-shell pellets.[14] This enhancement in strength was believed to be from the formation of a binding calcium aluminate phase formed during high temperature calcination.

Subsequent development of the core-in-shell concept for application as an advanced material for sorption enhanced steam-methane reforming showed that Ni could be added to the shell material by wet impregnation with a $Ni(NO_3)_2$ solution.[20] Then it was shown that the activity of the Ni catalyst could be improved by replacing some of the low surface area α-Al_2O_3 with a higher surface area amorphous Al_2O_3. However this change also decreased the physical strength of the material. Testing of the core-in-shell concept demonstrated the ability of the advanced material to produce H_2 in large concentrations by reacting steam with CH_4 at 580-600°C or with C_3H_8 at 560°C.[20] Furthermore, the use of the core-in-shell pellets produced H_2 in high concentrations by reacting toluene and steam at 600°C and 1.0 atm.[21]

Since the addition of high surface area alumina was determined to be detrimental to the strength of the core-in-shell pellets,[20] further development of the shell formulation was undertaken to produce a high surface area alumina-based material with enhanced physical strength.[22] Two methods of enhancing the strength of the core-in-shell pellets were investigated. First, finer size limestone than that had previously been used was added to the shell formulation to create more of a binding calcium aluminate phase by providing more intimate contact between Al_2O_3 and CaO particles during high temperature calcination. The addition of 10 wt% limestone (3.2 μm mean particle size) and subsequent calcination at 900°C for 3 hr or 1100°C for 2 hr in flowing air was determined to increase the physical strength of the alumina-based material compared to similar samples made without limestone. Secondly, the addition of La_2O_3 to the shell formulation through doping the alumina mixture with lanthanum nitrate followed by calcination at 900°for 3 hr or 1100°C for 2 hr also significantly increased the strength of the shell material. Interestingly, the addition of lanthanum to the shell formulation resulted in an increase in the strength of the material that was the same for either calcination temperature. However, all of the samples calcined at 1100°C for 2 hr had a lower surface area than those calcined at 900°C for 3 hr, which was probably due to sintering of the high surface area amorphous alumina.

The purpose of the present investigation was to test the performance of core-in-shell pellets impregnated with a Ni catalyst at producing high concentration H_2 from CH_4 and steam in a single stage. Two of the most promising shell formulations determined previously were used in the core-in-shell pellets. One of the shell formulations consisted of 90 wt% Al_2O_3 and 10 wt% 3.2μm mean particle size limestone. A second formulation consisted of Al_2O_3 doped with lanthanum nitrate. After calcination this formulation would have been

equivalent to a mixture composed of 7.7 wt% La_2O_3 and 92.3 wt% Al_2O_3. Both core-in-shell formulations utilized limestone with a 3.2 μm mean particle size in the core material. Additionally, both core-in-shell formulations were calcined at 900°C for 3 hr to strengthen the material. This temperature was selected over calcination at 1100°C because it resulted in less loss of shell surface area. While previous tests of the core-in-shell material were conducted at atmospheric pressure, present testing was extended to higher pressures up to 10.0 atm. After calcination followed by H_2 reduction, all of the pellets contained about 6 wt% Ni in the shell.

The current investigation also undertook limited lifecycle testing of the core-in-shell material. The core-in-shell pellets with the two different shell formulations were subjected separately to lifecycle testing. This testing was limited to 10 cycles of H_2 production and sorbent regeneration conducted at 1.0 atm and 650°C. Selected physical properties of the core-in-shell pellets were also measured before and after lifecycle testing to determine what the effect on the physical properties of the pellets.

Thermodynamic Analysis

To better understand the effects of temperature and pressure on the steam-methane reforming process, a thermodynamic analysis of the chemical reactions was carried out. This analysis was conducted by simultaneously solving the equilibrium expressions for the steam-methane reforming reaction, the water-gas shift reaction and the reaction between CaO and CO_2. The equilibrium constants for the steam-methane reforming and water-gas reactions were obtained from the *Catalyst Handbook*.[23] The equilibrium constant for the reaction between CaO and CO_2 was obtained from *Metallurgical Thermochemistry*[24] As a basis for comparison, the thermodynamic equilibrium expressions were also solved without the

absorption of CO_2 present. The analysis was based on an initial feed composed of 1 mol CH_4 and 3 mol H_2O and temperatures between 550°C and 850°C and pressures of 1, 5 and 10 atm.

Figure 1 indicates the concentration of H_2 in a system at thermodynamic equilibrium that was supplied initially with 3 mol of H_2O and 1 mol of CH_4. The H_2 concentrations are expressed on a dry basis. Figure 1 shows that the absorption of CO_2 by CaO greatly increases the H_2 concentration at equilibrium. For example, at 650°C and 1 atm, CO_2 absorption allows for a H_2 concentration of 95% to be produced. In comparison, without CO_2 absorption, a H_2 concentration of only 77% would be present at equilibrium. Thus, CO_2 absorption makes it possible to produce H_2 in much greater concentration than would be possible otherwise.

Figure 1 also demonstrates the effect of pressure on the H_2 concentration in a system at equilibrium. When CO_2 absorption is not present, the H_2 concentration of a system at equilibrium decreases as the pressure increases because of the effect of pressure on the steam-methane reforming reaction (equation 1). This effect also reduced the conversion of CH_4 at any temperature and pressure. When CaO is present to absorb CO_2, the system is more complex due to the reaction between CO_2 and CaO (equation 3), which is favored by increasing pressure. The net effect of the two reactions is to cause the H_2 concentration to decrease with increasing temperature once a critical temperature has been reached. At 1.0 atm, the critical temperature is about 600°C, at 5.0 atm it is about 675°C, and at 10.0 atm it is 725°C. In general, increasing the system pressure results in a decrease of H_2 concentration due to lowered CH_4 conversion. However, increased pressure allows for CaO to be utilized as a CO_2 sorbent at higher temperatures because of the increased partial pressure of CO_2.

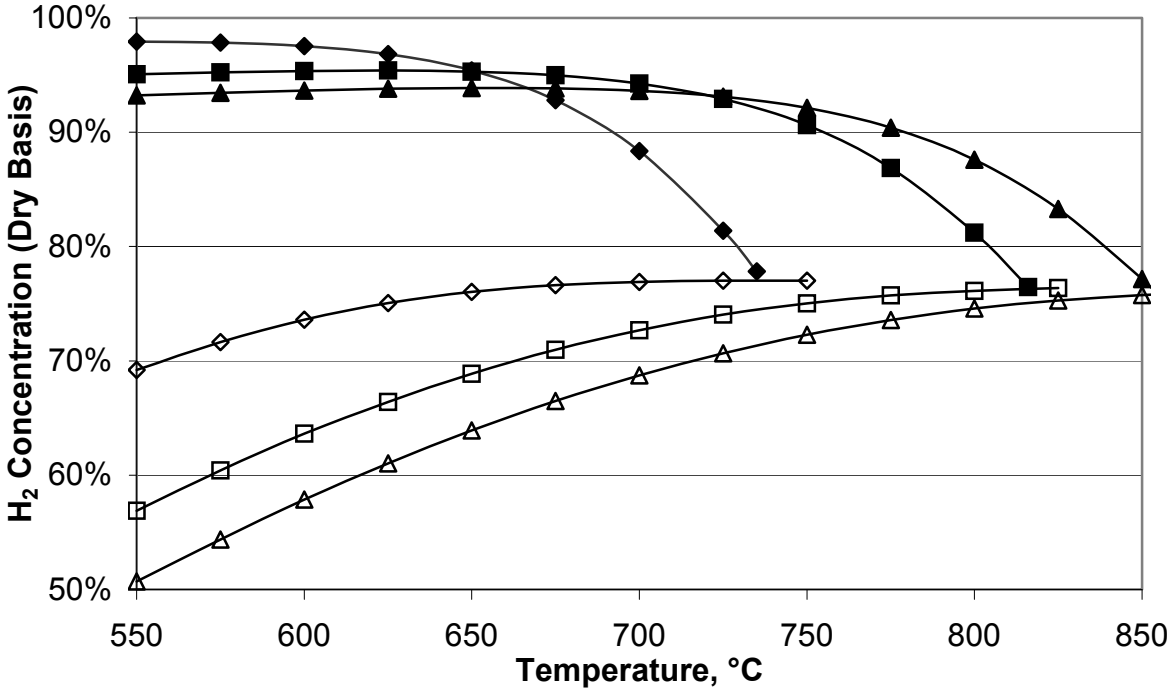

Figure 1. Equilibrium H_2 concentrations on a dry basis for a system supplied with 1.0 mol CH_4 and 3.0 mol steam. The closed symbols are with CO_2 absorption and the open symbols are without CO_2 absorption at 1 atm (◇), 5 atm (□) and 10 atm (△).

Figure 2 (a) and (b) shows the effects of temperature and pressure on the conversion of CH_4 and CO, respectively, on a reaction system in thermodynamic equilibrium. Figure 2 (a) indicates that the absorption of CO_2 allows for enhanced CH_4 conversion at lower temperatures. Since the steam-methane reforming reaction is highly endothermic, increased CH_4 conversion is favored by higher temperature. Thus, CH_4 conversions with and without CO_2 absorption eventually converge for a given system pressure at a high enough temperature. Figure 2 (a) also illustrates decreasing CH_4 conversion with increasing pressure as would be expected from equation 1. While the absorption of CO_2 by CaO does result in enhanced CH_4 conversions at temperatures lower than those applied industrially, CH_4 conversion is limited by thermodynamics even in the presence of CO_2 sorption.

In contrast to the endothermic steam-methane reforming reaction, the water-gas shift reaction is exothermic. Thus, the equilibrium conversion of CO decreases with increasing temperature, as indicated by Figure 2 (b). Additionally, increasing the pressure of the system results in a higher conversion of CO when the system is at equilibrium. The water-gas shift reaction itself is itself unaffected by system pressure at equilibrium due to the fact no net moles are produced by the forward reaction (equation 2). However, increasing the system pressure enhances the forward extent of the reaction between CaO and CO_2 (equation 3). Thus, while higher pressures inhibit CH_4 conversion, increasing the pressure results in a decreased amount of CO when CO_2 absorption is present and the system is at equilibrium. Increased system pressure could be utilized when creating a high concentration H_2 stream with a low CO concentration, which is important in applications such as H_2 produced for fuel cells.

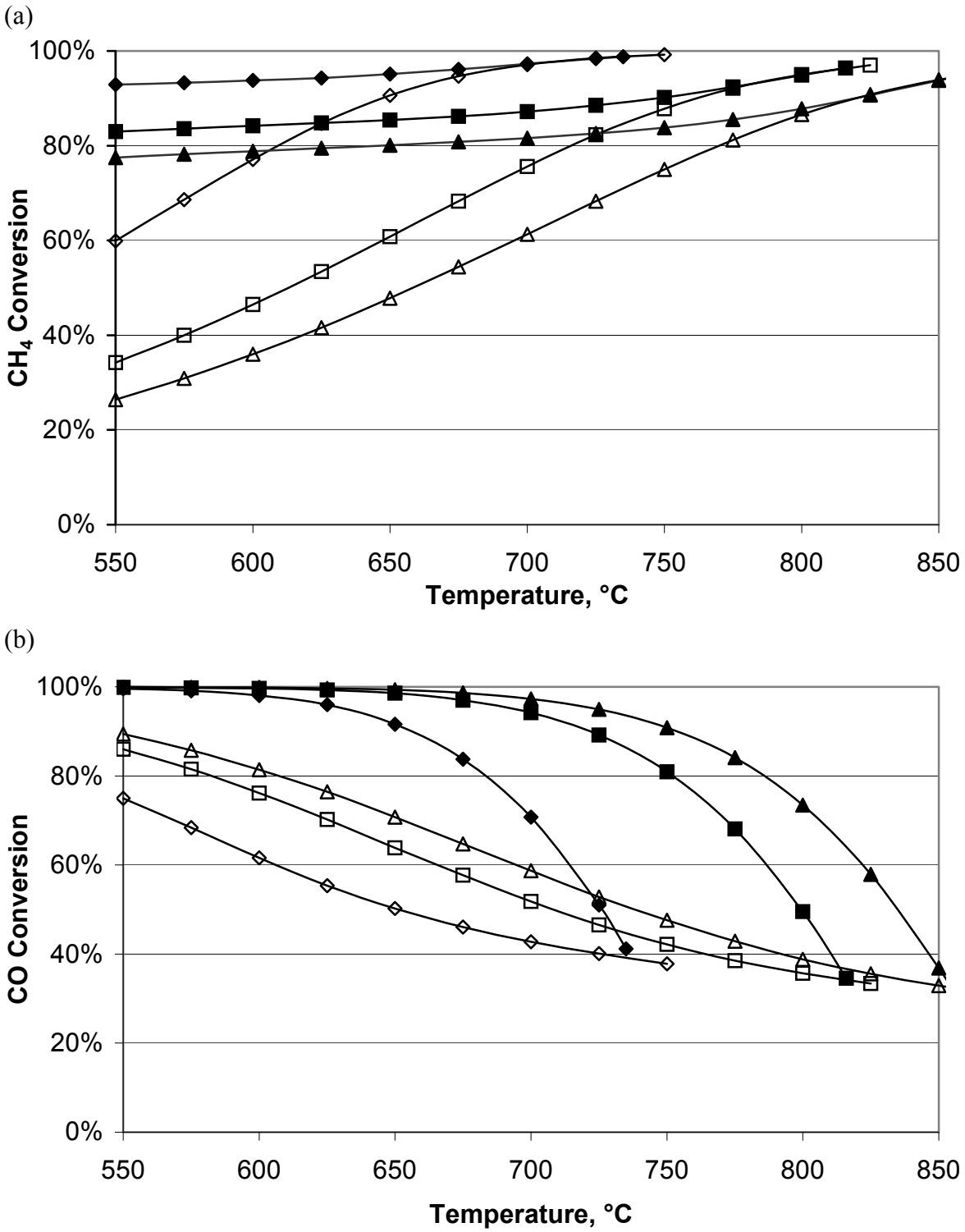

Figure 2. Conversions of (a) CH_4 and (b) CO determined by solving equilibrium expressions with a feed of 1 mol CH_4 and 3 mol H_2O. The closed symbols are with CO_2 absorption and the open symbols are without CO_2 absorption at 1 atm (◇), 5 atm (□) and 10 atm (△).

Experimental Methods and Materials

Materials

Limestone for this study was obtained from Columbia River Carbonates in Washington. The limestone designated as Microna 3 had a mean particle size of 3.2 μm and a $CaCO_3$ concentration greater than 97 wt% according to the producer. Three different types of alumina were utilized for the shell formulations of the core-in-shell pellets. Two types of α-Al_2O_3 were supplied by Almatis: one designated as A16-SG had a mean particle size of 0.4 μm and another designated as T-64 consisted of particles screened to –325 mesh, or -44μm. A third type of Al_2O_3 was an amorphous material supplied by Engelhard for use as a catalyst support precursor, and it was designated as DD-290. This material has a mean particles size of 9.8 μm and a surface area of 275 m^2/g according to the supplier who also claimed it to be identical to CP-7, formerly supplied by Almatis.

Saint-Gobain Norpro supplied three different sizes and/or shapes of SiC. SiC spheres having a diameter of 0.63 cm and denoted as SC 5232 were used to support the catalyst bed. Cylindrical SiC extrudes having a diameter of 0.64 cm and designated as SC 5132 were also used as a catalyst bed support. Finally, SiC spheres with a diameter of 0.13 cm and denoted as SC 52126 were interspersed within the bed of core-in-shell pellets to prevent gas channeling and to enhance heat transfer.

Nickel nitrate hexahydrate, $Ni(NO_3)_2 \bullet 6H_2O$, was obtained from Sigma-Aldrich and was reported to be 99.999% pure. Laboratory grade lanthanum nitrate hexahydrate ($La(NO_3)_3 \bullet 6H_2O$) was obtained from Fisher Scientific and was reported to be 98+% pure. Research grade CH_4 was obtained from Air Liquide and was used as a reactant for

performance and lifecycle testing. It was reported by the supplier to have a purity of 99.995%. Ultra-high purity Ar (99.999% pure) was supplied by Linweld to pressurize the system prior to reactant introduction. Hydrogen (99.5% pure) from Air Products was used for reduction of the Ni catalyst before reaction testing of the core-in-shell pellets.

Preparation of Core-in-Shell Pellets

Spherical core-in-shell pellets were prepared by pan rolling the powder formulations for the core and then the shell in a conical rotating drum that had a maximum diameter of 25 cm and was operated at 30 rpm. The cores of the spherical pellets were prepared first by placing Microna 3 limestone powder in the rotating drum and spraying it with water intermittently so that it balled up as the drum rotated. Cores were built up in this way until about 20 g of pellets ranging between 5 and 6 mesh, or between 3.96 mm and 3.35 mm in diameter, were produced. The cores were then hardened by operating the drum at the following speed and time settings: 10 rpm for 10 min., 30 rpm for 20 min., 60 rpm for 30 min., and 90 rpm for 30 min.

The cores were coated with a formulation composed largely of powdered Al_2O_3 that also contained either Microna 3 limestone (10 wt%) or $La(NO_3)_3$ (corresponding to 7.7 wt% La_2O_3). These concentrations were based on the results obtained previously.[22] The formulation with 10 wt% limestone also contained 27 wt% DD-290 amorphous Al_2O_3, 27 wt% T-64 and 36 wt% A16-SG. The powders were mixed by placing 600 g of the mixture in a plastic drum that was alternately rolled and shaken until the material appeared well mixed. The mixed powder was then applied to pre-made cores by employing the drum pelletizer.

The shell formulation with $La(NO_3)_3 \bullet 6H_2O$ was prepared by first weighing out 400 g of a mixture consisting of 30 wt% DD-290, 30 wt% T64 and 40 wt% A16-SG. A solution of

1 M $La(NO_3)_3 \bullet 6H_2O$ dissolved in tetrahydrofuran (THF) was then added to the alumina mixture to produce a formulation with a La:Al atomic ratio of 0.026, which corresponded to 7.7 wt% La_2O_3 in terms of the oxides. THF was then added to the mixture to produce a thick paste. The paste was thoroughly mixed, and the THF was allowed to evaporate overnight under atmospheric conditions in a fume hood. The resulting powder was then dried at 110°C for 4 hr and reground in a mortar and pestle. The prepared powder was then applied to pre-made pellet cores by employing the revolving drum pelletizer. As the drum revolved, the pellets were sprayed intermittently with de-ionized water while the shell powder was gradually added. In this way, the diameter of the pellets increased to a size between 4 and 5 mesh, or between 4.76 and 3.96 mm in diameter. After about 50 g of pellets had been produced of the correct size, the pellets were hardened by employing the same procedure used for hardening the cores.

All of the pellets were calcined at high temperature in an atmosphere of flowing air to increase the physical integrity of the pellets. The samples were calcined at 900°C for 3 hr after being heated gradually from room temperature over a two-hour period. The pellets were then cooled using a 2 hr ramp back to room temperature. After calcination, the pellets were placed in a tube oven at 650°C for 1 hr in flowing CO_2 in order to recarbonate the CaO cores. The prepared core-in-shell pellets were stored in a desiccator.

Impregnation with Nickel Nitrate

The core-in-shell pellets used in this investigation were impregnated with a Ni catalyst. Prepared core-in-shell pellets were treated in a 50 mL round bottom flask that was placed in a vacuum oven at 110°C for 3 hr. After this treatment, the sample was removed from the vacuum oven, capped, and allowed to cool for 5 min. Then without further cooling,

25 mL of 2 M $Ni(NO_3)_2 \bullet 6H_2O$ in tetrahydrofuran (THF) was slowly added to the pellets. The pellets were allowed to soak for 1 hr in this solution where upon the pellets were removed from the solution and allowed to dry under atmospheric conditions overnight. After drying, the pellets were placed in an oven at 1.0 atm and 110°C for 4 hr. The pellets were then heated in a tube oven as the temperature was ramped from room temperature to 500°C at 25°C/min in flowing air. Once 500°C was reached, the pellets remained in the oven for 2.0 hr to convert nickel nitrate into NiO. The impregnation process was then repeated so that the pellets were impregnated with nickel twice prior to testing in the fixed bed reactor. The gain in weight of the pellets resulting from impregnation corresponded to an added Ni content of 6 wt%. Prior to reaction testing of the core-in-shell pellets, the NiO was reduced in-situ by raising the catalyst bed temperature to 550°C and flowing H_2 at 1.3 mmol/min for 4 hr through the bed.

Fixed Bed Reactor Loading

The performance of the core-in-shell pellets was evaluated by testing the pellets in a fixed bed reactor. Performance testing at 1.0, 3.0 and 5.0 atm was conducted with a vertical tubular reactor consisting of a stainless steel tube that was 61 cm long and 1.27 cm in diameter. At the bottom of the tube, a porous stainless steel plate was placed to support the catalyst bed. On top of the plate, 35 g of SC 5232 SiC spheres were placed, resulting in a layer 23 cm deep. On top of this layer, 5 g of SC 5132 SiC extrudes were added, resulting in a layer 2.5 cm deep. The inert SiC bed ensured that the bed of core-in-shell pellets was in the middle third of the electric resistance furnace used to control the bed temperature. Reaction testing at 1.0, 3.0 and 5.0 atm was carried out with 13.7 g of core-in-shell pellets that were interspersed with 8.2 g of SC 52126 SiC pellets, which reduced channeling around the core-

in-shell pellets and improved the heat transfer in the catalyst bed. The mixture of core-in-shell pellets and SiC pellets resulted in a bed length of 10-11 cm. In the middle of the catalyst bed, a thermocouple was placed to record the bed temperature throughout reaction testing. On top of the catalyst bed, 16 g of SC 5132 SiC extrudes were added, resulting in a 10 cm deep layer that served to mix and preheat the entering reactant gas mixture.

Fixed bed reactor testing at 10.0 atm used a greater reactant flow rate that required more than 13.7 g of core-in-shell pellets in order to adequately observe the period of CO_2 absorption. Thus, the mass of core-in-shell pellets loaded into the reactor was doubled. The same vertical tubular reactor was employed as before, but the different layers of materials were altered. The first layer of SiC pellets on top of the porous metal plate was reduced to 26 g, resulting in a layer 16.5 cm deep. However the next layer of SiC pellets remained the same, while on top of this layer was placed 27.4 g of core-in-shell pellets mixed with 16.4 g of SC 52126 SiC pellets resulting in a bed depth of 21 cm. On top of this was placed the same quantity of SC 5132 SiC extrudes used before.

Fixed Bed Reactor Testing

Table 1 shows the reaction conditions used in the performance testing of the core-in-shell pellets. A molar ratio of 3:1 H_2O:CH_4 was used in all tests. As the pressure of the system increased, the molar flow rate of the reactants fed to the reactor increased proportionally. Thus, the residence time of the reaction mixture in the bed of core-in-shell pellets was the same during testing at 1.0, 3.0 and 5.0 atm. At 10.0 atm, the residence time of the reaction mixture in the bed of pellets doubled because the length of the catalyst bed was doubled.

Table 1. Summary of experimental conditions employed for a series of test runs made with the core-in-shell pellets.

Temperature, °C	Pressure, atm	Flow Rate, mmol/min	H_2O:CH_4 Ratio	Core-in-shell pellets, g
Hydrogen Production Period				
550	1	2.41	3	13.7
600	1	2.41	3	13.7
	3	7.23	3	13.7
	5	12.1	3	13.7
	10	24.1	3	27.4
650	1	2.41	3	13.7
	3	7.23	3	13.7
	5	12.1	3	13.7
	10	24.1	3	27.4
Sorbent Regeneration Period				
850	1	2.41	3	

Figure 3 is a schematic diagram of the reactor used to test the performance of the core-in-shell pellets for producing H_2 in a single step. A LabAlliance Series I HPLC pump delivered a metered flow of de-ionized water to a pre-heater furnace where it was vaporized and mixed with CH_4. Brooks Instruments mass flow controllers metered the CH_4 flow rate. After mixing in the pre-heater furnace, the steam and CH_4 were conducted through heat-taped stainless steel tubing to the heated fixed bed reactor. After passing through the reactor, the gas mixture was cooled to condense unreacted steam and then vented through a line with a back pressure regulator that maintained the required system pressure. A bypass line was provided around the reactor for use before starting a test run. Reactants could be fed through

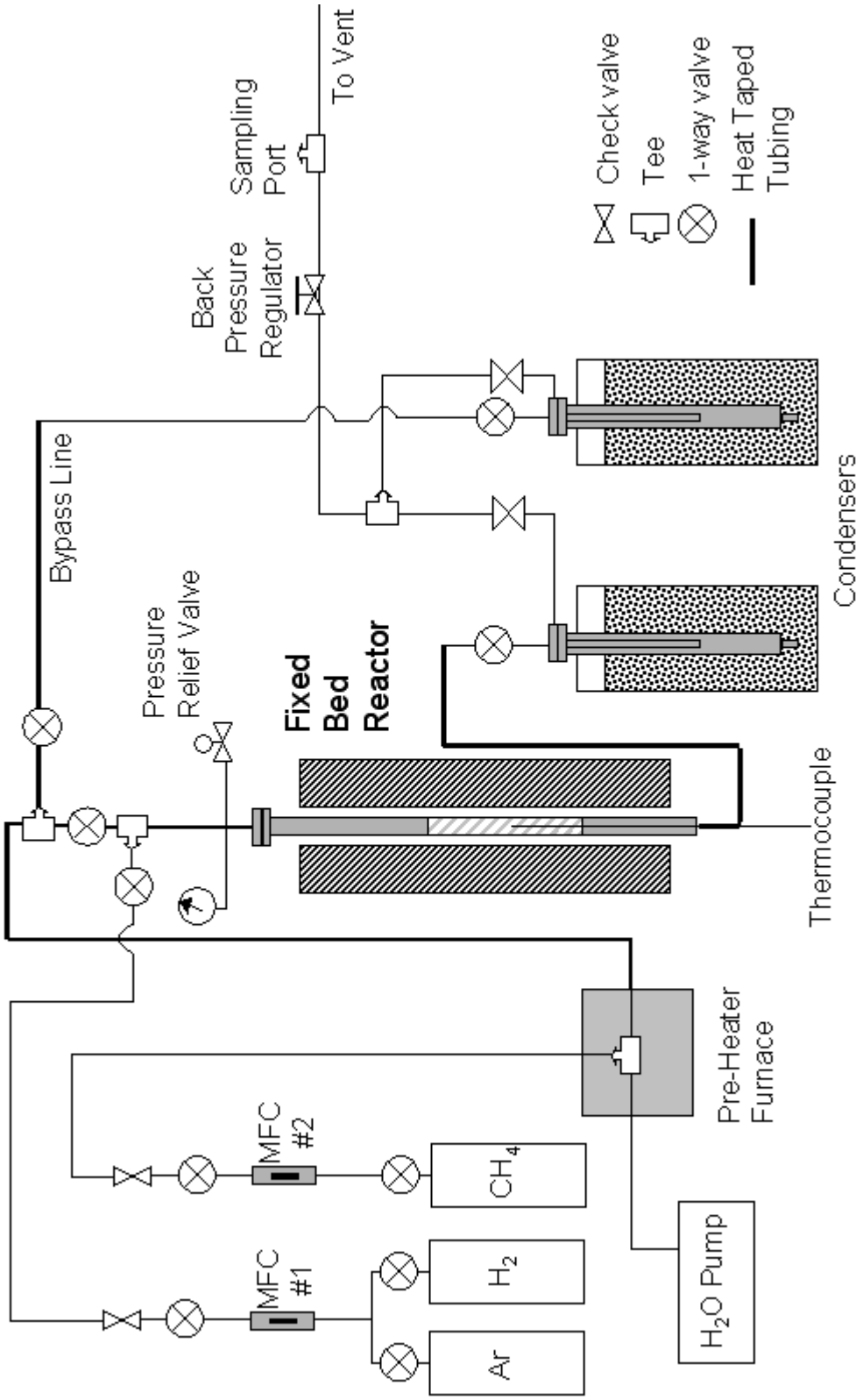

Figure 3. Schematic of the fixed bed reactor used for performance and lifecycle testing of the combined catalyst and sorbent core-in-shell pellets.

the bypass line at the appropriate flow rate and pressure for the particular conditions being tested, which insured that a well-mixed, steady flow of reactants could be introduced into the fixed bed reactor at the beginning of a performance test.

Before starting a test run, the bed of core-in-shell pellets was heated to 850°C to ensure that the sorbent was fully regenerated. This step was conducted by passing steam and CH_4 in a 3:1 mole ratio at a flow rate of 2.41 mmol/min through the bed for 1.0 to 1.5 hr. After this step was completed, the flow of CH_4 and steam was diverted around the reactor through the bypass while the reactor was cooled to the required temperature for the test run. During this cooling period, no gas was passed through the reactor when it was to be used for a test conducted at 1.0 atm. However, when it was to be used at higher pressures, Ar at a rate of 3.08 mmol/min was supplied to the reactor to pressurize the system. The flow of Ar was continued until other preparations had been completed. At this point an appropriate flow rate of CH_4 and steam was established through the bypass line. At elevated pressures, the reactants were then passed through the bypass line for at least 15 min to ensure that a steady stream of reactants of the required composition would be supplied to the fixed bed reactor. For tests at elevated pressures, the Ar flow was stopped just before introducing the reactant mixture into the fixed bed.

As the test run proceeded, samples of the reactor effluent were periodically drawn with Gastight syringes manufactured by the Hamilton Company. The effluent gas was analyzed with an SRI 8610C gas chromatograph (GC) equipped with a thermal conductivity detector and flame ionization detector. The samples were analyzed and the concentrations of H_2, CO, CO_2 and CH_4 were normalized to 100%. The gas concentrations reported are the average of several samples drawn during reaction testing at a given temperature and pressure.

Lifecycle Testing

Lifecycle testing was also conducted on the core-in-shell pellets. The core-in-shell pellets with limestone or lanthanum added to the shell formulation were separately subjected to lifecycle testing. A batch of 13.7 g of core-in-shell pellets was loaded into the fixed bed reactor as described above. The pellets were initially reduced at 550°C for 4 hr in H_2 flowing at 1.3 mmol/min. The bed temperature was then increased to 650°C at 1.0 atm for lifecycle testing. One cycle consisted of passing the reactant stream through the bed of core-in-shell pellets at this temperature for 155 min followed by subsequent sorbent regeneration at 850°C. The reactant stream had a flow rate of 2.41 mmol/min and a steam to CH_4 ratio of 3:1. During the steam-methane reforming period, samples of the reactor effluent were drawn every 10 min. At the end of the reforming period, the reactor temperature was raised to 850°C at 10°C/min for sorbent regeneration. During both the reaction and regeneration phases of the cycle, the feed composition and flow rate remained unchanged. Therefore, while the sorbent was being regenerated, CO_2 was desorbed and swept from the system and the Ni catalyst remained reduced. The composition of the reactor effluent was monitored during sorbent regeneration. The sorbent was considered regenerated when the CO_2 gas concentration stabilized, which typically took 1.0-1.5 hr. The reactant stream was then diverted through the bypass line as the reactor was cooled to 650°C at 10°C/min. Once the temperature reached 650°C, the reactant stream was reintroduced and a new cycle began. Ten cycles were completed for lifecycle testing. However, the sorbent was not regenerated at the end of the final cycle so that the sorbent remained in the more stable $CaCO_3$ form.

The 10 cycles of H_2 production at 650°C and subsequent sorbent regeneration at 850°C were not conducted without interruption due to the length of each cycle. When left overnight, the testing was interrupted at the end of a H_2 production period of a cycle so that the core was left in the $CaCO_3$ form. During the pauses in lifecycle testing, Ar was flowed through the reactor at 0.44 mmol/min. Additionally, the temperature was left at 650°C during lifecycle testing pauses in order to limit the amount of thermal stress experienced by the core-in-shell pellets.

Physical characterization of the core-in-shell pellets was also conducted before and after lifecycle testing. The BET surface area of the core-in-shell pellets was determined by using N_2 adsorption measurements. A Micromeritics ASAP 2020 was used for surface area determination. Approximately 1.0 g of core-in-shell pellets was analyzed. Pellets that were analyzed prior to lifecycle testing did not undergo a reduction treatment to convert NiO to metallic Ni.

Selective H_2 chemisorption by the metallic Ni surface was used to determine the Ni surface area present in core-in-shell pellets. H_2 chemisorption measurements were conducted with a Micromeritics ASAP 2020 with the chemisorption attachment. Chemisorption measurements were conducted at 35°C. In order to reduce NiO to Ni prior to chemisorption measurements, each sample was reduced at 550°C for 4 hr in flowing H_2 as part of the chemisorption program carried out by the ASAP 2020. Only the results of H_2 chemisorption measurements of core-in-shell pellets that had not been subjected to lifecycle testing are reported. When H_2 chemisorption measurements were carried out on core-in-shell pellets that had been subjected to lifecycle testing, the amount of H_2 chemisorbed was very low, which was probably due to coking and the deposition of carbon on the Ni surface.

The size of Ni crystallites was determined through powder X-ray diffraction (XRD) measurements using a Siemens D-500 Diffractometer and Cu Kα radiation with a graphite monochromator. A voltage of 50 kV and a current of 27 mA were employed. The divergence slits used were 1.0°, and the detector slit used was 0.15°. A counting time of 2 sec was used. The Scherrer equation was used to calculate the mean crystallite dimensions from the measured line breadth of the peaks. Since metallic Ni was required to measure the Ni crystallite size, samples that had been previously subjected to H_2 chemisorption measurements were used as the fresh core-in-shell samples. Core-in-shell pellets that had been subjected to lifecycle testing were also subjected to XRD to determine the Ni crystallite size after being unloaded from the fixed bed reactor.

The effect of lifecycle testing on the physical integrity of core-in-shell pellets was also investigated. Core-in-shell pellets that were broken or otherwise found to contain visual shell cracks following lifecycle testing were considered "fractured." The percentage of pellets fractured during lifecycle testing is reported.

The compressive force required to break the core-in-shell pellets was also determined. For this determination, the diameter of an individual pellet was measured with digital calipers, and then the compressive force required to break the pellet was measured with an Accuforce EZ 250 instrument. For this measurement the pellet was placed between two flat plates and between pieces of cardboard, which distributed the force. The top plate was lowered at a rate of 10 mm/min and the force required to break the pellet was recorded. The crushing force divided by the pellet diameter is reported. Fifteen pellets were individually measured during this test and the average of the breaking force per unit of pellet diameter, or N/mm, was determined. This average is reported with 95% confidence intervals. Pellets that

had not been reduced or subjected to lifecycle testing were used for determining the average breaking force of fresh pellets. In the case of pellets subjected to lifecycle testing, only intact and fracture-free pellets were selected for the breaking force determination.

Experimental Results and Discussion

Satrio et al.[20, 21] prepared a combined catalyst and sorbent in the form of core-in-shell pellets capable of producing high concentration H_2 by steam reforming methane, propane or toluene. However, to prepare an active Ni catalyst for steam-methane reforming, the material required an extended activation period involving the reaction of propane or methane with steam at 750-770°C over several hours. To determine why such a long activation period had been required, the present study focused initially on changes in the composition of the core-in-shell pellets that had taken place. Pellets prepared in the same way as before were examined by X-ray fluorescence (XRF) before and after catalyst activation. This examination revealed the presence of sulfate in the freshly prepared pellets. After the Ni catalyst had been activated by reforming propane for several hours, the concentration of sulfur compounds was reduced significantly and the sulfate form was converted to sulfide. The source of the sulfur was ultimately traced to the lignin solution that was used as a binder while the shell material was being applied to prepare the core-in-shell pellets. Subsequent batches of core-in-shell pellets were prepared without using the lignin solution. After these batches had been impregnated with a Ni catalyst and the Ni had been reduced to the metallic state by employing H_2 at 550°C, no further activation of the catalyst was required. Thus, the long activation period previously required was needed to remove the sulfur from the Ni

catalyst surface. Therefore, all of the core-in-shell pellets utilized in the present investigation were prepared without lignin.

The results of a typical steam-methane reforming test with fresh core-in-shell pellets conducted with a 3:1 mole ratio of H_2O:CH_4 at 600°C and 1.0 atm are presented in Figure 4.

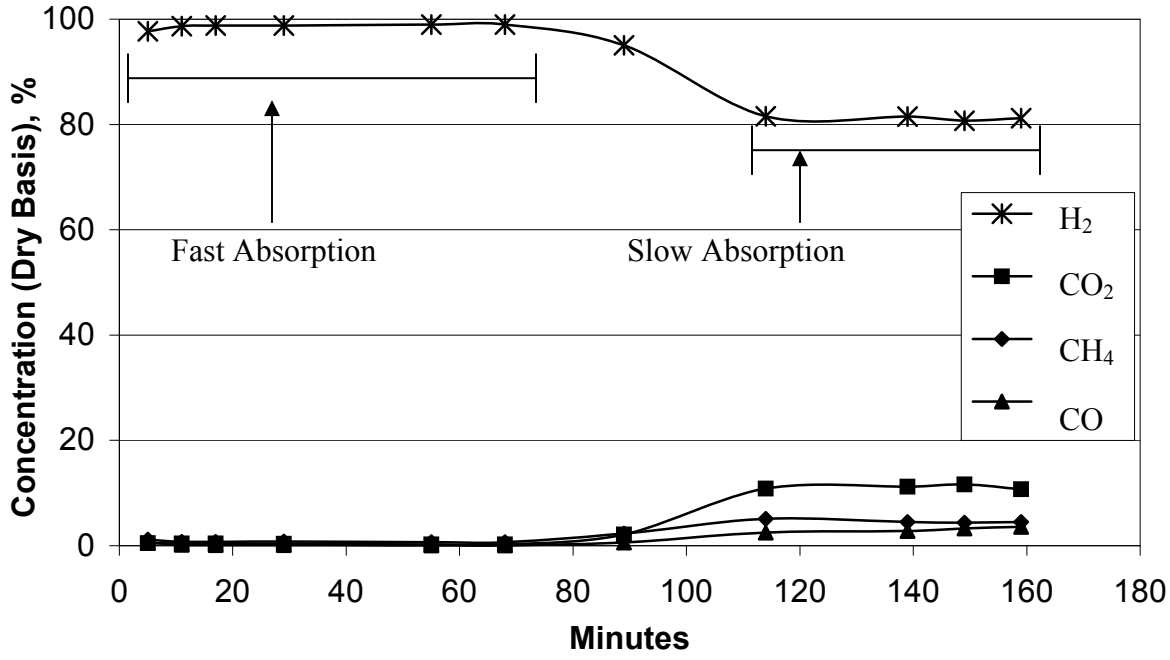

Figure 4. Gas concentrations observed in the reactor effluent during fixed bed reactor testing of a fresh batch of core-in-shell pellets with limestone added to the shell formulation and impregnated with Ni at 600°C and 1.0 atm.

During the initial 70 min of the test, most of the CH_4 was converted and virtually all of the CO_2 was absorbed, resulting in a large H_2 concentration. This period will be referred to as the Fast Absorption period. As time progressed, the CaO sorbent was gradually converted to $CaCO_3$, and the rate of CO_2 absorption slowed significantly. However, an analysis performed on the gas concentrations observed during the Slow Absorption period revealed that the steam-methane reforming and water-gas shift reactions could not solely account for the observed reactor effluent concentrations. On the other hand, when CO_2 absorption was

taken into account, the conversions obtained were consistent. Thus, the slow absorption of CO_2 by the CaO sorbent appeared to be taking place even after an extended time. Hence, this phase of reaction testing will be referred to as the Slow Absorption period.

During the Slow Absorption period, the H_2 concentration was much lower than during the Fast Absorption period, whereas the CO, CO_2 and CH_4 concentrations were higher. The Slow Absorption period was characterized by a loaded CaO sorbent that slowly absorbed CO_2 through a diffusion-limited reaction. The phenomenon of CaO slowly absorbing CO_2 after an initial rapid, kinetically controlled period is a well known property of CaO-based sorbents.[25, 26] Furthermore, the Slow Absorption period is a rough approximation of the gas concentrations that would be obtained without a sorbent present. Therefore, a single reaction test provided a comparison of the regimes with and without CO_2 absorption. The terms Fast Absorption period and Slow Absorption period are utilized throughout this investigation.

Performance Testing at Atmospheric Pressure

The performance of core-in-shell pellets used to produce H_2 in high concentrations from CH_4 and steam in a 3:1 mole ratio was investigated over a 550-650°C temperature range and a 1.0-10.0 atm pressure range by employing the fixed bed reactor. The experimental conditions employed for a series of test runs are summarized in Table 1. The results achieved in these runs are presented below in terms of the reactor effluent gas composition and the conversions of CH_4 and CO, respectively. For the initial series of runs conducted at 1.0 atm with core-in-shell pellets made with the shell formulation containing limestone, the reactor effluent composition is presented in Table 2 and the CH_4 and CO conversion are presented in Figure 5. A comparison of these conversions with the

Table 2. Reactor effluent concentrations observed from reaction testing core-in-shell pellets with limestone added to the shell formulation at 1.0 atm.

Temperature, °C	Absorption Period	Concentration (Dry Basis), mol%			
		CH_4	CO	CO_2	H_2
550	Fast	1.7	0.2	0.2	97.9
	Slow	10.4	2.2	14.3	73.1
600	Fast	0.8	0.1	0.4	98.7
	Slow	5.0	2.8	12.8	79.4
650	Fast	0.8	0.5	0.8	98.0
	Slow	2.0	5.7	12.3	80.1

equilibrium conversions shown in Figure 2 and calculated equilibrium concentrations in Appendix 2 indicates that the rates of the steam-methane reforming reaction, water-gas shift reaction and reaction of CaO and CO_2 were rapid enough to produce conversions limited by equilibrium during the Fast Absorption period. A product stream with 98 mol% H_2 was produced between 550-650°C. The level of CH_4 conversion during the Fast Absorption period increased slightly as the temperature increased, which was expected due to the endothermic nature of the steam-methane reforming reaction. Additionally, conversions observed during the Fast Absorption period were greater than the conversions during the Slow Absorption period. The greatest enhancement in CH_4 conversion due to rapid CO_2 absorption was experienced at 550°C, which allowed for the endothermic steam-methane reforming reaction to be enhanced. The greatest enhancement in CO conversion due to rapid CO_2 absorption was observed at 650°C, which allowed for the exothermic water-gas shift reaction to be enhanced. Thus, rapid CO_2 absorption resulted in CH_4 and CO conversions at levels greater than those possible without a sorbent.

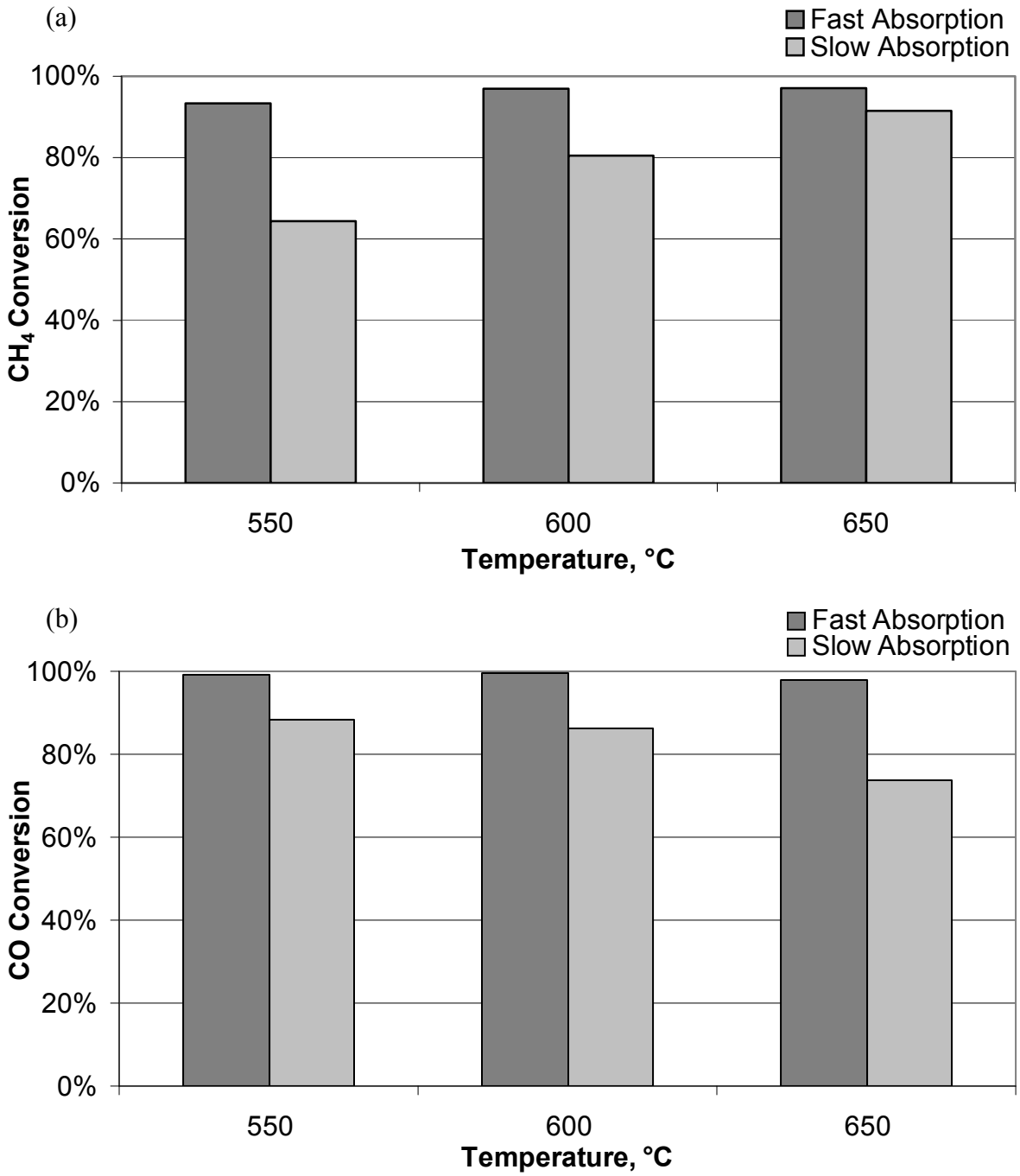

Figure 5. The observed CH_4 (a) and CO (b) conversions recorded during fixed bed reaction testing of core-in-shell pellets with limestone added to the shell formulation at 1.0 atm.

The gas compositions shown for the Slow Absorption period can best be explained by the slow absorption of CO_2 during this period. Furthermore, the absorption of some CO_2 during this period could explain why the CO conversions recorded in Figure 5 (b) are higher than the equilibrium CO conversions indicated in Figure 2 (b) for 1.0 atm and no CO_2 absorption. A possible alternative explanation is that a temperature gradient across the fixed bed could have been present due to the large endothermicity of the steam-methane reforming reaction. Since the bed temperature was measured at the center of the bed, the bed exit temperature could have been cooler, which would have resulted in a higher than expected CO conversion due to the exothermic nature of the water-gas shift reaction. Overall, the CO conversion decreased with increasing temperature, which was probably due to the exothermic nature of the water-gas shift reaction.

For the next series of runs, core-in-shell pellets with lanthanum added to the alumina shell formulation were prepared and then tested in the fixed bed reactor using the same conditions as before. Previous investigations determined that the addition of lanthanum nitrate to the alumina shell formulation resulted in increased physical strength after calcination.[22] Therefore, lanthanum was added to the alumina shell formulation and reaction testing was performed to determine any effects that the addition of lanthanum might have on the production of H_2.

The product gas composition observed during testing of the pellets with the lanthanum shell formulation is tabulated in Table 3. The gas concentrations in Table 3 were used to determine the CH_4 and CO conversion levels reported in Figure 6 (a) and (b), respectively. The results obtained with the lanthanum shell formulation were very similar to the results obtained with the limestone shell formulation. The CH_4 and CO conversions

Table 3. Reactor effluent concentrations observed from reaction testing core-in-shell pellets with lanthanum added to the shell formulation at 1.0 atm.

Temperature, °C	Absorption Period	Concentration (Dry Basis), mol%			
		CH_4	CO	CO_2	H_2
550	Fast	1.4	0.1	0.4	98.1
	Slow	10.7	1.6	12.3	75.4
600	Fast	1.1	0.1	0.6	98.1
	Slow	4.9	3.2	12.8	79.1
650	Fast	0.7	0.4	0.5	98.5
	Slow	1.7	5.0	12.3	81.0

observed during the Fast Absorption period of reaction testing were near calculated equilibrium levels (Figure 2) and calculated equilibrium concentrations (Appendix 2). The absorption of CO_2 by CaO, which took place rapidly during the Fast Absorption period, resulted in the production of a product stream with over 98 mol% H_2 on a dry basis between 550-650°C. Additionally, CH_4 and CO conversions were enhanced by the rapid absorption of CO_2, which allowed for greater conversions than would have otherwise been possible without the sorbent. Again, during the Slow Absorption period the product gas composition could best be explained by allowing for the absorption of CO_2. Overall, the addition of lanthanum to the shell formulation did not hinder the ability of the pellets to produce H_2 in large concentrations. Furthermore, the results obtained with the different pellet formulations were consistent and reproducible.

Performance Testing at Elevated Pressures

The performance of core-in-shell pellets was also evaluated with the fixed bed reactor at elevated pressures. Reaction testing was conducted at absolute pressures of 3.0, 5.0 and 10.0 atm and at temperatures of 600°C and 650°C. Core-in-shell pellets with limestone or

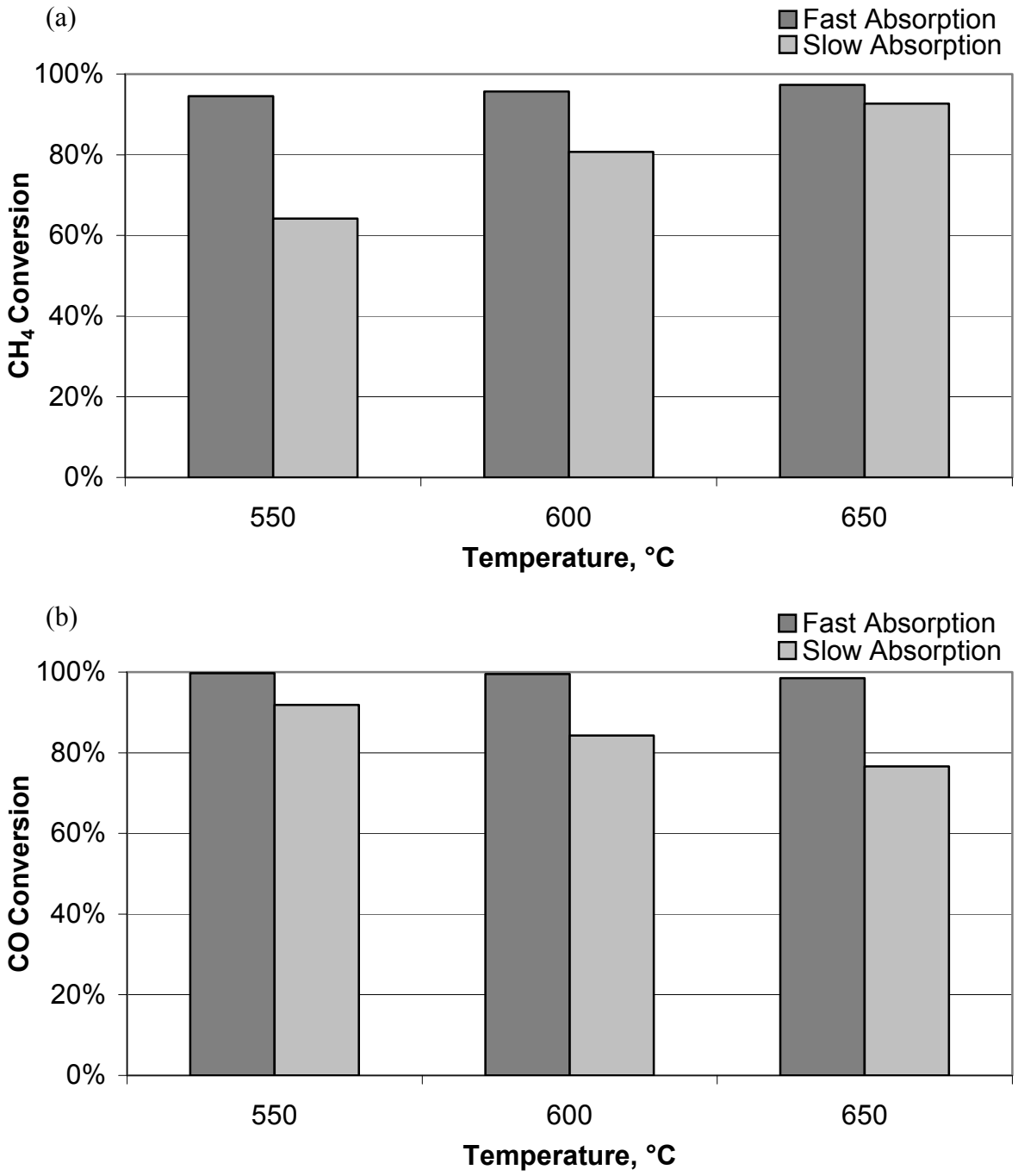

Figure 6. The observed CH_4 (a) and CO (b) conversions recorded during fixed bed reaction testing of core-in-shell pellets with lanthanum added to the shell formulation at 1.0 atm.

with lanthanum added to the shell formulation were separately tested. A steam to methane feed ratio of 3:1 was employed throughout the series of tests while the total molar flow rate of feed was increased in proportion to the pressure. Thus, the residence time of the reactants passing through the bed remained the same at 1.0, 3.0 and 5.0 atm. At 10.0 atm, the increased flow rate necessitated doubling the mass of core-in-shell pellets so that adequate CaO was present for the Fast Absorption period. Doubling the mass of pellets also doubled the length of the catalyst bed, effectively doubling the residence time of the gas passing through the bed.

The product gas concentrations observed while operating the reactor filled with pellets having the limestone shell formulation are shown in Table 4 for the runs made at elevated pressures. The CH_4 and CO conversions calculated from the gas concentrations presented in Table 4 are illustrated in Figure 7 (a) and (b). The CH_4 conversions for the Fast Absorption period are approximately equal to the thermodynamic equilibrium levels shown in Figure 2. Additionally, the observed concentrations in Table 4 are comparable to the calculated equilibrium concentrations in Appendix 2. In both Figures 2 and 7 (a) it can be seen that for a given pressure, CH_4 conversion does not have a strong dependence on temperature during the Fast Absorption period. This result is probably due to the balance between the endothermic and exothermic heats of reaction for the three reactions involved.

It can also be seen in Figure 7 (a) that an increase in pressure reduced the CH_4 conversion, which was expected based on the change in the number of moles of gas as all three reactions take place during the Fast Absorption period. Table 4 shows that during the Fast Absorption period H_2 in high concentrations was produced at all pressures and temperatures investigated. Also, unreacted CH_4 was the principle impurity while CO and,

Table 4. Reactor effluent concentrations observed from reaction testing core-in-shell pellets with limestone added to the shell formulation at elevated pressures.

Temperature, °C	Pressure, atm	Absorption Period	Concentration (Dry Basis), mol%			
			CH_4	CO	CO_2	H_2
600	3	Fast	2.5	0.1	0.3	97.2
		Slow	14.5	3.5	12.2	69.9
	5	Fast	3.1	0.1	0.2	96.6
		Slow	19.0	2.5	12.3	66.3
	10	Fast	6.0	0.0[a]	<0.1	93.8
		Slow	41.8	0.7	9.2	48.2
650	3	Fast	2.0	0.2	0.2	97.6
		Slow	8.9	4.9	11.7	74.5
	5	Fast	2.9	0.1	0.6	96.4
		Slow	11.7	4.0	12.3	72.0
	10	Fast	4.8	0.0[a]	<0.1	95.1
		Slow	31.0	2.8	11.1	55.0

[a]Below detection limits

CO_2 were present in very low concentrations. At 10.0 atm, the concentration of CO_2 was less than 0.1 mol%, and the concentration of CO was below the detection limits of the GC. Thus increasing the system pressure during the Fast Absorption period diminished CH_4 conversion and increased CO conversion, resulting in lower concentrations of H_2, CO and CO_2. A comparison of the actual CH_4 conversions for the Slow Absorption period in Figure 7 with the equilibrium values appearing in Figure 2 shows good agreement except for the values at 10.0 atm where the actual CH_4 conversions were considerably lower than the equilibrium

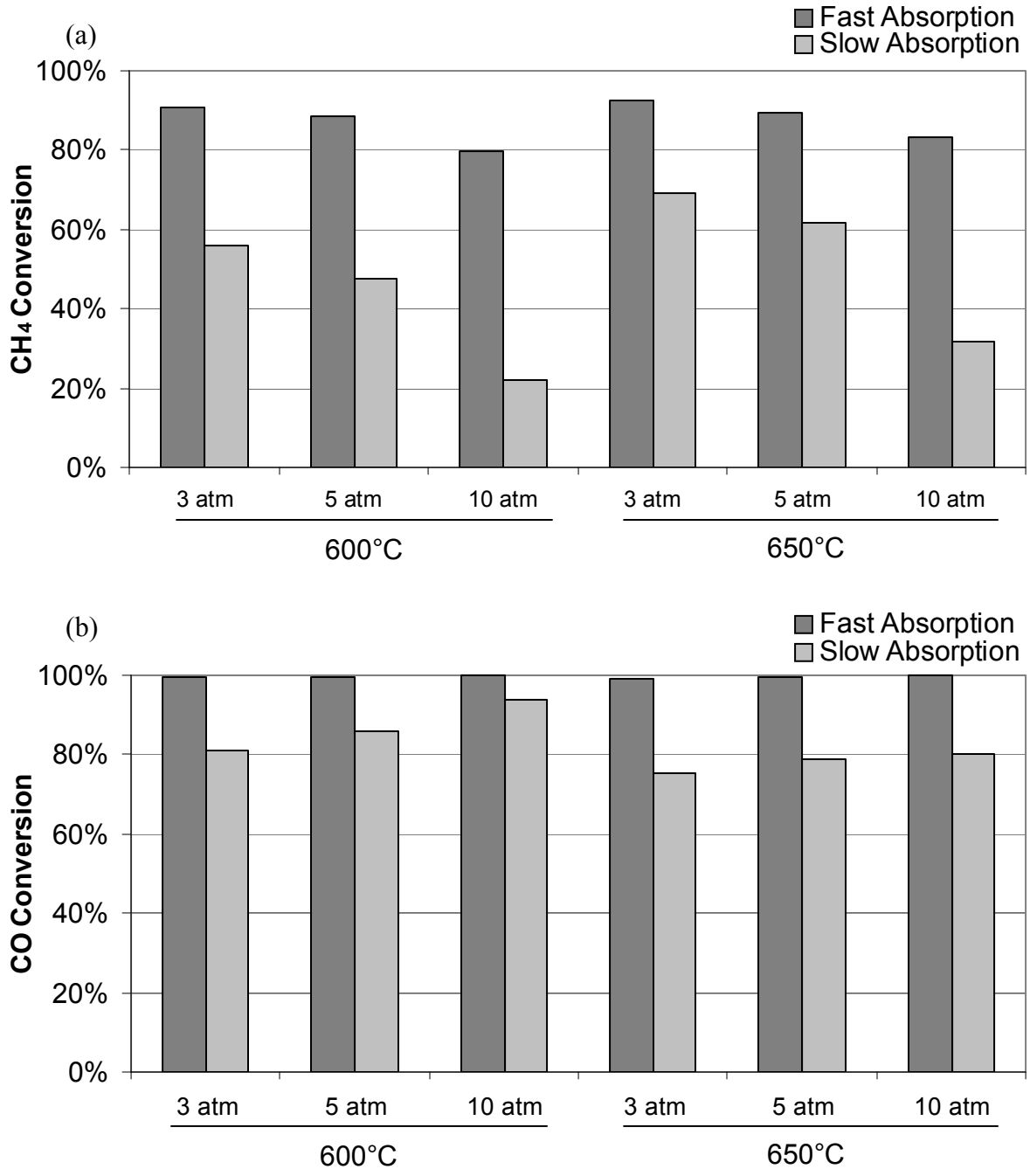

Figure 7. The observed CH_4 (a) and CO (b) conversions recorded during fixed bed reaction testing of core-in-shell pellets with limestone added to the shell formulation at elevated pressures.

values. The diminished CH_4 conversion during the Slow Absorption period at 10.0 atm was most likely due to heat transfer limitations that prevented the conversion of CH_4 to near equilibrium levels because of the strongly endothermic steam-methane reforming reaction. Of greater interest are the effects of temperature and pressure on the CO conversion where at any specific temperature and pressure the actual CO conversion is always greater than the equilibrium conversion, which does not take into account CO_2 absorption. Therefore, these results further suggest that CO_2 is being absorbed during the Slow Absorption period.

Core-in-shell pellets with lanthanum added to the shell formulation were also tested at pressures of 3.0, 5.0 and 10.0 atm and at both 600 and 650°C. The gas concentrations are presented in Table 5 as well as CH_4 and CO conversions in Figure 8.

Table 5. Reactor effluent concentrations observed from reaction testing core-in-shell pellets with lanthanum added to the shell formulation at elevated pressures.

Temperature, °C	Pressure, atm	Absorption Period	Concentration (Dry Basis), mol%			
			CH_4	CO	CO_2	H_2
600	3	Fast	2.2	0.1	0.2	97.5
		Slow	15.3	2.3	11.9	70.5
	5	Fast	3.5	0.1	0.2	96.2
		Slow	19.7	2.0	11.6	66.7
	10	Fast	5.1	0.0[a]	<0.1	94.9
		Slow	39.9	0.9	8.6	50.6
650	3	Fast	1.7	0.2	0.8	97.4
		Slow	8.4	4.5	11.9	75.2
	5	Fast	3.0	0.2	0.6	96.2
		Slow	11.7	3.7	12.0	72.6
	10	Fast	5.3	0.0[a]	<0.1	94.7
		Slow	30.5	1.3	11.0	57.2

[a]Below detection limits

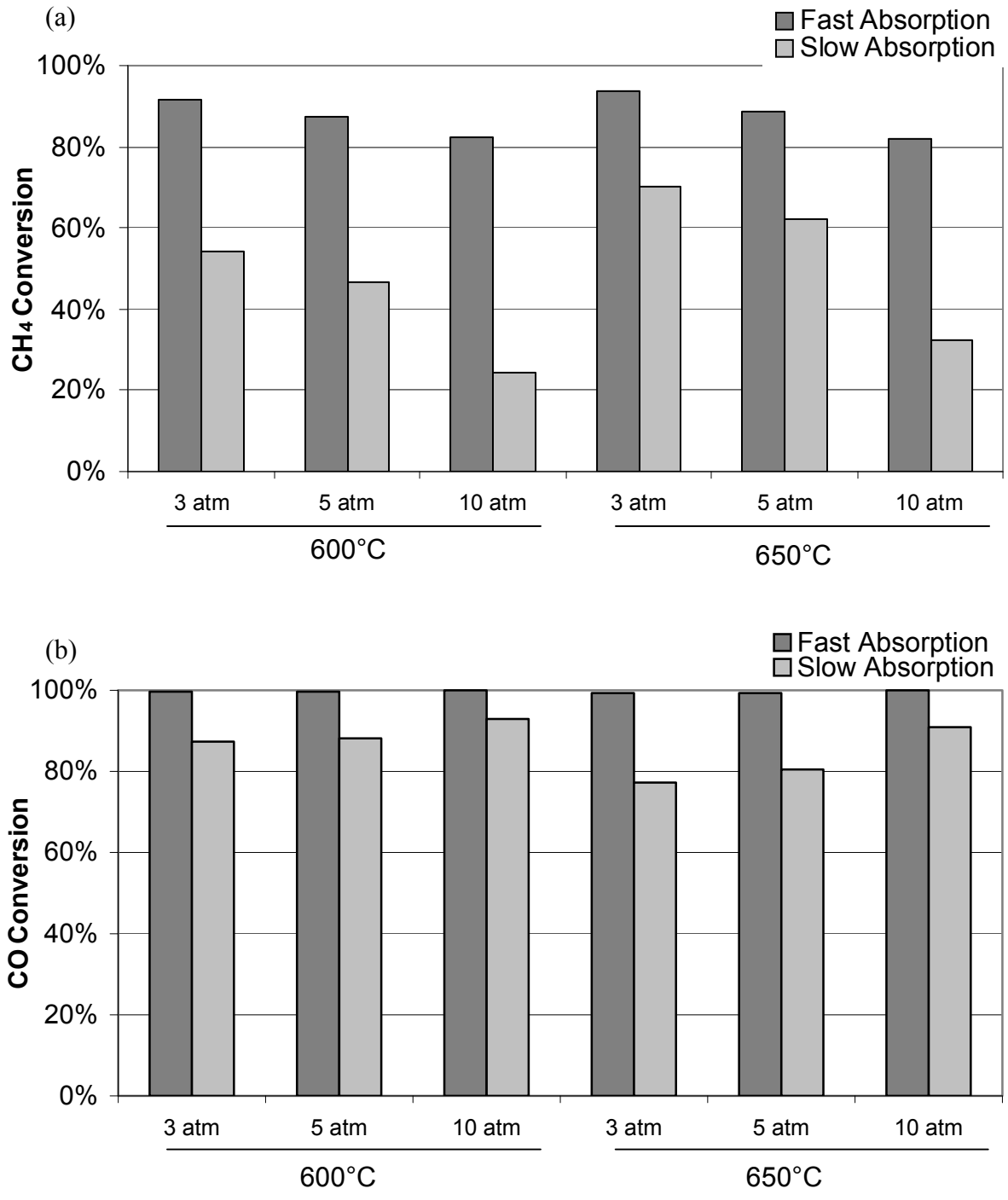

Figure 8. The observed CH_4 (a) and CO (b) conversions recorded during fixed bed reaction testing of core-in-shell pellets with lanthanum added to the shell formulation at elevated pressures.

The results with pellets having lanthanum in the shell formulation were very similar to results obtained with pellets having limestone in the shell formulation. The gas compositions in Table 5 for the lanthanum shell formulations were very similar to those in Table 4 for the limestone shell formulation. Furthermore, the CH_4 and CO conversions indicated by Figure 8 for the lanthanum formulations were very similar to those shown in Figure 7 for the limestone formulation.

Lifecycle Testing

Limited lifecycle testing of the core-in-shell pellets was conducted to evaluate the performance of the pellets as they were subjected to 10 cycles of H_2 production and subsequent sorbent regeneration. Selected physical properties of the pellets were also measured before and after lifecycle testing. Core-in-shell pellets with either the limestone shell formulation or the lanthanum shell formulation were prepared for fixed bed reactor testing. A fresh batch of 13.7 g of core-in-shell pellets was loaded into the fixed bed reactor for each test. After an initial reduction of the NiO catalyst to Ni by flowing H_2 at 550°C, the performance of the core-in-shell pellets was evaluated by passing steam and CH_4 in a 3:1 molar ratio through the pellet bed at 2.41mmol/min at 650°C and 1.0 atm for 155 min. During this time, a sample of the reactor effluent was drawn every 10 min to record the reactor response curve. After 155 min, the reactor temperature was raised from 650°C to 850°C at 10°C/min while continuing the flow of reactants to regenerate the CaO sorbent. When the CO_2 concentration in the reactor effluent reached a constant level at 850°C, the sorbent was considered regenerated. The sorbent was regenerated while the reactants continued to flow through the reactor to ensure that the Ni catalyst remained reduced during

sorbent regeneration. Regeneration took 1.0-1.5 hr at 850°C. The period of reaction testing for 155 min at 650°C followed by the regeneration step at 850°C constituted a complete cycle. Each pellet formulation was subjected to 10 cycles. However, the sorbent was not regenerated after the 10^{th} reaction stage at 650°C so that it was left in the more stable $CaCO_3$ form for further evaluation.

Core-in-shell pellets with limestone added to the shell formulation were tested first. As each test cycle proceeded, the concentrations of H_2 and CO_2 in the reactor effluent were recorded (see Figure 9 (a) and (b), respectively). Initially and for extended periods, CO_2 was rapidly absorbed so the concentration of CO_2 was only 0.8 mol% in the reactor effluent. During this period, the rates of the steam-methane reforming reaction, water-gas shift reaction and reaction between CaO and CO_2 were sufficiently rapid to produce H_2 in 98 mol% concentration. Eventually as time progressed, the rate of CO_2 absorption by CaO slowed so its concentration rose to about 12 mol% while the H_2 concentration fell to 81 mol%. As the number of cycles increased, the time that H_2 in high concentration was produced also decreased from 95-100 min for the first cycle to 50 min for the last cycle. Also, Figure 9 (b) indicates that as the number of cycles increased the period during which CO_2 was rapidly absorbed decreased form 100 min for the first cycle to 50 min for the last cycle. Thus the amount of CO_2 that was absorbed rapidly diminished as the sorbent absorption capacity decreased, which is in line with the results of previous work.[8] While the length of time that CO_2 was rapidly absorbed decreased as the number of cycles increased, H_2 in high concentration was produced during a portion of each cycle. Thus, more mature samples of combined catalyst and sorbent were still capable of producing H_2 in high concentration but the length of time high concentration H_2 is produced was diminished.

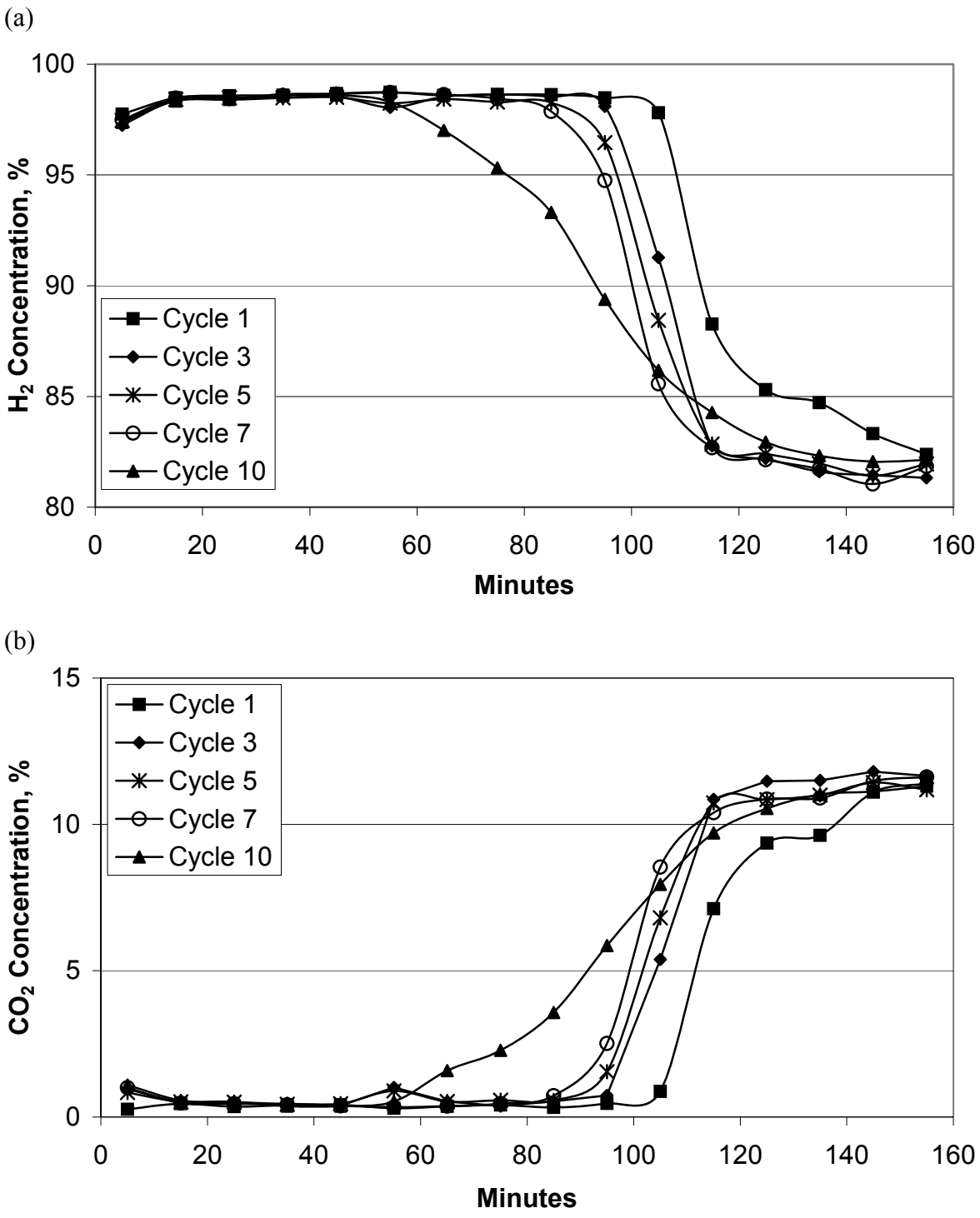

Figure 9. The concentration of (a) H_2 and (b) CO_2 at 650°C and 1.0 atm in the reactor effluent during lifecycle testing utilizing core-in-shell pellets with the limestone shell formulation.

For the first seven cycles the transition time between the rapid and slow CO_2 absorption periods was relatively short. However, for the 10th cycle, the transition time between the two absorption periods was prolonged, which could have been due to changes either in the core material or shell material. As the number of cycles increased, the CaO cores probably became denser due to expansion and contraction associated with the change in molar volume as the sorbent was transformed between CaO and $CaCO_3$. Also, since the melting point of $CaCO_3$ is 1330°C,[27] it has a Tamman temperature of half the melting point, or 665ºC. Therefore, enhanced sintering of the core could take place at 650ºC when the core was in the form of $CaCO_3$. Densification and sintering of the core would tend to reduce the rate of diffusion of CO_2 into the core and thereby reduce its overall rate of absorption.

The performance of core-in-shell pellets with lanthanum added to the shell formulation was also investigated over 10 cycles of reaction and sorbent regeneration. Figure 10 shows the concentrations of H_2 and CO_2 observed during lifecycle testing of the pellets. While the results were generally similar to those observed with the previous pellets, there were some important differences that seemed due to the difference in shell formulations. In both cases, H_2 in 98 mol% concentration was produced during the initial rapid CO_2 absorption period followed by the production of H_2 in 82 mol% concentration during the slow CO_2 absorption period. However, after the first cycle, the concentration profile differed greatly between shell formulations during the transition from one CO_2 absorption period to the next. Furthermore, this difference appeared to increase as the number of cycles increased. The results suggest that the two materials will need to be tested over many more cycles before a definite conclusion can be reached about their relative merits.

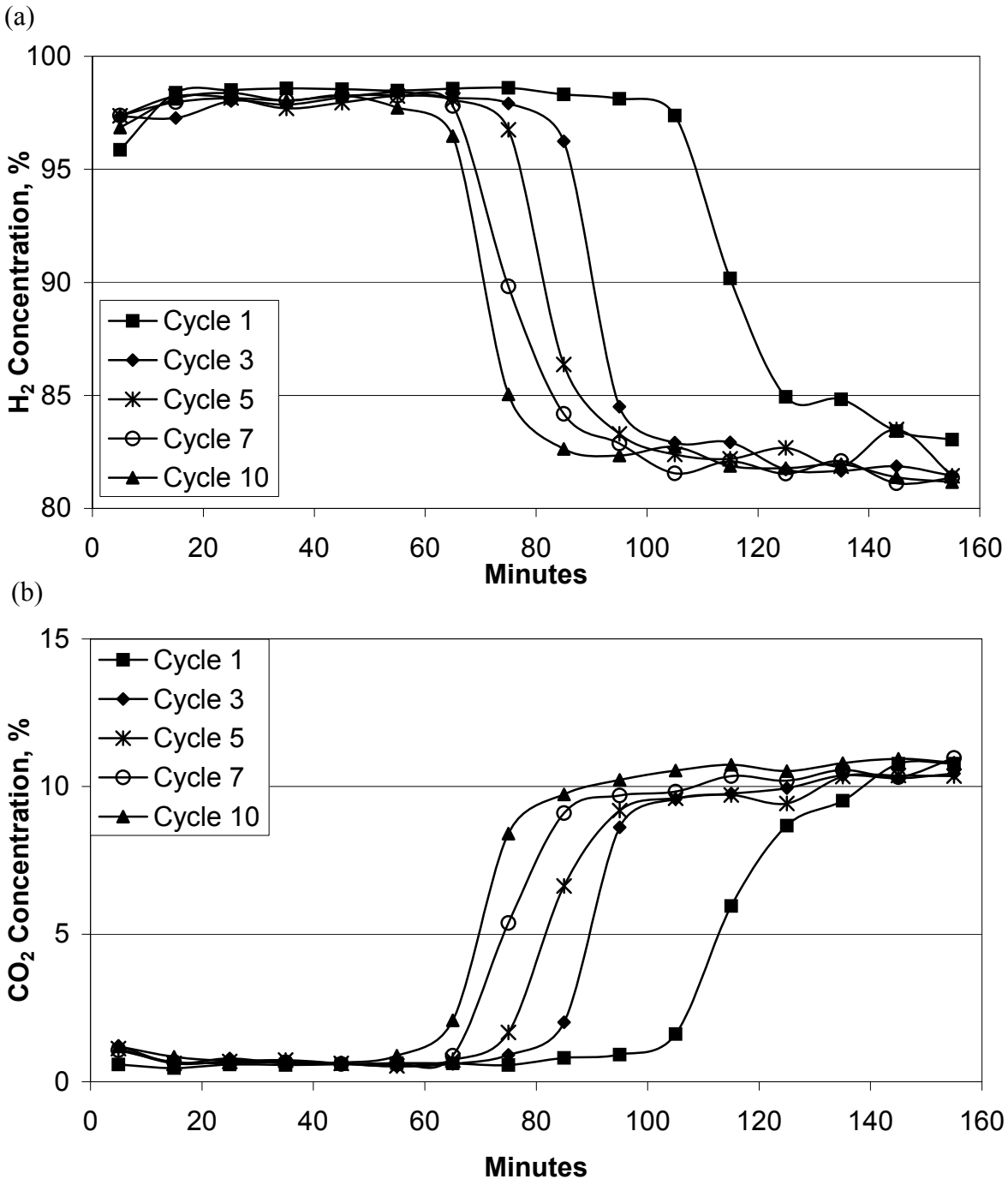

Figure 10. The concentration of H_2 (a) and CO_2 (b) in the reactor effluent during cyclic reaction testing at 650°C and 1.0 atm utilizing core-in-shell pellets with the lanthanum shell formulation.

The maximum amount of CO_2 absorbed per gram of sorbent present was also determined for both shell formulations. The amount of CaO present in the core-in-shell pellets was determined gravimetrically. After lifecycle testing, the average weight of 7 carbonated core-in-shell pellets was measured. The shells were then carefully removed from the cores, which were then subjected to high temperature heat treatment at 800°C for 1 hr in flowing air to convert the $CaCO_3$ to CaO. The weight percent of CaO present in carbonated core-in-shell pellets with the reduced Ni catalyst was based on the following equation:

$$CaO(wt\%) = \frac{W_{CalcinedCore}}{W_{Core-in-Shell}} \tag{4}$$

where $W_{Calcined\ Core}$ is the mass of the separated cores after high temperature heat treatment, and $W_{Core\text{-}in\text{-}Shell}$ is the mass of the core-in-shell pellets after being unloaded from the reactor. The amount of CaO in the uncalcined pellets was found to be 32 wt% for pellets made with either the limestone or lanthanum shell formulation. A mass of 13.7 g of unreduced core-in-shell pellets were loaded into the reactor for both the limestone and lanthanum samples. The amount of Ni recorded for both samples was 6 wt%. Thus, reduction of NiO to Ni resulted in a mass of 13.5 g of reduced pellets loaded into the reactor. Therefore, the mass of CaO calculated to be present in the reactor was 4.3 g. Appendix 1 of the present dissertation illustrates an example of how the absorption capacity of the material was determined for the first cycle of the limestone lifecycle test. The absorption capacity of the pellets with respect to the cycle number is illustrated in Figure 11. The CO_2 absorption capacity of Microna 3 limestone determined previously[8] by thermogravimetric analysis is also given in Figure 11. In general, the absorption capacity of the core-in-shell pellets decreased in a similar manner as that of the powdered Microna 3 limestone as the number of cycles increased.

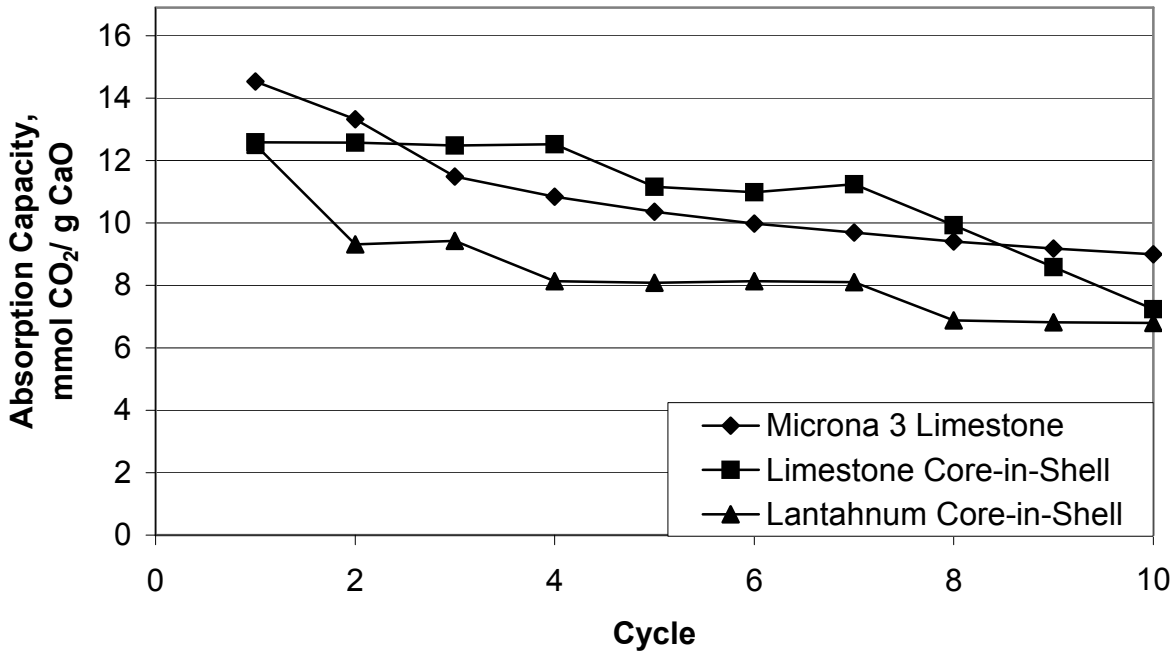

Figure 11. The calculated CO_2 absorption capacity during the Fast Absorption period of cyclic reaction testing of core-in-shell pellets with limestone or lanthanum added to the shell formulation. For reference, the absorption capacity of powdered Microna 3 limestone measured by thermogravimetric analysis from Albrecht et al.[8] is also included.

To determine the effect that lifecycle testing had on the physical properties of the core-in-shell pellets, the pellets were characterized by various methods before and after testing, and the results are presented in Table 6. One method of characterization was the determination of the surface area of the pellets by the BET method involving physisorption of N_2. This method showed that the initial surface area was 8 m^2/g for either pellet formulation and that after lifecycle testing, the surface area decreased to 5 m^2/g for the limestone formulation and 6 m^2/g for the lanthanum formulation. The loss of surface area was most likely due to the sintering of the amorphous DD-290 alumina in the shell formulation. The slightly higher surface area observed in the lanthanum shell formulation after testing could have been due to the stabilizing effect of lanthanum on alumina at high

Table 6. Physical properties of core-in-shell pellets with limestone or lanthanum added to the shell formulation before and after lifecycle testing in the fixed bed reactor.

	Limestone Shell Formulation		Lanthanum Shell Formulation	
	Before Lifecycle Testing	After Lifecycle Testing	Before Lifecycle Testing	After Lifecycle Testing
BET Surface Area, m^2/g	8	5	8	6
Ni Crystallite Size, nm[a]	12	54	8	39
Ni Surface Area, m^2/g[b]	3.1	--	3.3	--
Ni Dispersion, %				
By XRD	8	2	12	3
By H_2 Chemisorption	7	--	9	--
Fractured Pellets, %	--	18	--	26
Compressive Strength, N/mm	4.9 ± 1.0	9.0 ± 2.2	5.5 ± 1.0	12.6 ± 2.3

[a]Measured with X-ray diffraction (XRD)
[b]Measured with H_2 chemisorption

temperatures.[28] However further testing would be required to verify that the observed difference in surface area was indeed statistically significant.

The effect of lifecycle testing on the size of the Ni crystallites present in the core-in-shell pellets was determined by X-ray diffraction measurements (XRD). The mean Ni crystallite size was based on the measured line breadth of the Ni crystallite peak using the Scherrer equation. Since metallic Ni was required for these measurements, pellets that had been subjected to H_2 chemisorption measurements but not lifecycle testing were used for the "fresh" pellet XRD measurements. Such measurements were also conducted on core-in-shell pellets that had been subjected to lifecycle testing in the fixed bed reactor. The results of these measurements are presented in Table 6, and they indicated that sintering of the Ni

crystallites occurred in both the limestone and lanthanum shell formulations. Consequently, the size of the Ni crystallites in the limestone shell formulation grew from 12 nm to 54 nm as a result of lifecycle testing. Also, the size of the Ni crystallites in the lanthanum formulation grew from 8 nm to 39 nm. By comparison, Ortiz and Harrison[12] reported that the size of Ni crystallites in an industrial reforming catalyst grew from 19.8 nm to 32.2 nm as a result of being subjected to 15 cycles of H_2 production and sorbent regeneration. While sintering of the Ni catalyst did occur during the present testing of the core-in-shell pellets, the catalytic activity of both pellet formulations was sufficient to reform CH_4 to nearly equilibrium levels during each lifecycle test.

The surface area of the Ni catalyst was measured by selective H_2 chemisorption on the catalyst present in core-in-shell pellets. Only the results of selective H_2 chemisorption on fresh core-in-shell pellets are reported in Table 6 because very little H_2 was chemisorbed on pellets that had been subjected to lifecycle testing, which was probably due to carbon deposited on the Ni surface due to coking. The Ni surface area of fresh pellets was found to be 3.1 m^2/g and 3.3 m^2/g for the limestone and lanthanum shell formulations, respectively. By comparison, the Ni surface area of Süd Chemie Reformax 330 LDP, an industrial reforming catalyst, was 3.5 m^2 Ni/g of sample. Thus, the Ni surface area of the fresh core-in-shell pellets was similar to that of an industrial reforming catalyst.

The dispersion of the Ni catalyst was also evaluated. The dispersion is the fraction of metallic Ni atoms in a crystallite that are exposed on the surface and, thus, assumed to be catalytically active. The dispersion of Ni was determined by two different methods. In the first method, XRD was used to determine the dispersion of Ni atoms based on the size of the

Ni crystallites. If spherical crystals are assumed, the dispersion of Ni and crystallite size are related by the equation:

$$D(\%) = \frac{C}{d} \tag{5}$$

where D is the dispersion, d is the crystallite diameter in nm obtained from XRD measurements, and C is a constant specific to the metal that incorporates several physical properties of the metal catalyst.[29] C is equal to 97 for Ni. The dispersion of Ni atoms based on the size of Ni crystallites determined by XRD measurements are shown in Table 6. Due to sintering of the Ni crystallites, the dispersion of Ni atoms decreased from 8% to 2% as a result of lifecycle testing of the core-in-shell pellets with limestone added to the shell formulation. Likewise, sintering of the Ni crystallites in the pellets with lanthanum added in the shell reduced the dispersion of Ni from 12% to 3% as a result of lifecycle testing.

In the second method, H_2 chemisorption is used as a basis for determining the dispersion of Ni by relating the amount of H_2 adsorbed to the total concentration of Ni present. This method showed that the dispersion of Ni was 7% and 9% in fresh pellets containing limestone and lanthanum, respectively, in the shell formulations. As noted above, pellets subjected to lifecycle testing did not adsorb significant amounts of H_2 and, therefore, could not be used for application of the second method. However, the Ni dispersion determined by the two methods was in good general agreement for fresh, untested core-in-shell pellets.

The effect of lifecycle testing on the physical integrity of the core-in-shell pellets was also evaluated. During lifecycle testing, it was observed that some core-in-shell pellets were fractured, which could have been due to thermal stress as the pellets were heated and cooled,

expansion and contraction of the cores as CO_2 was absorbed and desorbed or to mechanical stress as the pellets were loaded and unloaded. The percentage of fractured pellets resulting from lifecycle testing is listed in Table 6, where it can be seen that a slightly higher percentage of pellets with lanthanum than with limestone were fractured. This result could have been due to the formation of different aluminate phases. When limestone was added to the formulation, CaO would have been formed, which could have reacted with Al_2O_3 to form $CaAl_2O_4$. On the other hand, the addition of $La(NO_3)_3$ could have resulted in the formation of $LaAlO_3$. Since the thermal expansion coefficients of the alumina phases are 7.1 ppm/°C[30] and 9.8 ppm/°C[31] for $CaAl_2O_4$ and $LaAlO_3$, respectively, the larger coefficient of thermal expansion of $LaAlO_3$ could have resulted in a higher thermal stress during lifecycle testing, resulting in more fracturing of the core-in-shell pellets. However, further testing is needed to justify this supposition.

Finally, the compressive force required to break the core-in-shell pellets before and after lifecycle testing was determined since this is an important physical property of pellets that will be subjected to mechanical stresses in various practical applications. For this determination, 15 unreduced, core-in-shell pellets were taken from the batch used to load the fixed bed reactor for lifecycle testing. The core-in-shell pellets were subjected individually to a compression test after having its diameter measured. The results are reported in terms of the force required to break a pellet divided by its diameter. The average of 15 breaking force tests and 95% confidence intervals were determined and are reported in Table 6. Likewise, 15 core-in-shell pellets unloaded from the reactor after lifecycle testing that had not fractured were also subjected to the breaking force test.

The addition of lanthanum to the alumina shell formulation was previously shown to enhance the strength of the core-in-shell pellets compared to pellets with only alumina in the shell formulation.[22] However, in the present study, the compressive strength of fresh, unreduced core-in-shell pellets was almost the same for pellets made with either lanthanum or limestone added to the shell formulation. The difference was not statistically significant. But the present study also included the Ni catalyst in the shell whereas the previous studies of the compressive strength did not. Overall, the recorded compressive strength of the fresh core-in-shell pellets reported in Table 6 are similar to the 4.5 ± 1.2 N/mm reported previously by Satrio et al.[20]

Table 6 also includes the measured compressive strength of core-in-shell pellets that had been subjected to lifecycle testing. Average values are reported with 95% confidence intervals. Interestingly, the compressive strength of the tested pellets was approximately twice that of the fresh pellets. Further examination of the core-in-shell pellets revealed that the increase in compressive strength may not have been due only to further strengthening of the shell material but also to densification of the core material. As the CaO core absorbed CO_2 and was subsequently regenerated, it appeared to become more compact and denser. The shell of pellets that had been subjected to lifecycle testing could be separated from the core, but the core retained a high strength. Thus, the increase in compressive strength required to break the cycled core-in-shell pellets could be due to densification of the core as well as further sintering of the shell.

Conclusions

An advanced catalyst and sorbent material in the form of core-in-shell pellets was successfully tested for the production of H_2 in a single step from CH_4 and steam. Two different core-in-shell formulations were tested. One core-in-shell formulation utilized limestone in the alumina shell mixture whereas the second formulation used lanthanum in the alumina shell mixture. The operating conditions tested were in the range of 550-650°C and 1.0-10.0 atm in a fixed bed reactor. A distinct period characterized by rapid absorption of CO_2 by the CaO sorbent and termed the Fast Absorption period was observed at all reaction conditions. Observations made during the Fast Absorption period indicated that CH_4 and CO conversions were at or very near calculated equilibrium conversions for both core-in-shell formulations at all temperatures and pressures investigated. Thus, the reaction rates of the steam-methane reforming and water-gas shift reactions coupled with the reaction of CaO and CO_2 were all sufficiently rapid to achieve nearly thermodynamic equilibrium. Furthermore, the rapid absorption of CO_2 allowed for the conversions of CH_4 and CO to overcome thermodynamic limitations that would have been present without selective CO_2 absorption. Increasing the pressure of the reaction system facilitated the conversion of CO, resulting in a CO concentration lower than detectable limits during the Fast Absorption phase of testing at 10.0 atm.

A second steady state period observed during performance testing of the core-in-shell pellets was characterized by a slower rate of CO_2 absorption and was identified as the Slow Absorption period. During the Slow Absorption period, the H_2 concentration was lower and the CH_4, CO and CO_2 concentrations were higher compared to the Fast Absorption period. Slow, diffusion limited CO_2 absorption by the CaO sorbent seemed a likely explanation for

the Slow Absorption period, which resulted in CO conversions greater than those predicted by the equilibrium expressions that assumed no CO_2 absorption. The steady state material balance expressions that accounted for the absorption of CO_2 fit the experimental results closely, which showed that the absorption of CO_2 had to be included.

The heat produced from the exothermic reaction of CaO and CO_2 was found to supply heat to the endothermic steam-methane reforming reaction during performance testing at 10.0 atm. During the Fast Absorption phase, the CH_4 conversion appeared to reach near calculated equilibrium levels at 600°C and 650°C when both core-in-shell formulations were tested. However, during the Slow Absorption phase, less heat was produced by the reaction of CaO and CO_2. Subsequently, CH_4 conversion during the Slow Absorption phase of testing at 10.0 atm was significantly below equilibrium levels. The likely explanation for this phenomenon was heat transfer limitations during the Slow Absorption period. Thus, the highly endothermic steam-methane reforming reaction was benefited not only through the absorption of CO_2 to induce greater conversion but also through the supply of heat generated from the reaction of CaO and CO_2.

Lifecycle testing was also performed to determine the effects of multiple H_2 production and sorbent regeneration cycles on the core-in-shell pellets. Core-in-shell pellets with limestone or lanthanum added to the shell formulation were tested separately. During 10 cycles of H_2 production and subsequent sorbent regeneration, a product stream with 98 mol% H_2 (dry basis) was produced during the Fast Absorption period. However, the length of the Fast Absorption period decreased as the number of cycles increased due to a decrease in the absorption capacity of the CaO sorbent. Lifecycle testing of the core-in-shell pellets also revealed that 18% of the pellets with limestone in the shell fractured during testing.

Likewise, 26% of the pellets with lanthanum in the shell formulation fractured during lifecycle testing. XRD measurements of core-in-shell pellets before and after lifecycle also revealed the growth of Ni crystallites during lifecycle testing, which was attributed to sintering of the Ni catalyst. Interestingly, the compressive force required to break core-in-shell pellets that had been subjected to lifecycle testing was found to be higher than that of fresh core-in-shell pellets. This may have been due to both further sintering of the shell material as well as densification of the core during lifecycle testing.

Acknowledgement

This report was prepared with the support of the U.S. Department of Energy, under Award No. DE-FG26-04NT 42182. However, any opinions, findings, conclusions, or recommendations expressed herein are those of the authors and do not necessarily reflect the views of DOE.

Literature Cited

(1) Bartholomew, C. H.; Farrauto, R. J., *Fundamentals of Industrial Catalytic Processes*. Second ed.; John Wiley & Sons, Inc.: Hoboken, 2006; p 340-486.

(2) Agrawal, R.; Offutt, M.; Ramage, M. P., Hydrogen economy - an opportunity for chemical engineers? *AIChE Journal* **2005,** 51, (6), 1582-1589.

(3) Harrison, D. P., Sorption-Enhanced Hydrogen Production: A Review. *Industrial & Engineering Chemistry Research* **2008,** 47, (17), 6486-6501.

(4) Hufton, J. R.; Mayorga, S.; Sircar, S., Sorption-enhanced reaction process for hydrogen production. *AIChE Journal* **1999,** 45, (2), 248-256.

(5) Ding, Y.; Alpay, E., Adsorption-enhanced steam-methane reforming. *Chemical Engineering Science* **2000,** 55, (18), 3929-3940.

(6) Cobden, P. D.; van Beurden, P.; Reijers, H. T. J.; Elzinga, G. D.; Kluiters, S. C. A.; Dijkstra, J. W.; Jansen, D.; van den Brink, R. W., Sorption-enhanced hydrogen production for pre-combustion CO2 capture: thermodynamic analysis and experimental results. *International Journal of Greenhouse Gas Control* **2007,** 1, (2), 170-179.

(7) Ochoa-Fernandez, E.; Haugen, G.; Zhao, T.; Ronning, M.; Aartun, I.; Borresen, B.; Rytter, E.; Ronnekleiv, M.; Chen, D., Process design simulation of H2 production by sorption enhanced steam methane reforming: evaluation of potential CO2 acceptors. *Green Chemistry* **2007,** 9, (6), 654-662.

(8) Albrecht, K. O.; Wagenbach, K. S.; Satrio, J. A.; Shanks, B. H.; Wheelock, T. D., Development of a CaO-Based CO2 Sorbent with Improved Cyclic Stability. *Industrial & Engineering Chemistry Research* **2008,** 47, (20), 7841-7848.

(9) Ding, Y.; Alpay, E., Equilibria and kinetics of CO2 adsorption on hydrotalcite adsorbent. *Chemical Engineering Science* **2000,** 55, (17), 3461-3474.

(10) Abanades, J. C.; Rubin, E. S.; Anthony, E. J., Sorbent Cost and Performance in CO2 Capture Systems. *Industrial & Engineering Chemistry Research* **2004,** 43, (13), 3462-3466.

(11) Balasubramanian, B.; Ortiz, A. L.; Kaytakoglu, S.; Harrison, D. P., Hydrogen from methane in a single-step process. *Chemical Engineering Science* **1999,** 54, (15-16), 3543-3552.

(12) Ortiz, A. L.; Harrison, D. P., Hydrogen Production Using Sorption-Enhanced Reaction. *Industrial & Engineering Chemistry Research* **2001,** 40, (23), 5102-5109.

(13) Yi, K. B.; Harrison, D. P., Low-Pressure Sorption-Enhanced Hydrogen Production. *Industrial & Engineering Chemistry Research* **2005,** 44, (6), 1665-1669.

(14) Akiti, T. T., Jr.; Constant, K. P.; Doraiswamy, L. K.; Wheelock, T. D., A Regenerable Calcium-Based Core-in-Shell Sorbent for Desulfurizing Hot Coal Gas. *Industrial & Engineering Chemistry Research* **2002,** 41, (3), 587-597.

(15) Akiti, T. T.; Constant, K. P.; Doraiswamy, L. K.; Wheelock, T. D., An improved core-in-shell sorbent for desulfurizing hot coal gas. *Advances in Environmental Research* **2002,** 6, (4), 419-428.

(16) Akiti, T. T., Jr.; Constant, K. P.; Doraiswamy, L. K.; Wheelock, T. D., Development of an advanced calcium-based sorbent for desulfurizing hot coal gas. *Advances in Environmental Research* **2001,** 5, (1), 31-38.

(17) Wheelock, T. D.; Akiti, T. T. Core-in-shell sorbent for hot coal gas desulfurization. Patent:2002103074, 2002.

(18) Hasler, D. J.; Wheelock, T. D.; Doraiswamy, L. K.; Constant, K. P., Physical Properties and Composition Effects on the Reactivity of Calcium-Based Sulfur Sorbents. *Industrial & Engineering Chemistry Research* **2007,** 46, (18), 5913-5921.

(19) Hasler, D. J. L.; Doraiswamy, L. K.; Wheelock, T. D., A Plausible Model for the Sulfidation of a Calcium-Based Core-in-Shell Sorbent. *Industrial & Engineering Chemistry Research* **2003,** 42, (12), 2644-2653.

(20) Satrio, J. A.; Shanks, B. H.; Wheelock, T. D., Development of a Novel Combined Catalyst and Sorbent for Hydrocarbon Reforming. *Industrial & Engineering Chemistry Research* **2005,** 44, (11), 3901-3911.

(21) Satrio, J. A.; Shanks, B. H.; Wheelock, T. D., A Combined Catalyst and Sorbent for Enhancing Hydrogen Production from Coal or Biomass. *Energy & Fuels* **2007,** 21, (1), 322-326.

(22) Albrecht, K. O.; Satrio, J. A.; Shanks, B. H.; Wheelock, T. D., Development of an Alumina-Based Material for Use as the Shell of a Combined Catalyst/Sorbent Core-in-Shell Material. *In Preparation* **2008**.

(23) *Catalyst Handbook*. Second Edition ed.; Wolfe Publishing, Ltd.: Frome, England, 1989; p 537-548.

(24) Kubaschewski, O.; Evans, E. L.; Alcock, C. B., *Metallurgical Thermochemistry*. Fourth ed.; Pergamon Press Ltd.: Oxford, 1967; Vol. 1, p 379.

(25) Barker, R., Reversibility of the reaction of calcium carbonate to give calcium oxide and carbon dioxide. *Journal of Applied Chemistry & Biotechnology* **1973,** 23, (10), 733-42.

(26) Bhatia, S. K.; Perlmutter, D. D., Effect of the product layer on the kinetics of the carbon dioxide-lime reaction. *AIChE Journal* **1983,** 29, (1), 79-86.

(27) *CRC Handbook of Chemistry and Physics*. 87th Edition ed.; Taylor & Francis Group: Boca Raton, Fl, 2006-2007.

(28) Yamamoto, T.; Hatsui, T.; Matsuyama, T.; Tanaka, T.; Funabiki, T., Structures and Acid-Base Properties of La/Al2O3 - Role of La Addition to Enhance Thermal Stability of g-Al2O3. *Chemistry of Materials* **2003,** 15, (25), 4830-4840.

(29) Bartholomew, C. H.; Farrauto, R. J., *Fundamentals of Industrial Catalytic Processes*. Second ed.; John Wiley & Sons, Inc.: Hoboken, 2006; p 83.

(30) Kanclir, E.; Ambruz, V., Thermal expansion of minerals in the system CaO-Al2O3. *Chemicke Zvesti* **1964,** 18, (9), 702-4.

(31) Zhai, H. Y.; Chu, W. K., Effect of interfacial strain on critical temperature of YBa2Cu3O7-d thin films. *Applied Physics Letters* **2000,** 76, (23), 3469-3471.

Chapter 5. High Concentration H_2 Production via the Water-Gas Shift Reaction Utilizing a Combined Catalyst/Sorbent Core-in-Shell Material

A paper to be submitted to *Industrial & Engineering Chemistry Research*

Karl O. Albrecht,[a] Justinus A. Satrio,[b] Brent H. Shanks[a] and Thomas D. Wheelock[a,*]

Abstract

The water-gas shift reaction is being strongly considered for the production of hydrogen form synthesis gas ($CO + H_2$) produced by gasifying coal or biomass. However, this exothermic reaction is limited by thermodynamic equilibrium. This limitation can be largely overcome by mixing a sorbent for the by-product CO_2 with a catalyst for the reaction. For the present investigation, three different catalyst formulations were combined with limestone in the form of pellets made with limestone cores surrounded by shells made largely of sintered alumina. One catalyst formulation consisted almost entirely of the sintered alumina. A second formulation included some Fe_2O_3 in the shell material while the third formulation included elemental Ni in the shell material.

A test of these formulations showed that all three formulations were highly effective for catalyzing the water-gas shift reaction at temperatures ranging from 480°C to 600°C when the reactants were supplied in a 3:1 mole ratio of H_2O:CO as long as CO_2 was being absorbed. However, without CO_2 absorption, only the Ni formulation achieved a large CO conversion. Therefore, by removing CO_2 from the reaction mixture as it is produced through

[a]Dept of Chemical and Biological Engineering, Iowa State University, Ames, Iowa 50011.

[b]Center for Sustainable Environmental Technologies, 0411 Marston Hall, Iowa State University, Ames, Iowa 50011

*Corresponding Author: wheel@iastate.edu

absorption, it would be possible to rely on Al_2O_3 as a catalyst. This material offers the advantages of being rugged, relatively inexpensive, and not easily poisoned by sulfur compounds or other impurities in the feed.

Introduction

Hydrogen is an important chemical used in petroleum refining and in the production of various products such as methanol and ammonia. Additionally, H_2 has the potential to become a transportation fuel in a H_2-based economy. One of the more widely used industrial processes for making H_2 is based on the water-gas shift reaction in which CO and steam are reacted to produce H_2 and CO_2. The CO can be produced by gasifying coal or biomass or by reforming natural gas.[1, 2]

The reversible water-gas shift reaction converts one mole of carbon monoxide and one mole of steam into one mole of carbon dioxide and one mole of hydrogen.

$$CO + H_2O \leftrightarrow CO_2 + H_2 \quad (1)$$

The exothermic water-gas shift reaction is limited by thermodynamic equilibrium; as the temperature increases, the equilibrium conversion of CO decreases. In order to obtain maximum conversion of carbon monoxide, the industrial application of the water-gas shift reaction is performed in two steps. First, a high temperature shift (HTS) step is performed at 350-500^{o}C using an iron oxide/chromium oxide catalyst.[3] The HTS step is followed by a low temperature shift (LTS) step at 200-215^{o}C, which uses a copper-zinc oxide-aluminum oxide catalyst.[3] A decrease in temperature and the use of two reactors in series is needed to maximize the rate of the water-gas shift reaction in the first reactor while increasing overall CO conversion in the second, cooler reactor.

Recent research has focused on overcoming the equilibrium limitation by catalyzing the water-gas shift reaction in the presence of a selective CO_2 sorbent. Lee et al.[4] investigated a Na_2O-promoted alumina sorbent that can selectively absorb CO_2 in the presence of steam. When the Na_2O-promoted alumina becomes saturated with CO_2, it can be regenerated through a thermal swing desorption procedure. The Na_2O-promoted alumina was demonstrated by physically mixing it with an industrial LTS catalyst. When the mixture was tested at 150°C, the rate of the water-gas shift reaction was low and unreacted CO was observed in the effluent from the reactor even though CO_2 was being absorbed. Increasing the temperature from 150°C to either 200°C or 300°C resulted in an increase in the rate of the water-gas shift reaction, enabling a fuel-cell-grade H_2 stream to be produced while CO_2 was being absorbed.

Another sorbent for CO_2 that has been investigated for the water-gas shift reaction system is CaO. Han and Harrison[5] utilized dolomite as a precursor for CaO in a reactor without any catalyst. The kinetics of the water-gas shift and CaO absorption reactions were sufficiently fast so that the results closely approached equilibrium between 500°C and 650°C under a pressure of 15 atm. Total combined conversion of CO and absorption of CO_2 were greater than 99.9% at 500°C. Above 500°C, the carbon oxide levels increased with an increase in temperature due to the equilibrium limitation. However, CO and CO_2 removal was 98% or greater up to 600°C, demonstrating that high concentration H_2 can be produced at temperatures greater than industrially employed for the water-gas shift reaction at present without any catalyst present.

Utilizing CaO as a sorbent requires consideration of the fact that CaO can form $Ca(OH)_2$ in the presence of steam. At 470°C, the equilibrium partial pressure of water vapor is 1.0 atm in the presence of $Ca(OH)_2$.[6] Thus, at atmospheric pressure, $Ca(OH)_2$ formation is not thermodynamically favorable above 470°C. Therefore, tests in the current investigation were limited to atmospheric pressure at temperatures of 480°C and above.

Another method of combining a catalyst and sorbent for production of high concentration H_2 has been under development for several years.[7, 8] This method utilizes spherical pellets consisting of a CaO core surrounded by a shell of alumina impregnated with a catalyst. Although the core is generally made of limestone, other CaO precursors such as dolomite can be used. Since the CaO is soft and friable, a strong shell made of sintered alumina is essential. The core-in-shell pellets were developed initially for the steam-reforming of hydrocarbons, and for this purpose the shell was impregnated with a Ni catalyst.[7] Since this application also involved the water-gas shift reaction, the results were directly applicable in the present investigation.

While Satrio et al.[7] found it necessary to incorporate a Ni catalyst in the core-in-shell material for the combined steam-methane reforming and water-gas shift reactions, other investigations have used catalysts for the water-gas shift reaction that may be more suitable than Ni for the present application. At 550°C and 15 atm with a $CO:H_2O$ ratio of approximately 1:4, Han and Harrison[5] demonstrated that Al_2O_3 was slightly more active than a traditional HTS catalyst for the water-gas shift reaction in the absence of CO_2 absorption. These investigators also demonstrated the catalytic activity of dolomite, limestone and marble chips for the water-gas shift reaction. These results indicated that core-in-shell pellets made with Al_2O_3 shells and CaO cores might already possess sufficient catalytic activity for

the water-gas shift reaction so that an additional catalyst was unnecessary. Such material could prove advantageous for treating synthesis gas produced by the gasification of coal or biomass that has been shown to contain sulfur that poisons traditional HTS and LTS catalysts.[2] In the iron oxide/chromium oxide HTS catalyst, iron oxide can be converted to less active iron sulfide if the sulfur content of the synthesis gas is greater than or equal to 100 ppm.[1] Sulfur would also poison the catalytically active Cu phase in the LTS catalyst.[3] On the other hand, by utilizing Al_2O_3 as a water-gas shift catalyst in combination with CaO as a sorbent for CO_2, a robust material that is more resistant to sulfur poisoning can be made. Furthermore, if the CaO core is converted to CaS, the sorbent can be regenerated by a proven method.[9, 10]

In addition to the ability to overcome equilibrium limitations, Lee and co-workers have claimed that the removal of CO_2 also enhances the forward rate of the water-gas shift reaction.[11] Han and Harrison[5] also achieved very high CO conversion with only a CaO-based sorbent with no catalyst present. In order to better understand the effect of CO_2 absorption on the forward rate of the water-gas shift reaction, it is instructive to analyze previous studies of the kinetics and mechanism of the reaction over a HTS catalyst. While several different mechanisms and rate equations have been proposed,[12] the Langmuir-Hinshelwood type rate equation that was proposed by Fott et al.[13] shares characteristics with several rate expressions for the water-gas shift reaction that are documented in the literature.

$$r = \frac{k K_{CO} K_{H_2O} \left\{ [CO][H_2O] - \frac{[CO_2][H_2]}{K} \right\}}{\{1 + K_{CO}[CO] + K_{H_2O}[H_2O] + K_{CO_2}[CO_2] + K_{H_2}[H_2]\}^2} \qquad (2)$$

In equation 2, r is the rate of the water-gas shift reaction, k is the kinetic rate constant, K is the equilibrium constant for the water-gas shift reaction, K_i is the equilibrium constant for the adsorption of species i on an active catalytic site and $[i]$ is the concentration of species i. Fott et al.[13] derived Equation 2 and also observed that reducing the CO_2 concentration led to an increase in the rate of reaction over the HTS catalyst. Qualitatively, Equation 2 indicates that if the concentration of CO_2 were to decrease through selective absorption, the overall rate would increase. This can be seen from the effect of CO_2 concentration on both the numerator and denominator of Equation 2. While a kinetic expression for the results observed in the present investigation is not likely to be identical to Equation 2, the results are generally in agreement with this expression. Therefore, CO_2 absorption can not only overcome equilibrium limitations associated with the exothermic water-gas shift reaction but also has the potential to enhance the forward rate of the reaction.

The purpose of the present investigation was to evaluate the performance of a combined catalyst and sorbent in the form of spherical core-in-shell pellets for the production of high concentration H_2 by means of the water-gas shift reaction. Carbon monoxide and steam were fed to a fixed bed reactor to produce H_2 and CO_2. Three different catalyst formulations were investigated whereas only CaO derived from limestone was employed as a sorbent core for CO_2. The first catalyst formulation consisted almost entirely of the alumina shell material and a small amount of limestone as described below. This formulation was tested to determine if Al_2O_3 could catalyze the water-gas shift reaction as reported above. The second formulation was similar to the first except that 10 wt% Fe_2O_3 was added to the shell formulation in order to approximate a HTS catalyst. The third formulation was also similar to the first but with a Ni catalyst impregnated in the shell. The samples were tested at

atmospheric pressure and temperatures between 480°C and 600°C and the results were compared with calculated thermodynamic equilibrium conversion values.

Experimental Methods and Materials

Materials

Limestone for this study was obtained from two different sources. Columbia River Carbonates in Washington provided Microna 3 limestone, with a mean particle size of 3.2 μm and a $CaCO_3$ content greater than 97 wt% according to the producer. Coarser limestone with 97 wt% $CaCO_3$ was obtained from the Ames, Iowa quarry of Martin Marietta Aggregates. This material was ground and screened to a size of -212/+63 μm.

Three different types of alumina were utilized for the shell formulation of the core-in-shell pellets. An α-alumina supplied by Almatis and designated as A16-SG had a mean particle size of 0.4 μm. Another α-alumina consisting of particles screened to -325 mesh, or –44 μm size, was also supplied by Almatis and was designated as T-64 alumina. The Engelhard Corporation supplied an amorphous alumina designated as DD-290 that is sometimes used as a catalyst support precursor. According to the supplier, DD-290 has a mean particle size of 9.8 μm and a surface area of 275 m^2/g. DD-290 is identical to CP-7 alumina formerly supplied by Almatis.

Ferric oxide, Fe_2O_3, was supplied by the J.T. Baker Chemical Co., which reported a purity of 99.6 wt% Fe_2O_3. Nickel nitrate hexahydrate, $Ni(NO_3)_2 \bullet 6H_2O$ was supplied by Sigma-Aldrich, which claimed the material to be 99.999% pure. Matheson Tri-Gas supplied CO with a Technical Purity grade of 99.8%.

Preparation of Core-in-Shell Pellets

Spherical core-in-shell pellets were prepared for testing by pan rolling powders in a rotating drum pelletizer that had a maximum diameter of 25 cm and was operated at 30 rpm. The cores of the spherical pellets were prepared first by placing the limestone powder in the rotating drum and spraying it with water intermittently so that it balled up as the drum rotated. Cores were built up in this way until about 20 g of pellets ranging between 5 and 6 mesh, or between 3.96 mm and 3.35 mm in diameter, were produced. The cores were then hardened in the rotating drum operated at the following speeds and time settings: 10 rpm for 10 min., 30 rpm for 20 min., 60 rpm for 30 min., and 90 rpm for 30 min.

The shell material formulation was prepared by weighing out 600 g of the appropriate shell mixture. The dry shell mixture was placed in a container and rolled for at least 1.0 hr to produce a homogenous mixture of dry powders. Shells were applied to pre-made cores by using the pelletizer operating at 30 rpm while spraying the pellets intermittently with a 5 wt% lignin/95 wt% water solution and gradually adding the shell powder. In this way, the size of the pellets gradually increased to a diameter between 3.96 and 4.76 mm, or between 5 and 4 mesh. After about 50 g of pellets had been made, the pellets were hardened as described above for the cores.

Calcination of Pellets

All of the pellets tested were calcined at high temperature in an atmosphere of flowing air to increase the physical integrity of the pellets. About 25 g of pellets would be subjected to calcination at one time. Some samples were calcined at 900°C for 3 hr after being heated gradually from room temperature over a two hour period. Other samples were

calcined at 800°C for 2 hr following a 2 hr heating ramp to 800°C. All of the calcined materials were cooled using a 2 hr ramp back to room temperature.

Impregnation of Nickel Nitrate

One batch of core-in-shell pellets tested in this investigation was impregnated with a Ni catalyst. About 25 g of core-in-shell pellets were produced and calcined at 800°C for 2 hr. After calcination, the pellets were placed in a tube oven at 650°C for 1 hr in flowing CO_2 in order to recarbonate the CaO core. After recarbonation, the pellets were placed in a 50 mL round bottom flask and subjected to a moderate vacuum and temperature of 110°C for 3 hr. After this treatment, the sample was removed from the vacuum oven, capped, and allowed to cool for 5 min. Then, 25 mL of 2 M $Ni(NO_3)_2 \bullet 6H_2O$ in tetrahydrofuran (THF) was slowly added to the pellets. After soaking in this solution for 1 hr, the pellets were removed from the solution and allowed to dry under atmospheric conditions overnight. The pellets were subsequently dried at 110°C for 4 hr under atmospheric pressure. The pellets were then placed in a tube oven and the temperature was ramped from room temperature to 500°C at 25°C/min in flowing air. Once 500°C was reached, the pellets remained in the oven for 2 hr to convert nickel nitrate into NiO. The impregnation process was then repeated so that the pellets were impregnated with nickel nitrate twice prior to testing in the fixed bed reactor. After loading of the Ni impregnated sample into the fixed bed reactor, the NiO was reduced in-situ to metallic Ni by raising the catalyst bed temperature to 550°C and passing H_2 through the bed at a rate of 1.3 mmol/min for 4 hr.

Core-in-Shell Samples Tested

Three batches of core-in-shell pellets were prepared and tested in a fixed bed reactor for conducting the water-gas shift reaction with simultaneous absorption of CO_2. Table 1 shows the formulations used in preparing the three core-in-shell samples, and it also indicates how the formulations are identified throughout this presentation.

Table 1. Core-in-shell pellet formulations tested for the water-gas shift reaction.

Sample I.D.	Limestone Core	Shell Formulation, wt%				Calcination Conditions
		A16-SG	T64	DD-290	Limestone	
F(Al_2O_3)	Microna 3	36	27	27	10[c]	900°C, 3 hr
F(Fe_2O_3)[a]	Microna 3	32.4	24.3	24.3	9[c]	900°C, 3 hr
F(Ni-Al_2O_3)[b]	-212/+63 μm	38	28.5	28.5	5[d]	800°C, 2 hr

[a]10 wt% Fe_2O_3 was also added
[b]6.1 wt% Ni after being impregnated with $Ni(NO_3)_2$
[c]Microna 3 limestone
[d]–212/+63 μm limestone

The first formulation, denoted as F(Al_2O_3), had only limestone and alumina present in the shell before calcination. Microna 3 limestone was added to the shell formulation to enhance the physical strength of the shell material upon calcination at 900°C for 3 hr. This 3.2 μm size material proved to be more effective than the –210/+44 μm material used previously for strengthening the shell material.[7, 8] In addition, Microna 3 limestone was utilized as the CaO precursor for the cores of the core-in-shell pellets.

The second formulation, designated F(Fe_2O_3), was generally similar to the first except for the addition of 10 wt% Fe_2O_3 to the shell material in order to approximate a HTS catalyst.

Industrial HTS catalysts are made with approximately 90 wt% Fe_2O_3 and 10 wt% Cr_2O_3.[12] The active phase in HTS catalysts is Fe_3O_4, which forms upon reduction of Fe_2O_3. The Cr_2O_3 acts as a refractory to stabilize the Fe_3O_4 crystallites. For industrial applications, HTS catalysts undergo a controlled reduction procedure to ensure that Fe_3O_4 is produced as the major phase. In this investigation, no initial reduction of iron oxide was performed. Microna 3 limestone was again utilized as the CaO precursor for the cores of the core-in-shell pellets.

The third shell formulation, denoted as F(Ni-Al_2O_3), was similar to one of the shell formulations used by Satrio et al.[7] for steam-methane reforming. In order to activate the Ni catalyst, methane and propane were reformed at 850°C for several hours after the Ni had been reduced with H_2 at 550°C for 4 hr. A similar procedure had been used previously when such a catalyst had been used for steam-methane reforming.[7]

Fixed Bed Reactor Loading

The performance of the core-in-shell pellets was evaluated with a fixed bed tubular reactor made of stainless steel and having a length of 61 cm and an inner diameter of 1.27 cm. A stainless steel plate with holes drilled in it supported the bed of pellets in the vertical tube. Approximately 35 g of inert spherical pellets having a diameter of 0.63 cm were placed on top of the plate, resulting in a 23 cm deep layer. On top of this layer was placed another 2.5 cm deep layer of extruded SiC pellets, each having a diameter of 0.32 cm. The two layers of inert SiC supported the bed of core-in-shell pellets tested, which was 10-11 cm deep and consisted of a mixture of 13.7 g of core-in-shell pellets and 8.2 g of SiC pellets having a diameter of 0.1cm. The interspersed SiC pellets reduced channeling around the core-in-shell pellets and improved heat transfer in the catalyst bed. In the middle of the catalyst bed, a thermocouple was placed to record the bed temperature when the reactor was in use. Above

the bed of core-in-shell pellets was placed another layer of extruded SiC pellets to mix and preheat the entering gas stream of reactants. This layer was 10 cm deep and consisted of 16 g of cylindrical pellets having a diameter of 0.32 cm.

Fixed Bed Reactor Operating Procedure

For testing a core-in-shell pellet formulation, the fixed bed reactor was supplied with a mixture of steam and carbon monoxide in a 3:1 mole ratio while also employing a total gas flow rate of 3.6 mmol/min. Steam was generated by pumping de-ionized water at a controlled flow rate into a preheater furnace where it was mixed with CO, which was metered by a Brooks mass flow controller. The mixture of steam and CO was conducted through heat-taped stainless steel tubing to the reactor inlet.

Before undertaking a new test cycle of the core-in-shell pellets, the pellets were regenerated to desorb any CO_2 absorbed during a previous cycle. The F(Al_2O_3) formulation was regenerated by increasing the bed temperature to 775°C with Ar flowing through the bed at a rate of 1.8 mmol/min. Under these conditions, desorption was slow and a long time was required for the reactor effluent to be devoid of CO_2. Therefore, a different procedure was employed for regenerating the sorbent in the case of other formulations. For these formulations, a CO and steam mixture flowing at 3.6 mmol/min was used as the sweep gas while the bed temperature was raised to 850°C. Under these conditions, desorption of CO_2 was complete when the CO_2 concentration in the reactor effluent remained constant. Sorbent regeneration at 850°C typically took about 1.0-1.5 hr. Additionally, the use of CO and steam as the sweep gas ensured that the Ni catalyst remained reduced during sorbent regeneration of the F(Ni-Al_2O_3) sample.

After regenerating the sorbent, the reactor temperature was reduced to a temperature more appropriate for the water-gas shift reaction. While the reactor was being cooled, Ar was passed through the bed at a rate of 1.8 mmol/min in the case of the F(Al_2O_3) formulation. For the other formulations, no gas was passed through the bed during cooling. When the desired reaction temperature was achieved, the reactants were introduced at a total flow rate of 3.6 mmol/min with a molar ratio of 3:1 CO:H_2O. Samples of the reactor effluent were periodically drawn with Gastight syringes supplied by the Hamilton Co. These samples were analyzed with an SRI 8610C gas chromatograph (GC) equipped with a thermal conductivity detector and flame ionization detector to determine the concentrations of H_2, CO, CO_2 and CH_4, which were then normalized to 100%.

Experimental Results and Discussion

The performance of the different core-in-shell pellet formulations listed in Table 1 was evaluated by conducting the water-gas shift reaction in the fixed bed reactor starting with a freshly regenerated sample and continuing a run until the sorbent was saturated and CO_2 absorption effectively ceased. The results of such a run are presented in Figure 1. For this run the reactor was charged with the F(Ni-Al_2O_3) pellet formulation, and it was operated at 600°C. During the "Absorption" period, most of the CO_2 was absorbed and a high concentration of H_2 was produced. Later, as the sorbent became saturated, the concentration of H_2 fell to a level of approximately 50 mol% and the concentration of CO_2 reached a level of 47 mol%. Figure 1 illustrates a run with a F(Ni-Al_2O_3) sample that had undergone several absorption and regeneration cycles, which shortened the length of Absorption period compared to a fresh sample.

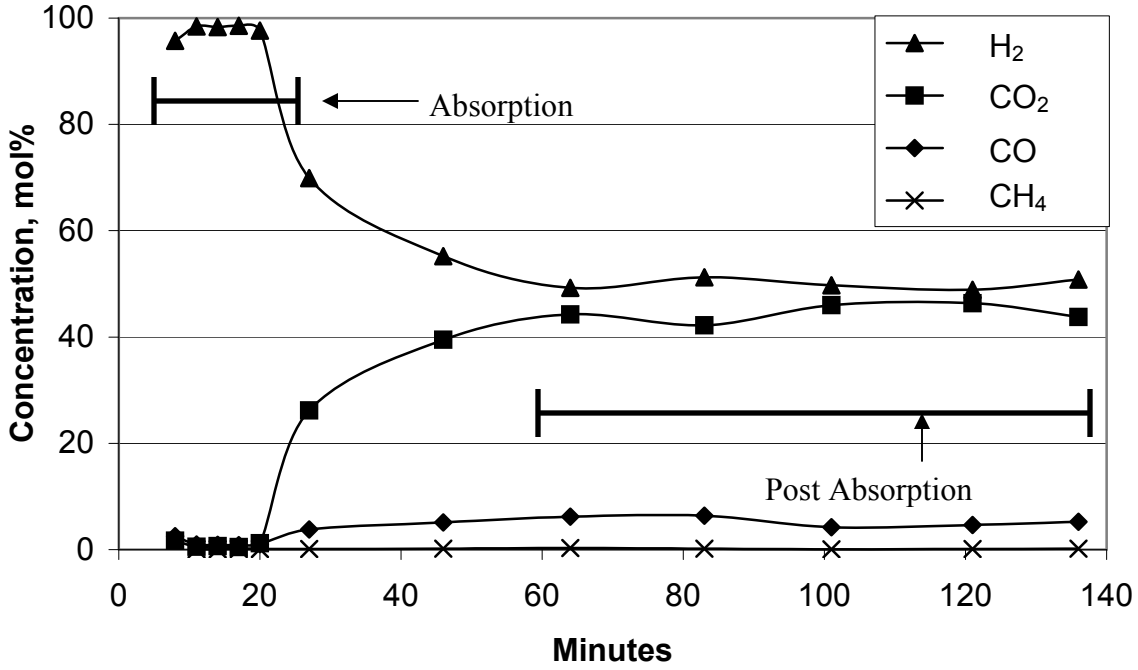

Figure 1. Dry basis gas concentrations observed in the reactor effluent from testing the F(Ni-Al_2O_3) formulation at 600°C. The period marked "Absorption" indicates when strong CO_2 absorption was present and "Post Absorption" indicates that the CaO sorbent had become saturated and CO_2 absorption had effectively ceased.

The Post Absorption phase should produce the gas concentrations that would result if no sorbent was present in the reactor. Interestingly, every test run observed in this investigation resulted in a H_2 concentration slightly higher than the CO_2 concentration during the Post Absorption period. This is interesting because H_2 and CO_2 should be present in equimolar quantities when only the water-gas shift reaction takes place. A check of the GC did not reveal an error in calibration that would account for the disparity. A possible explanation for this disparity is that CO_2 continued to be slowly absorbed well into the so-called Post Absorption period. When CaO produced from limestone undergoes recarbonation after calcination, the CaO goes through a period of rapid, kinetically controlled reaction with CO_2, followed by the buildup of a carbonate layer. When the thickness of the carbonate layer

becomes significant, the rate of absorption of CO_2 becomes controlled by diffusion through the carbonate layer.[14] This slow, diffusion-controlled period of CO_2 absorption can last for an extended period of time. Thus, it is plausible that CaO would slowly absorb CO_2 even during the Post Absorption period.

Each of the core-in-shell pellet formulations were subjected to a series of tests of the water-gas shift reaction conducted at four different temperatures. The results of the first series conducted with the F(Al_2O_3) formulation are tabulated in Table 2. The gas concentrations in Table 2 can be compared with calculated thermodynamic equilibrium gas concentrations in Appendix 4. The gas concentrations recorded in this table were used to calculate the CO conversions for both the Absorption and Post Absorption periods of operation, which are presented in Figure 2. The black bars outlining the Post Absorption period indicate the calculated equilibrium CO conversion for the water-gas shift reaction based on equilibrium data found in the *Catalyst Handbook.*[12] The equilibrium data for the reaction of CaO and CO_2 present during the Absorption period was obtained from *Metallurgical Thermochemistry.*[15] For the Absorption period of operation, the calculated equilibrium conversion of CO was essentially 100% over the 480-600°C temperature range. Hence, black bars outlining the equilibrium conversions for the Absorption period are not shown in order to refrain from obscuring the data.

Figure 2 and Table 2 indicate that a large CO conversion and a high concentration of H_2 were produced at all temperatures during the Absorption period with the F(Al_2O_3) formulation. The large CO conversions observed during this period were due to the rapid rate of the water-gas shift reaction, which was not inhibited by the reverse reaction. As

Table 2. Dry basis gas concentrations observed exiting the fixed-bed reactor during water-gas shift testing of the F(Al_2O_3) formulation.

Temperature, °C	Period of Operation	Component, mol%			
		CH_4	CO	CO_2	H_2
480	Absorption	0.0	4.4	0.1	95.4
	Post Absorption	0.0	76.0	8.5	15.5
520	Absorption	0.0	3.1	0.6	96.1
	Post Absorption	0.0	63.9	15.6	20.5
550	Absorption	0.0	1.8	0.6	97.6
	Post Absorption	0.0	52.3	20.5	27.2
600	Absorption	0.0	1.5	0.9	97.6
	Post Absorption	0.0	30.1	30.6	39.3

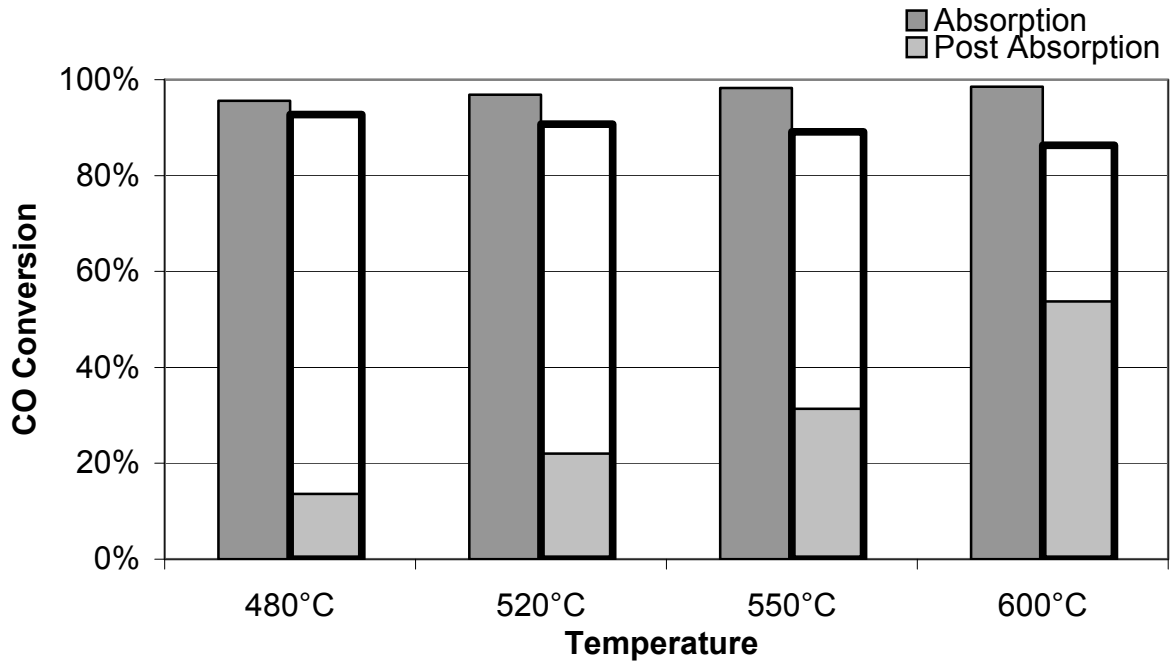

Figure 2. CO conversion observed during water-gas shift testing of the F(Al_2O_3) core-in-shell pellet formulation. The black bars outlining the Post Absorption bars represent the calculated water-gas shift equilibrium in the absence of CO_2 absorption. The shaded areas represent actual conversion observed in all cases.

equation 2 indicates, the rate of the water-gas shift reaction can be strongly reduced by the presence of CO_2. The presence of CO_2 appears to have reduced the forward rate of the water-gas shift reaction during the Post Absorption period. During this period, the CO conversion increased directly with an increase in temperature, which was probably due to kinetic limitations of the water-gas shift reaction. Han and Harrison[5] had claimed previously that Al_2O_3 and limestone catalyze the water-gas shift reaction at 550°C, but the present results indicate that the catalytic activity of the F(Al_2O_3) core-in-shell pellets was not sufficient to achieve equilibrium CO conversion levels during the Post Absorption period. However, the removal of CO_2 via absorption by CaO during the Absorption period allowed for the forward rate of the reaction to be substantially increased.

During the Absorption period, the system appeared to approach equilibrium but was still slightly limited by either the rate of diffusion of CO_2 through the shell to the CaO core or the rate of reaction between CaO and CO_2. A limitation is indicated by the gradual increase in CO conversion with increasing temperature, which is opposite to the decrease in CO conversion expected in an exothermic system limited by thermodynamic equilibrium. However, a comparison of actual CO conversion levels during the Absorption period with calculated equilibrium limited CO conversions for the Post Absorption period in Figure 2 indicates that the equilibrium limitation of the water-gas shift reaction was largely overcome by the absorption of CO_2. In other words, since the CO conversion during the Absorption period as indicated by Figure 2 was higher than the equilibrium conversion indicated for the Post Absorption period, the absorption of CO_2 made it possible to overcome the thermodynamic equilibrium limitation of the water-gas shift reaction. The maximum benefit

was observed at 600°C where a CO conversion of 98.5% was achieved when CO_2 was being absorbed compared to a calculated equilibrium conversion of 86.3% without CO_2 absorption.

The second series of tests of the water-gas shift reaction was conducted with the F(Fe_2O_3) formulation of the core-in-shell pellets. The results of this series are reported in Table 3 and Figure 3. Gas concentrations that were observed in the reactor effluent during this series are shown in Table 3 and the CO conversions based on these concentrations are shown in Figure 3. The gas concentrations in Table 3 can be compared with calculated thermodynamic equilibrium gas concentrations in Appendix 4. As before, the black borders above the unshaded areas correspond to calculated thermodynamic equilibrium values, where as the shaded areas correspond to the actual conversion achieved. Of most interest was the higher conversion achieved with the F(Fe_2O_3) formulation compared to the F(Al_2O_3) formulation at each temperature during the Post Absorption period. These results clearly indicated that the F(Fe_2O_3) formulation had a higher catalytic activity for the water-gas shift reaction than the F(Al_2O_3) formulation for this reaction.

Somewhat puzzling were the results in Figure 3 that indicated that the CO conversion achieved during the Absorption period at either 480°C or 520°C were less than those achieved with the F(Al_2O_3) formulation. Furthermore, a comparison of the results in Table 3 with those in Table 2 showed that the H_2 concentration produced at these temperatures was lower for the second formulation than for the first. The lower conversions produced by the F(Fe_2O_3) formulation did not appear to be due to reduced catalytic activity of this material because the CO conversion achieved at these temperatures during the Post Absorption period was greater than those achieved with F(Al_2O_3). Likewise, Microna 3 limestone was utilized as the CaO sorbent precursor in both samples, making different absorption rates by

Table 3. Dry basis gas concentrations observed exiting the fixed-bed reactor during water-gas shift testing of the F(Fe_2O_3) formulation.

Temperature, °C	Period of Operation	Component, mol%			
		CH_4	CO	CO_2	H_2
480	Absorption	0.0	26.1	1.2	72.8
	Post Absorption	0.0	58.6	15.8	25.6
520	Absorption	0.0	7.2	0.7	92.1
	Post Absorption	0.0	40.6	26.3	33.0
550	Absorption	0.0	2.9	0.7	96.5
	Post Absorption	0.0	28.3	31.1	40.6
600	Absorption	0.0	3.4	1.2	95.4
	Post Absorption	0.0	15.8	38.2	46.0

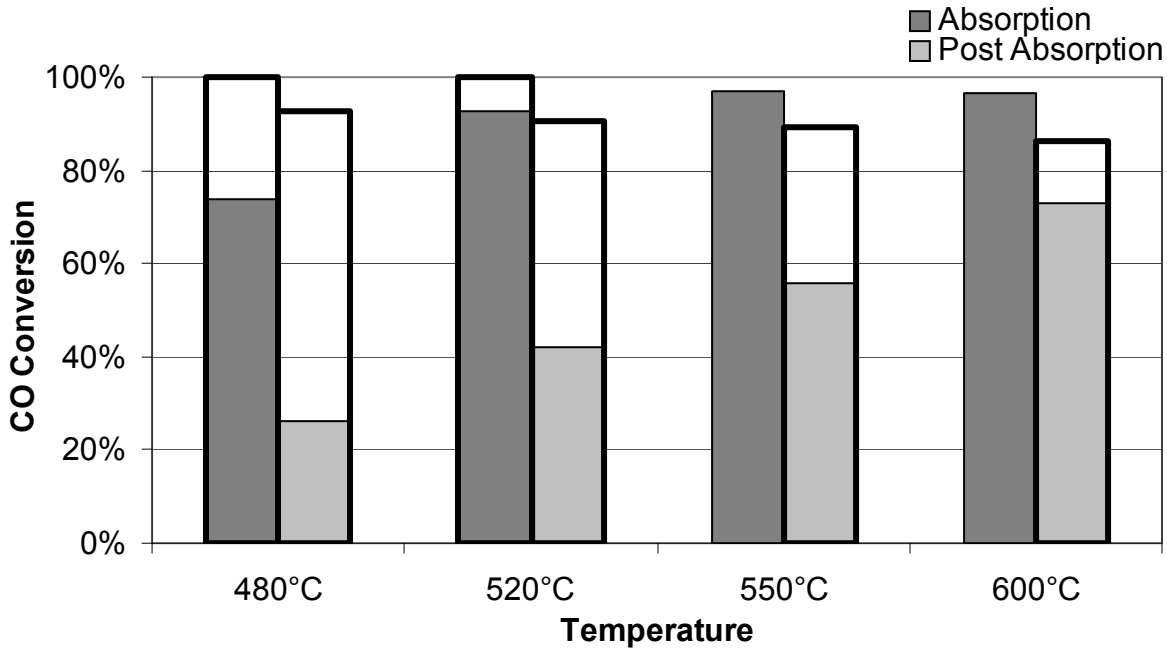

Figure 3. CO conversion observed during water-gas shift testing of the F(Fe_2O_3) formulation. The black outlining bars illustrate calculated CO conversions based on thermodynamic equilibrium. The shaded areas represent actual conversions in all cases.

the sorbent unlikely. A more likely explanation is that the addition of ultra-fine sized Fe_2O_3 to the second formulation reduced the porosity and increased the resistance to diffusion of CO_2 through the shell material. Consequently, the CO_2 produced by the water-gas shift reaction was not absorbed as rapidly. However, as the temperature was raised, the rate of CO_2 diffusion could have increased so that at the higher temperatures, this rate was virtually non-limiting. At both 550°C and 600°C, the CO conversion achieved with F(Fe_2O_3) were only slightly lower than those obtained with F(Al_2O_3) during the Absorption period.

The third series of tests was conducted with a core-in-shell pellet formulation similar to the one used by Satrio et al.[7] for steam-methane reforming. When this formulation was utilized for steam-methane reforming, an active Ni catalyst was required in order for the CH_4 conversion to approach the value predicted by thermodynamic equilibrium.[7] Since this core-in-shell formulation included a Ni catalyst, the material will be referred to as the F(Ni-Al_2O_3) formulation. This formulation also utilized –212/+63 μm limestone in place of Microna 3 limestone for both the core and shell materials. The limestone was crushed and sieved to provide the necessary size range.

The results of applying the F(Ni-Al_2O_3) formulation to the water-gas shift reaction at different temperatures are presented in Table 4 and Figure 4. As before, the observed gas concentrations in Table 4 can be compared with calculated thermodynamic equilibrium gas concentrations in Appendix 4. These results indicate that for every temperature and for both the Absorption and Post Absorption periods the CO conversion was very large and similar in magnitude to that predicted by thermodynamic equilibrium provided the formation of CH_4 was neglected. Since the concentration of CH_4 in the product was only 0.1 to 0.6 mol%, it probably did not have a major effect on the outcome.

Table 4. Dry basis gas concentrations observed exiting the fixed-bed reactor during water-gas shift testing of the F(Ni-Al_2O_3) sample.

Temperature, °C	Period of Operation	Component, mol%			
		CH_4	CO	CO_2	H_2
480	Absorption	0.6	2.1	0.7	96.6
	Post Absorption	0.6	2.5	46.0	50.9
520	Absorption	0.3	2.3	1.1	96.3
	Post Absorption	0.3	3.7	47.8	48.2
550	Absorption	0.3	1.5	0.8	97.4
	Post Absorption	0.3	5.2	43.9	50.6
600	Absorption	0.1	0.9	0.7	98.2
	Post Absorption	0.2	6.3	43.2	50.2

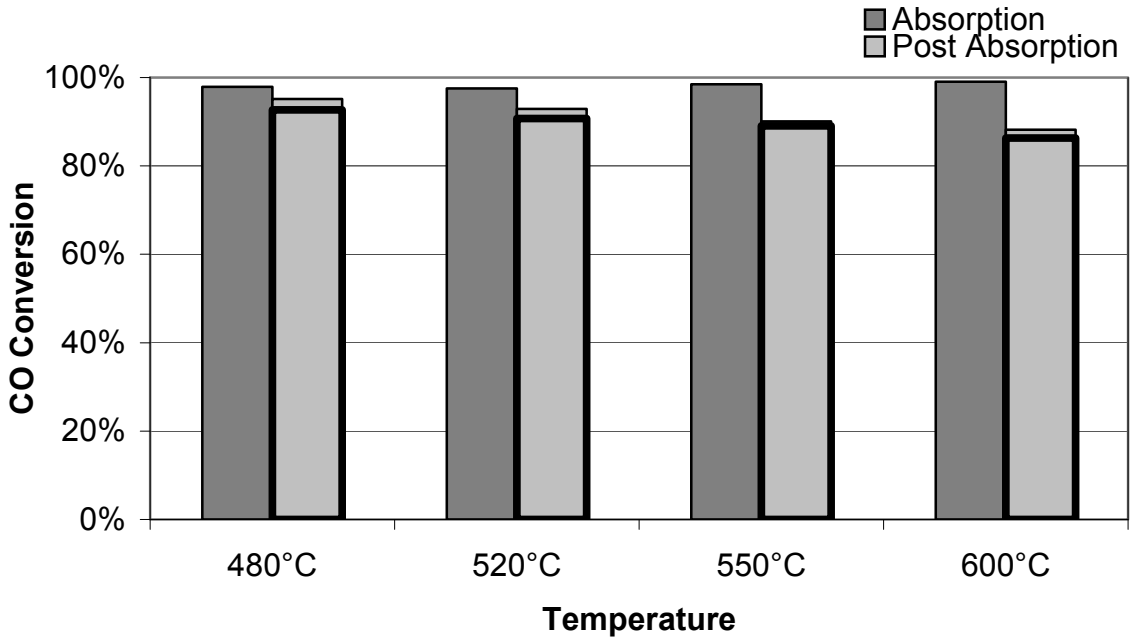

Figure 4. CO conversion observed during water-gas shift testing of the F(Ni-Al_2O_3) formulation. The black bars outlining the Post Absorption bars indicate the predicted CO conversions based on thermodynamic equilibrium. The shaded areas represent actual conversions in all cases.

In contrast to results obtained with the previous formulations, the CO conversion achieved with the F(Ni-Al_2O_3) formulation during the Post Absorption period was within 3% of the calculated equilibrium conversion for each temperature. Also, the conversion during the Post Absorption declined as the temperature increased, which corresponded with the effect of temperature on the equilibrium conversion. All of these results show that the Ni-based catalyst was superior to the other two catalysts for the water-gas shift reaction.

Since small amounts of CH_4 appeared in the reactor effluent while applying the F(Ni-Al_2O_3) catalyst formulation to the water-gas shift reaction, it is likely that the CH_4 was produced by the following exothermic reaction:

$$CO + 3H_2 \leftrightarrow CH_4 + H_2O \qquad (3)$$

Because this reaction is the reverse of the endothermic steam-methane reforming reaction that is catalyzed by Ni, the Principle of Microscopic Reversibility indicates that it should also be catalyzed by Ni.[16] Furthermore, as the temperature increased, the concentration of CH_4 in the effluent (Table 4) decreased in agreement with the effect of temperature on an equilibrium controlled exothermic reaction. No CH_4 was observed while testing the F(Al_2O_3) and F(Fe_2O_3) formulations, which is an additional benefit of using a catalyst that does not catalyze the steam-methane reforming reaction for the production of high concentration H_2 from CO and steam.

Conclusion

Three different catalyst formulations were prepared and tested as the shell material of core-in-shell pellets that combine a catalyst for the water-gas shift reaction with a sorbent for the CO_2 produced by the reaction. All three formulations proved highly effective for

converting CO through the water-gas shift reaction at 550°C and 600°C in the presence of an active sorbent core of CaO. At 480°C and 550°C, both the F(Al_2O_3) and F(Ni-Al_2O_3) formulations continued to be highly effective whereas the effectiveness of the F(Fe_2O_3) formulation declined, possibly because of the reduced permeability of the shell material.

After the CaO sorbent became saturated with CO_2, the F(Ni-Al_2O_3) formulation continued to be highly effective at converting CO at all temperatures tested, while the effectiveness of the other two formulations declined considerably, especially as the temperature was reduced. For this period of operation, the effectiveness of the different catalysts increased in the following order: F(Al_2O_3), F(Fe_2O_3) and F(Ni-Al_2O_3).

Although these results indicate that the F(Ni-Al_2O_3) formulation was the most effective catalyst for all conditions tested, the F(Al_2O_3) formulation was nearly as effective while CO_2 was being absorbed, which corresponds to the most likely operating mode in an industrial H_2 production application. The F(Al_2O_3) formulation is also much less likely to become poisoned by impurities in the feed gas, such as sulfur compounds. Furthermore, no CH_4 was observed during testing of the F(Al_2O_3) formulation. Therefore, the F(Al_2O_3) formulation warrants further development.

Acknowledgement

This report was prepared with the support of the U.S. Department of Energy, under Award No. DE-FG26-04NT 42182. However, any opinions, findings, conclusions, or recommendations expressed herein are those of the authors and do not necessarily reflect the views of DOE.

Literature Cited

(1) Aznar, M. P.; Caballero, M. A.; Corella, J.; Molina, G.; Toledo, J. M., Hydrogen Production by Biomass Gasification with Steam-O2 Mixtures Followed by a Catalytic Steam Reformer and a CO-Shift System. *Energy & Fuels* **2006,** 20, (3), 1305-1309.

(2) Zhang, R.; Brown, R. C.; Suby, A., Thermochemical Generation of Hydrogen from Switchgrass. *Energy & Fuels* **2004,** 18, (1), 251-256.

(3) Bartholomew, C. H.; Farrauto, R. J., *Fundamentals of Industrial Catalytic Processes*. Second ed.; John Wiley & Sons, Inc.: Hoboken, 2006; p 340-486.

(4) Lee, K. B.; Beaver, M. G.; Caram, H. S.; Sircar, S., Effect of Reaction Temperature on the Performance of Thermal Swing Sorption-Enhanced Reaction Process for Simultaneous Production of Fuel-Cell-Grade H2 and Compressed CO2 from Synthesis Gas. *Industrial & Engineering Chemistry Research* **2008,** 47, (17), 6759-6764.

(5) Han, C.; Harrison, D. P., Simultaneous shift reaction and carbon dioxide separation for the direct production of hydrogen. *Chemical Engineering Science* **1994,** 49, (24B), 5875-83.

(6) Babushkin, V. I.; Matveyev, G. M.; Mchedlov-Petrossyan, O. P., *Thermodynamics of Silicates*. Fourth Edition ed.; Springer-Verlag Berlin Heidelberg: Berlin, 1985.

(7) Satrio, J. A.; Shanks, B. H.; Wheelock, T. D., Development of a Novel Combined Catalyst and Sorbent for Hydrocarbon Reforming. *Industrial & Engineering Chemistry Research* **2005,** 44, (11), 3901-3911.

(8) Satrio, J. A.; Shanks, B. H.; Wheelock, T. D., A Combined Catalyst and Sorbent for Enhancing Hydrogen Production from Coal or Biomass. *Energy & Fuels* **2007,** 21, (1), 322-326.

(9) Akiti, T. T., Jr.; Constant, K. P.; Doraiswamy, L. K.; Wheelock, T. D., A Regenerable Calcium-Based Core-in-Shell Sorbent for Desulfurizing Hot Coal Gas. *Industrial & Engineering Chemistry Research* **2002,** 41, (3), 587-597.

(10) Wheelock, T. D.; Akiti, T. T. Core-in-shell sorbent for hot coal gas desulfurization. Patent 2002103074:2002103074, 2002.

(11) Lee, K. B.; Beaver, M. G.; Caram, H. S.; Sircar, S., Reversible chemisorption of carbon dioxide: simultaneous production of fuel-cell grade H2 and compressed CO2 from synthesis gas. *Adsorption* **2007,** 13, (3/4), 385-397.

(12) Twigg, M. V., *Catalyst Handbook*. Third Edition ed.; Wolfe Publishing, Ltd.: Frome, England, 1996; p 537-548.

(13) Fott, P.; Vosolsobe, J.; Glaser, V., Kinetics of carbon monoxide conversion with steam at elevated pressures. *Collection of Czechoslovak Chemical Communications* **1979,** 44, (3), 652-9.

(14) Barker, R., Reversibility of the reaction of calcium carbonate to give calcium oxide and carbon dioxide. *Journal of Applied Chemistry & Biotechnology* **1973,** 23, (10), 733-42.

(15) Kubaschewski, O.; Evans, E. L.; Alcock, C. B., *Metallurgical Thermochemistry*. Fourth ed.; Pergamon Press Ltd.: Oxford, 1967; Vol. 1, p 379.

(16) Satterfield, C. N., *Heterogeneous Catalysis in Industrial Practice*. Second Edition ed.; Krieger Publishing Company: Malabar, Florida, 1996; p 554.

Chapter 6. General Conclusions and Recommended Future Research

General Conclusions

The goal of this innovative research project was to further develop and test an improved combined catalyst/sorbent material for steam reforming CH_4 and for the water-gas shift reaction. The material was in the form of core-in-shell pellets that contained a CaO-based sorbent core for the absorption of CO_2 and a strong outer shell composed mainly of alumina to protect the inner core and to support a Ni catalyst. The present dissertation focuses on improvements to the CaO-based core in Chapter 2 as well as the development of the alumina-based shell material in Chapter 3. Results of testing the core-in-shell material for producing H_2 from a mixture of CH_4 and steam at pressures between 1.0 and 10.0 atm and between 550 and 650°C are presented in Chapter 4. Alternate core-in-shell formulations for producing H_2 from CO and steam via the water-gas shift reaction are presented in Chapter 5. Overall, several significant advances in the materials used for the core-in-shell pellets are described. Additionally, it is shown that the core-in-shell material is capable of producing H_2 at nearly thermodynamic equilibrium levels in most cases from steam and CH_4 or steam and CO.

Development of a stable CaO-based sorbent is described in Chapter 2. The investigation focused on modification of the Microna 3 limestone to produce a stable CaO-based sorbent that could absorb CO_2 and be regenerated over many cycles. The addition of MgO to the precursor limestone produced a sorbent that did not sinter as severely as a similar sorbent without MgO present. Additionally, initial calcination of Microna 3 limestone at 1100°C for 5 hr produced a more stable sorbent than calcination of the limestone at 900°C

for 3 hr. Therefore, a sorbent with 0.25 g MgO/g CaO was more stable than a sorbent without MgO so that after 750 absorption and regeneration cycles, the stabilized sorbent had a greater absorption capacity than the unstabilized sorbent. Additionally, Microna 3 limestone calcined at 1100°C for 5 hr had a higher absorption capacity after 500 cycles than a similar sorbent initially calcined at 900°C for 3 hr.

The development of a strong but porous Al_2O_3-based material with high surface area for use as the shell of core-in-shell pellets is described in Chapter 3. In order to rapidly screen several different formulations, the shell material was prepared in the form of cast cylindrical tablets. Enhancing the physical strength of the shell material by forming a binding aluminate phase proved rewarding. This phase was formed by the addition of limestone or metal nitrates to the alumina formulation and subsequent calcination at a high temperature. Testing revealed that the addition of fine limestone to the alumina formulation resulted in an increase in strength of the cast tablets that was proportional to the concentration of limestone in the samples calcined at 1100°C for 2 hr. Similar samples calcined at 900°C for 3 hr did not respond nearly as well to the addition of limestone, although the addition of 10 wt% limestone to the tablets calcined at the lower temperature did significantly increase the strength of the cast tablets. The addition of lanthanum nitrate to the alumina shell formulation substantially increased the compressive strength of the alumina shell formulation when it was calcined at 900°C or 1100°C.

The surface area of the shell material was not affected greatly by the addition of either limestone or La_2O_3. However, calcination of any shell formulation at 1100°C reduced the surface area of the material much more than calcination at 900°C, which was most likely

due to unavoidable sintering of the high surface area catalyst precursor alumina. Core-in-shell pellets with lanthanum nitrate added to the shell formulation were prepared and were determined to have improved physical strength compared to pellets without lanthanum, which showed a correlation between the physical strength of cast tablets and core-in-shell pellets.

Chapter 4 presents the results of reaction testing two of the promising core-in-shell pellet formulations described in Chapter 3 for the production of H_2 from a mixture of steam and CH_4. Namely, core-in-shell pellets either with 10 wt% limestone or 7.7 wt% La_2O_3 incorporated in the alumina shell formulation were prepared and reaction tested using a 3:1 molar ratio of H_2O:CH_4, a temperature between 550 and 650°C, and a pressure between 1.0 and 10.0 atm. Performance testing of the core-in-shell formulations showed that the rates of the steam-methane reforming and water-gas shift reactions combined with the reaction between CaO and CO_2 were sufficiently rapid to produce a high concentration H_2 stream that was nearly equal to that at thermodynamic equilibrium. Additionally, testing at 10.0 atm and at 600-650°C produced a product with 95 mol% H_2 on a dry basis and with less CO than could be detected by the gas chromatograph used for reactor effluent analysis.

Core-in-shell pellets with the limestone or lanthanum shell formulations were also subjected to lifecycle testing. Each test was conducted at 1.0 atm and included 10 cycles of H_2 production at 650°C followed by subsequent sorbent regeneration at 850°C. The core-in-shell material proved capable of producing a product with 98 mol% H_2 (dry basis) during each cycle. However, the length of time that this concentration of H_2 was produced decreased from cycle to cycle as the absorption capacity of the CaO-based sorbent decayed. Physical characterization of the core-in-shell formulations showed that lifecycle testing

resulted in sintering of the Ni catalyst. Additionally, 18% of the pellets with limestone in the shell and 26% of the pellets with lanthanum in the shell fractured during lifecycle testing either from thermal stresses or from handling of the material.

Chapter 4 also indicates that after the Ni catalyst had been added to the shell, the compressive strength of the shell formulations with limestone or lanthanum were nearly the same. In other words the difference in force required to break the pellets was not statistically significant. Thus, the addition of lanthanum was a costly addition to the core-in-shell formulation that appeared unnecessary when the shell formulation contained both limestone and Ni.

The combined catalyst and sorbent core-in-shell material was also applied to the production of hydrogen at 1.0 atm from a mixture of CO and steam via the water-gas shift reaction, and the results are presented in Chapter 5. For this application, three alternate shell formulations were investigated: (1) an alumina shell with 10 wt% limestone, (2) an alumina shell with 9 wt% limestone and 10 wt% Fe_2O_3 and (3) an alumina shell with 4.2 wt% limestone and 6.1 wt% Ni. The forward rate of the water-gas shift reaction was enhanced by the absorption of CO_2. With the first and third shell formulations a H_2 concentration in excess of 95 mol% was produced between 480-600°C during the period when CO_2 was rapidly absorbed. However, with the second shell formulation a H_2 concentration of 95 mol% or more was only produced at 550-600°C with rapid CO_2 absorption. At lower temperatures, the CO conversion observed with the second formulation was lower even while CO_2 was rapidly absorbed, possibly because of the low permeability of this shell formulation. Once CO_2 absorption had slowed significantly due to loading of the CaO sorbent, the CO conversion varied greatly among the three shell formulations. In this CO_2 absorption regime

only the third formulation produced a CO conversion approaching an equilibrium level at all temperatures tested. Much lower conversions were achieved with the second formulation and even lower conversions with the first formulation. However, since any of these shell formulations are most likely to be applied under conditions where CO_2 is rapidly absorbed, the first formulation may hold the greatest promise because it is likely to be the most economical as well as resistant to sulfur poisoning.

Recommended Future Research

The combined catalyst and sorbent core-in-shell pellets used for H_2 production were advanced significantly through the research presented in this dissertation. However, this research has also suggested opportunities for further investigation to extend the development and improvement of a very promising material.

CO_2 Sorbent Development

Development of a more stable CaO-based sorbent requires further consideration. Control of the calcination atmosphere during initial sorbent activation could lead to a more stable sorbent. Oneill and Keairns[1] reported that it is possible to control the pore size distribution of a sorbent derived from dolomite by controlling the CO_2 partial pressure and temperature during calcination. In this way, it is possible to produce a sorbent with larger pores that are more stable and that can absorb more material. This claim needs verification together with lifecycle testing of the material.

The lifecycle performance of other promising CaO-based sorbents deserves investigation. Hasler et al.[2] reported that a CaO-based sorbent derived from plaster of Paris had a high level of reactivity and good cyclic stability when used to remove H_2S from a hot

gas mixture. The reactivity and cyclic stability of this sorbent should be tested with CO_2 to determine if it is a superior sorbent compared to the sorbent derived from Microna 3 limestone.

Another potential sorbent for CO_2 is MgO, which could find application in systems operating at higher pressures or lower temperatures. Figure 1 illustrates the equilibrium partial pressure of CO_2 over MgO and CaO individually, based on equilibrium constants taken from *Metallurgical Thermochemsitry*.[3]

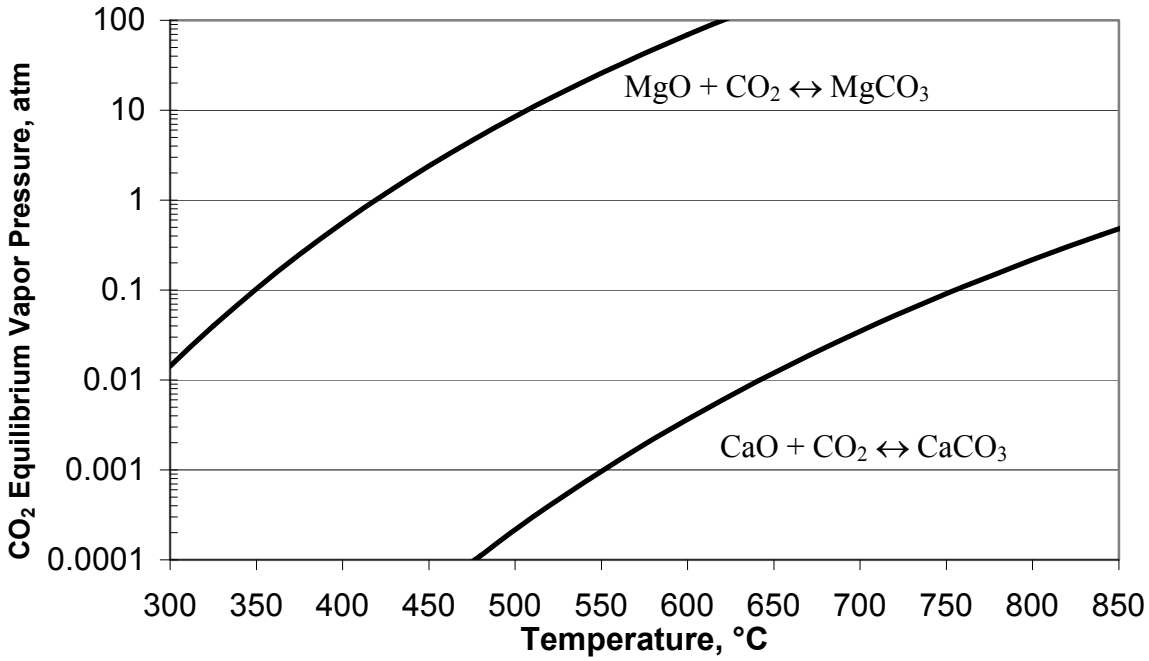

Figure 1. The equilibrium partial pressure of CO_2 over MgO and CaO.

Above the equilibrium lines in Figure 1, the sorbents absorb CO_2 while below the lines the sorbents can be regenerated. The use of MgO as a CO_2 sorbent would require lower temperatures and/or higher pressures than are used with CaO. Figure 1 suggests that MgO may be more suitable for use with the water-gas shift reaction than for the steam reforming reaction since the former can be conducted at a lower temperature than the latter. Figure 1

also indicates that MgO can be regenerated so as to provide a stream of pure CO_2 at 1.0 atm at about 430°C. This is an enormous advantage when a stream of nearly pure CO_2 is required for sequestration.

Alumina-Based Shell Development

An opportunity for the further development of the alumina-based shell could be performed through an alteration of the shell material formulation. Instead of mixing several different types of alumina with an additive such as limestone or lanthanum, it could be possible to use a single alumina precursor, such as pseudo-boehmite. A peptizing agent such as an acid could then be added to the pseudo-boehmite. For example, when the shell powder is applied to the core during pellet preparation, the water used to agglomerate the shell powder could have acid added to it, which would ideally bond the particles together through peptization. Under controlled calcination conditions, pseudo-boehmite would convert to high surface area, porous Al_2O_3 that would ideally be fused together by the peptizing agent. Additionally, if an organic acid were used, it would decompose during calcination in air. In this way, a homogenous Al_2O_3 material could be produced with high surface area and good physical strength to act as the shell of the core-in-shell material. Additionally, the homogenous shell material might be better suited to thermal cycling since it would presumably have a singular thermal expansion coefficient.

Reaction Testing

Any improvements made in either the core or shell materials should be confirmed by preparing core-in-shell pellets that are then subjected to reaction testing either by steam reforming CH_4 or conducting the water-gas shift reaction. Promising materials should be

subjected to lifecycle performance testing for greater than 10 cycles of H_2 production and sorbent regeneration.

A shell formulation without the addition of high surface area DD-290 amorphous alumina should also be tested for the sorption-enhanced production of hydrogen. The DD-290 alumina was originally added to produce a more active steam-methane reforming catalyst.[4] However, commercial reforming catalysts are often Ni supported on a low surface area ceramic, such as α-Al_2O_3. Since the Ni catalyst supported by the improved core-in-shell material no longer requires an activation period, it may be possible to prepare a sufficiently active catalyst by using a catalyst support composed entirely of α-Al_2O_3 and a small amount of limestone for strength.

Finally, the effect of employing different gases for sorbent regeneration should be investigated. Since CO_2 is a greenhouse gas that will need to be sequestered for disposal, a large concentration of CO_2 will be required for this purpose. One method of producing nearly pure CO_2 is to use steam for regenerating a CO_2 sorbent, since the steam can be condensed leaving only CO_2 as a gas. The ability of the sorbent to be regenerated with steam, and the effect of the steam on the performance and the physical properties of the core-in-shell pellets deserve further consideration and research.

Literature Cited

(1) O'Neill, E. P.; Keairns, D. L. Activation of calcium oxide as a sorbent. Patent:4226839, 1980.

(2) Hasler, D. J.; Wheelock, T. D.; Doraiswamy, L. K.; Constant, K. P., Physical Properties and Composition Effects on the Reactivity of Calcium-Based Sulfur Sorbents. *Industrial & Engineering Chemistry Research* **2007,** 46, (18), 5913-5921.

(3) Kubaschewski, O.; Evans, E. L.; Alcock, C. B., *Metallurgical Thermochemistry*. Fourth ed.; Pergamon Press Ltd.: Oxford, 1967; Vol. 1, p 379.

(4) Satrio, J. A.; Shanks, B. H.; Wheelock, T. D., Development of a Novel Combined Catalyst and Sorbent for Hydrocarbon Reforming. *Industrial & Engineering Chemistry Research* **2005,** 44, (11), 3901-3911.

Appendix 1. Mathematical Expressions Used for Data Analysis in Chapter 4

Equilibrium Expressions with CO_2 Absorption

Three reactions were assumed to take place during steam reforming of CH_4 in the presence of CO_2 absorption by a CaO sorbent: the steam-methane reforming reaction, the water-gas shift reaction and the reaction of CaO and CO_2, which are referred to as reactions 1-3, respectively. ξ_i is defined as the forward extent of each reaction.

$CH_4 + H_2O \leftrightarrow CO + 3H_2$ $\quad \xi_1$ = Extent of reaction 1

$CO + H_2O \leftrightarrow CO_2 + H_2$ $\quad \xi_2$ = Extent of reaction 2

$CaO + CO_2 \leftrightarrow CaCO_3$ $\quad \xi_3$ = Extent of reaction 3

The moles of each component in the gaseous phase at equilibrium are then determined on the basis of an initial charge of 1 mol CH_4 and 3 mol H_2O.

$$CH_4 = 1 - \xi_1 \quad H_2O = 3 - \xi_1 - \xi_2 \quad H_2 = 3\xi_1 + \xi_2$$

$$CO = \xi_1 - \xi_2 \quad CO_2 = \xi_2 - \xi_3$$

The total number of moles in the gaseous phase of the system is given by:

$$Total = 1 - \xi_1 + 3 - \xi_1 - \xi_2 + 3\xi_1 + \xi_2 + \xi_1 - \xi_2 + \xi_2 - \xi_3 = 4 + 2\xi_1 - \xi_3$$

Individual vapor phase concentrations in the system at equilibrium are given by:

$$y_{CH_4} = \frac{1 - \xi_1}{4 + 2\xi_1 - \xi_3} \quad y_{H_2O} = \frac{3 - \xi_1 - \xi_2}{4 + 2\xi_1 - \xi_3} \quad y_{H_2} = \frac{3\xi_1 + \xi_2}{4 + 2\xi_1 - \xi_3}$$

$$y_{CO} = \frac{\xi_1 - \xi_2}{4 + 2\xi_1 - \xi_3} \quad y_{CO_2} = \frac{\xi_2 - \xi_3}{4 + 2\xi_1 - \xi_3}$$

The equilibrium expressions are defined as:

$$K_1 = \left(\frac{P}{P_0}\right)^2 \frac{\left(y_{H_2}{}^3\right)\left(y_{CO}\right)}{\left(y_{CH_4}\right)\left(y_{H_2O}\right)}$$

$$K_2 = \frac{\left(y_{H_2}\right)\left(y_{CO_2}\right)}{\left(y_{CO}\right)\left(y_{H_2O}\right)}$$

$$K_3 = \left(\frac{P}{P_0}\right)^{-1} \frac{(1)}{\left(y_{CO_2}\right)}$$

where P is the total system pressure, P_0 is the reference pressure of 1.0 atm and K_1, K_2 and K_3 are equilibrium constants.

The equilibrium constants for the steam-methane reforming reaction and water-gas shift reaction were taken from the *Catalyst Handbook*.[1] The equilibrium constant for the reaction of CaO and CO_2 was taken from *Metallurgical Thermochemistry*.[2] The equilibrium constants are given by:

$$K_1 = \frac{1}{e^{Z[Z[Z(0.2513Z-0.3665)-0.58101]+27.1337]-3.2770}}$$

$$K_2 = e^{Z[Z(0.63508-0.29353Z)+4.1778]+0.31688}$$

$$K_3 = e^{\frac{-\left(-40250\frac{cal}{mol}+34.4\frac{cal}{mol^*K}{}^*T\right)}{R^*T}}$$

where:

$$Z = \frac{1000K}{T} - 1$$

and where R is the universal gas constant and T is the temperature in Kelvin.

The equilibrium expressions are then solved simultaneously for ξ_1, ξ_2, and ξ_3. The fractional equilibrium conversions of CH_4 and CO on a per mole basis are determined by:

$$CH_4 = \xi_1 \quad \text{and} \quad CO = \frac{\xi_2}{\xi_1}$$

Equilibrium Expressions without CO_2 Absorption

Two reactions are assumed to be taking in the absence of a CO_2 sorbent: the steam-methane reforming and water-gas shift reactions, which are referred to as reactions 1 and 2, respectively. ξ_i is defined as the forward extent of each reaction.

$CH_4 + H_2O \leftrightarrow CO + 3H_2$ ξ_1 = Extent of reaction 1

$CO + H_2O \leftrightarrow CO_2 + H_2$ ξ_2 = Extent of reaction 2

The moles of each component at equilibrium are then determined on the basis of an initial charge of 1 mol CH_4 and 3 mol H_2O by:

$$CH_4 = 1 - \xi_1 \quad H_2O = 3 - \xi_1 - \xi_2 \quad H_2 = 3\xi_1 + \xi_2 \quad CO = \xi_1 - \xi_2 \quad CO_2 = \xi_2$$

The total moles in the gaseous phase at equilibrium are given by:

$$Total = 1 - \xi_1 + 3 - \xi_1 - \xi_2 + 3\xi_1 + \xi_2 + \xi_1 - \xi_2 + \xi_2 = 4 + 2\xi_1$$

Individual vapor phase concentrations are given by:

$$y_{CH_4} = \frac{1 - \xi_1}{4 + 2\xi_1} \quad y_{H_2O} = \frac{3 - \xi_1 - \xi_2}{4 + 2\xi_1} \quad y_{H_2} = \frac{3\xi_1 + \xi_2}{4 + 2\xi_1}$$

$$y_{CO} = \frac{\xi_1 - \xi_2}{4 + 2\xi_1} \quad y_{CO_2} = \frac{\xi_2}{4 + 2\xi_1}$$

The equilibrium expressions are defined as:

$$K_1 = \left(\frac{P}{P_0}\right)^2 \frac{\left(y_{H_2}{}^3\right)(y_{CO})}{(y_{CH_4})(y_{H_2O})}$$

$$K_2 = \frac{(y_{H_2})(y_{CO_2})}{(y_{CO})(y_{H_2O})}$$

where P is the total system pressure, P_0 is the reference pressure of 1.0 atm and K_1 and K_2 are the equilibrium constants.

The equilibrium constants for the steam-methane reforming reaction and water-gas shift reaction were taken from the *Catalyst Handbook.*[1] The equilibrium constants are given by:

$$K_1 = \frac{1}{e^{Z[Z[Z(0.2513Z-0.3665)-0.58101]+27.1337]-3.2770}}$$

$$K_2 = e^{Z[Z(0.63508-0.29353Z)+4.1778]+0.31688}$$

where:

$$Z = \frac{1000K}{T} - 1$$

where T is the temperature in Kelvin.

The equations are then solved simultaneously for $\xi_{1,}$ and $\xi_{2,}$ in order to determine CH_4 and CO conversions as well as equilibrium gas concentrations. The fractional equilibrium conversions of CH_4 and CO on a per mole basis are determined by:

$$CH_4 = \xi_1 \quad \text{and} \quad CO = \frac{\xi_2}{\xi_1}$$

Determination of Observed Conversions

Determination of the observed conversions during the Fast and Slow Absorption periods are based on the assumption that the steam-methane reforming and water-gas shift

reactions occur simultaneously together with the reaction of CaO and CO_2, which are then referred to as reactions 1-3, respectively. ξ_i is defined as the forward extent of each reaction.

$CH_4 + H_2O \leftrightarrow CO + 3H_2$ ξ_1 = Extent of reaction 1

$CO + H_2O \leftrightarrow CO_2 + H_2$ ξ_2 = Extent of reaction 2

$CaO + CO_2 \leftrightarrow CaCO_3$ ξ_3 = Extent of reaction 3

Since the steam is condensed out of the reactor effluent prior to GC analysis, the observed conversions must be calculated on a dry basis. The moles of each component based on 1 mol of CH_4 on a dry basis are determined by:

$$CH_4 = 1 - \xi_1 \quad H_2 = 3\xi_1 + \xi_2 \quad CO = \xi_1 - \xi_2 \quad CO_2 = \xi_2 - \xi_3$$

The total moles are then given by:

$$Total = 1 - \xi_1 + 3\xi_1 + \xi_2 + \xi_1 - \xi_2 + \xi_2 - \xi_3 = 1 + 3\xi_1 + \xi_2 - \xi_3$$

Individual vapor phase concentrations are then given by:

$$y_{CH_4} = \frac{1 - \xi_1}{1 + 3\xi_1 + \xi_2 - \xi_3} \quad y_{H_2} = \frac{3\xi_1 + \xi_2}{1 + 3\xi_1 + \xi_2 - \xi_3}$$

$$y_{CO} = \frac{\xi_1 - \xi_2}{1 + 3\xi_1 + \xi_2 - \xi_3} \quad y_{CO_2} = \frac{\xi_2 - \xi_3}{1 + 3\xi_1 + \xi_2 - \xi_3}$$

The results presented in Chapter 4 were determined by utilizing the CH_4, CO and CO_2 gas concentrations expressed on a dry basis to solve the three vapor phase equations for ξ_1, ξ_2, and ξ_3. Since any combination of the three gas concentrations produced similar results when substituted into these equations, the gas concentrations were consistent for a given test. The observed conversions of CH_4 and CO were determined by:

$$CH_4 = \xi_1 \text{ and } CO = \frac{\xi_2}{\xi_1}$$

Example of Absorption Capacity Calculation

The lifecycle testing presented in Chapter 4 shows how the absorption capacity of the pellets varied with of cycle number (Chapter 4, Figure 11). The absorption capacity for the first cycle was used in the following example. Only the Fast Absorption period was used in determining the CO_2 absorption capacity (0-95 min).

First, the extent of the three reactions ξ_1, ξ_2 and ξ_3 was determined by the method outlined in the preceding section. The observed gas concentrations were 0.72% CH_4, 0.29% CO, 0.39% CO_2 and 98.60% H_2. The values of ξ_1, ξ_2 and ξ_3 were determined to be 0.9716, 0.9603 and 0.9449, respectively. However, ξ_1, ξ_2 and ξ_3 are fractional conversions based on 1 mole of CH_4. The extent of reactions 1-3 in terms of CH_4 feed rate in mmol/min were defined as η_i and were determined by:

$$\eta_1 = F_{CH_4} * \xi_1 = 0.6025 \frac{mmol}{\min} * 0.9716 = 0.5854 \frac{mmol}{\min}$$

$$\eta_2 = \eta_1 * \frac{\xi_2}{\xi_1} = 0.5854 \frac{mmol}{\min} * \frac{0.9603}{0.9716} = 0.5786 \frac{mmol}{\min}$$

$$\eta_3 = \eta_2 * \frac{\xi_3}{\xi_2} = 0.5786 \frac{mmol}{\min} * \frac{0.9449}{0.9603} = 0.5693 \frac{mmol}{\min}$$

where F_{CH4} is the molar flow rate of CH_4 fed to the reactor, or 0.6025 mmol/min. Therefore, the amount of CO_2 absorbed is 0.5693 mmol/min. The Fast Absorption period was determined to be 95 min long for this example, leading to 54.1 mmol of CO_2 that was absorbed. Furthermore, 4.3 g of CaO was determined to be present in the reactor, giving 12.6 mmol CO_2 absorbed/g CaO.

To verify that the correct CO_2 absorption rate was determined, the total molar flow rate without CO_2 absorption can be calculated for the following individual species:

$$CH_4 = F_{CH_4} - \eta_1 = 0.6025\frac{mmol}{\min} - 0.5854\frac{mmol}{\min} = 0.0171\frac{mmol}{\min}$$

$$CO = \eta_1 - \eta_2 = 0.5854\frac{mmol}{\min} - 0.5786\frac{mmol}{\min} = 0.0068\frac{mmol}{\min}$$

$$H_2 = 3\eta_1 + \eta_2 = 3 * 0.5854\frac{mmol}{\min} + 0.5786\frac{mmol}{\min} = 2.3348\frac{mmol}{\min}$$

$$CO_2 = \eta_2 = 0.5786\frac{mmol}{\min}$$

The total flow rate without CO_2 absorption is the sum of the individual species, given by:

$$Total = 0.0171\frac{mmol}{\min} + 0.0068\frac{mmol}{\min} + 2.3348\frac{mmol}{\min} + 0.5786\frac{mmol}{\min} = 2.9373\frac{mmol}{\min}$$

The amount of CO_2 absorbed per minute during the rapid absorption phase was 0.5693 mmol CO_2/min, which is given by η_3. Thus, the observed gas concentration of CO_2 is given by:

$$\frac{\eta_2 - \eta_3}{Total - \eta_3} = \frac{0.5786\frac{mmol}{\min} - 0.5693\frac{mmol}{\min}}{2.9373\frac{mmol}{\min} - 0.5693\frac{mmol}{\min}} = .0039$$

The CO_2 gas concentration of 0.39% is identical to the observed gas concentration, ensuring that the calculation was done correctly.

Literature Cited

(1) *Catalyst Handbook*. Second Edition ed.; Wolfe Publishing, Ltd.: Frome, England, 1989; p 537-548.

(2) Kubaschewski, O.; Evans, E. L.; Alcock, C. B., *Metallurgical Thermochemistry*. Fourth ed.; Pergamon Press Ltd.: Oxford, 1967; Vol. 1, p 379.

Appendix 2. Calculated Equilibrium Gas Concentrations for Reaction Conditions Reported in Chapter 4

Table 1. Calculated equilibrium dry basis gas concentrations based on a feed of 1 mol CH_4 and 3 mol H_2O.

Temperature, °C	Pressure, atm	CO_2 Absorption	Concentration (Dry Basis), %			
			CH_4	CO	CO_2	H_2
550	**1**	**With**	1.9	0.1	0.1	97.9
		Without	12.4	4.6	13.8	69.2
600	**1**	**With**	1.6	0.5	0.4	97.5
		Without	6.0	7.8	12.5	73.6
600	**3**	**With**	3.4	0.1	0.1	96.3
		Without	14.5	5.1	13.0	67.4
600	**5**	**With**	4.5	0.1	0.1	95.4
		Without	19.5	4.0	12.9	63.6
600	**10**	**With**	6.3	0.0	0.0	93.6
		Without	26.97	2.82	12.35	57.86
650	**1**	**With**	1.3	2.0	1.3	95.4
		Without	2.3	10.8	10.9	76.0
650	**3**	**With**	3.0	0.7	0.4	95.9
		Without	8.1	8.2	11.8	71.9
650	**5**	**With**	4.1	0.3	0.3	95.3
		Without	12.2	6.8	12.1	68.9
650	**10**	**With**	5.8	0.1	0.1	93.9
		Without	18.83	5.05	12.19	63.92

Appendix 3. Mathematical Expressions Used for Data Analysis in Chapter 5

Equilibrium Expressions for the Absorption Period

Two reactions were assumed to take place during the Absorption period of water-gas shift testing reported in Chapter 5: the water-gas shift reaction and the reaction of CaO and CO_2, which were referred to as reactions 1 and 2. ξ_i is defined as the forward extent of each reaction.

$CO + H_2O \leftrightarrow CO_2 + H_2$ ξ_1 = Extent of reaction 1

$CaO + CO_2 \leftrightarrow CaCO_3$ ξ_2 = Extent of reaction 2

The moles of each component in the gaseous phase at equilibrium are then expressed on the basis of the initial charge of 1 mole CO and 3 moles H_2O.

$$CO = 1 - \xi_1 \quad H_2O = 3 - \xi_1 \quad H_2 = \xi_1 \quad CO_2 = \xi_1 - \xi_2$$

The total number of moles in the gaseous phase of the system are given by:

$$Total = 1 - \xi_1 + 3 - \xi_1 + \xi_1 + \xi_1 - \xi_2 = 4 - \xi_2$$

Individual vapor phase concentrations in the system at equilibrium are given by:

$$y_{CO} = \frac{1 - \xi_1}{4 - \xi_2} \quad y_{H_2O} = \frac{3 - \xi_1}{4 - \xi_2} \quad y_{H_2} = \frac{\xi_1}{4 - \xi_2} \quad y_{CO_2} = \frac{\xi_1 - \xi_2}{4 - \xi_2}$$

The equilibrium expressions are defined as:

$$K_1 = \frac{(y_{H_2})(y_{CO_2})}{(y_{CO})(y_{H_2O})}$$

$$K_2 = \left(\frac{P}{P_0}\right)^{-1} \frac{1}{(y_{CO_2})}$$

where P is the system pressure, P_0 is the reference pressure of 1.0 atm and K_1 and K_2 are equilibrium constants.

The equilibrium constant for the water-gas shift reaction was taken from the *Catalyst Handbook.*[1] The equilibrium constant for the reaction of CaO and CO_2 was taken from *Metallurgical Thermochemistry.*[2] The equilibrium constants are given by:

$$K_1 = e^{Z[Z(0.68508-0.29358Z)+4.1778]+0.91688}$$

$$K_2 = e^{\frac{-\left(-40250\frac{cal}{mol}+34.4\frac{cal}{mol^*K}{}^*T\right)}{R^*T}}$$

where:

$$Z = \frac{1000K}{T} - 1$$

and where R is the universal gas constant and T is the temperature in Kelvin.

The equations were then solved simultaneously for ξ_1, and ξ_2. The fractional equilibrium conversions of CO on a per mole basis were determined by:

$$CO = \xi_1$$

Equilibrium Expressions for the Post Absorption Period

One reaction was assumed to be taking placed during the Post Absorption period: the water-gas shift reaction, which is referred to as reaction 1. ξ_1 is defined as the forward extent of the water-gas shift reaction.

$$CO + H_2O \leftrightarrow CO_2 + H_2 \qquad \xi_1 \text{ Extent of reaction 1}$$

The moles of each component at equilibrium were then based on an initial charge of 1 mole CO and 3 moles H_2O as shown below:

$$CO = 1 - \xi_1 \quad H_2O = 3 - \xi_1 \quad H_2 = \xi_1 \quad CO_2 = \xi_1$$

The total moles in the gaseous phase at equilibrium were given by:

$$Total = 1 - \xi_1 + 3 - \xi_1 + \xi_1 + \xi_1 = 4$$

Individual vapor phase concentrations were given by:

$$y_{CO} = \frac{1-\xi_1}{4} \quad y_{H_2O} = \frac{3-\xi_1}{4} \quad y_{H_2} = \frac{\xi_1}{4} \quad y_{CO_2} = \frac{\xi_1}{4}$$

The equilibrium expression for the water-gas shift was defined as:

$$K_1 = \frac{(y_{H_2})(y_{CO_2})}{(y_{CO})(y_{H_2O})}$$

where K_1 is the equilibrium constant.

The equilibrium constant for the water-gas shift reaction was taken from the *Catalyst Handbook.*[1] The equilibrium constant was given by:

$$K_1 = e^{Z[Z(0.63508 - 0.29358Z) + 4.1778] + 0.31688}$$

where:

$$Z = \frac{1000K}{T} - 1$$

and T is the temperature in Kelvin.

The equilibrium expression was then solved for ξ_1 in order to determine the CO conversion as well as equilibrium gas concentrations. The fractional equilibrium conversion of CO on a per mole basis was determined by:

$$CO = \xi_1$$

Determination of Observed Conversions During the Absorption Period

Determination of the observed conversion of CO during the Absorption period was based on the assumption that the water-gas shift reaction and the reaction of CO_2 and CaO

occurred simultaneously. These reactions are referred to as reactions 1 and 2, respectively. ξ_i was defined as the forward extent of each reaction.

$CO + H_2O \leftrightarrow CO_2 + H_2$ ξ_1 = Extent of reaction 1

$CaO + CO_2 \leftrightarrow CaCO_3$ ξ_2 = Extent of reaction 2

Since the steam was condensed out of the reactor effluent prior to GC analysis, the observed conversion determined during the Absorption phase of reaction testing was determined on a dry basis. The moles of each component based on 1 mole of CO and on a dry basis are expressed as:

$$CO = 1 - \xi_1 \quad H_2 = \xi_1 \quad CO_2 = \xi_1 - \xi_2$$

The total moles are then given by:

$$Total = 1 - \xi_1 + \xi_1 + \xi_1 - \xi_2 = 1 + \xi_1 - \xi_2$$

Individual vapor phase concentrations are then given by:

$$y_{CO} = \frac{1 - \xi_1}{1 + \xi_1 - \xi_2} \quad y_{H_2} = \frac{\xi_1}{1 + \xi_1 - \xi_2} \quad y_{CO_2} = \frac{\xi_1 - \xi_2}{1 + \xi_1 - \xi_2}$$

These equations are solved simultaneously for ξ_1 and ξ_2 after substituting measured values of the gas concentrations expressed on a dry basis. The observed conversion of CO was determined by:

$$CO = \xi_1$$

Determination of Observed Conversions During the Post Absorption Period

Determination of the observed conversion of CO during the Post Absorption period was based on the assumption that only the water-gas shift reaction occurred, which was referred to as reaction 1. ξ_1 was defined as the forward extent of the water-gas shift reaction.

$CO + H_2O \leftrightarrow CO_2 + H_2$ ξ_1 = Extent of reaction 1

Since the steam was condensed out of the reactor effluent prior to GC analysis, the observed conversion determined during the Post Absorption phase of reaction testing was determined on a dry basis. The moles of each component based on 1 mol of CO and on a dry basis were expressed as:

$$CO = 1 - \xi_1 \quad H_2 = \xi_1 \quad CO_2 = \xi_1$$

The total moles are then given by:

$$Total = 1 - \xi_1 + \xi_1 + \xi_1 = 1 + \xi_1$$

Individual vapor phase concentrations are then given by:

$$y_{CO} = \frac{1 - \xi_1}{1 + \xi_1} \quad y_{H_2} = \frac{\xi_1}{1 + \xi_1} \quad y_{CO_2} = \frac{\xi_1}{1 + \xi_1}$$

The work presented in Chapter 5 utilized the dry basis gas concentration of CO to solve the first of the preceding three equations for ξ_1. The observed conversion of CO was determined by:

$$CO = \xi_1$$

Literature Cited

(1) *Catalyst Handbook*. Second Edition ed.; Wolfe Publishing, Ltd.: Frome, England, 1989; p 537-548.

(2) Kubaschewski, O.; Evans, E. L.; Alcock, C. B., *Metallurgical Thermochemistry*. Fourth ed.; Pergamon Press Ltd.: Oxford, 1967; Vol. 1, p 379.

Appendix 4. Calculated Equilibrium Gas Concentrations for Reaction Conditions Reported in Chapter 5

Table 1. Calculated equilibrium gas concentrations based on a feed of 1 mol CO and 3 mol H_2O at 1.0 atm.

Temperature, °C	CO_2 Absorption	Concentration (Dry Basis), %		
		CO	CO_2	H_2
480	With	0.00	0.00	100.00
	Without	3.79	48.11	48.11
520	With	0.00	0.10	99.90
	Without	4.88	47.56	47.56
550	With	0.00	0.20	99.80
	Without	5.76	47.12	47.12
600	With	0.20	0.79	99.01
	Without	7.35	46.32	46.32

Acknowledgments

This report was prepared with the support of the U.S. Department of Energy, under Award No. DE-FG26-04NT 42182.

I would like to thank God for giving me the physical and emotional strength to perform this work.

I would like to thank Dr. Brent Shanks and Dr. Thomas Wheelock for their guidance, help and patience in helping me to perform this work. Also, I would like to thank Dr. Thomas McGee for his help with the shell portion of this dissertation.

Thank you to Dr. Justinus Satrio for your help in getting me started and for being a constant resource.

Thank you to my wife, Wendy, and my son, Samuel, for keeping me going and for being there for me.

Thank you to all my friends and family for your constant encouragement.